HIV-1 Reservoir Formation, Stability and Dynamics during early Therapy

Inauguraldissertation

zur

Erlangung der Würde eines Doktors der Philosophie

vorgelegt der Philosophisch-Naturwissenschaftlichen Fakultät

der Universität Basel

von

Fabian Otte

Basel, 2021

Genehmigt von der Philosophisch-Naturwissenschaftlichen Fakultät

auf Antrag von

Prof. Dr. rer. nat. Thomas Klimkait, Prof. Dr. Christoph Dehio und Prof. Dr. Angela Teresa Ciuffi

Basel, den 13.10.2020

Prof. Dr. Martin Spiess
Dekan der Philosophisch-
Naturwissenschaftlichen Fakultät

“May the wind always be at your back and the sun upon your face. And may the wings of destiny carry you aloft to dance with the stars.”

- **George Jung, Blow**

Für Mama un Baba,

für min Brüda Daniel,

für mini zwei Herzchäfa Mats un Leno

Table of Contents

I. List of Tables

II. List of Figures

III. List of Supplemental Figures

IV. Abbreviations

Abbreviations

AGM	African green monkey
AIDS	Acquired immunodeficiency syndrome
APOBEC3G/F	Apolipoprotein B mRNA-editing enzyme, catalytic polypeptide 3G/F
ARV	Antiretroviral
A4B7	Integrin $\alpha_4\beta_7$
bNAb	broadly neutralizing Antibody
cART	Combination antiretroviral therapy
CI	Confidence interval
CLA	Cutaneous Lymphocyte Antigen
CRF	Circulating recombinant form
CTL	Cytotoxic T-Lymphocyte
CCR5	CC-motive chemokine receptor 5
CCR7	CC-motive chemokine receptor 7
CD	Cluster of differentiation
CFSE	Carboxyfluorescein succinimidyl ester
CXCR4	CXC-motive chemokine receptor 4
DBSCAN	Density-Based Spatial Clustering of Applications with Noise
DM	Dual-/mixed tropic
DMSO	Dimethylsulfoxid
DN	double negative
DNA	Deoxyribonucleic acid

DP	double positive
DPI	Days post infection
EDTA	Ethylenediaminetetraacetic acid
EFV	Efavirenz
Env	Envelope
FACS	Flourescence activated cell sorting/scanning
FBS	Fetal Bovine Serum
FDA	Food and Drug administration
FPR	False positive rate
GALT	Gut associated lymphoid tissue
gDNA	Genomic DNA
GERDA	Gag and Envelope Reactivation Detection Assay
gp41	Glycoprotein 41
gp120	Glycoprotein 120
GPCR	G-protein coupled receptor
HIV	Human immunodeficiency virus
HSCT	Hematopoietic stem-cell transplantation
IC	Intracellular
IQR	Inter quartile range
INSTI	Integrase strand transfer inhibitor
IUPM	infectious units per million

kb	Kilo base
LN	Lymph node
LRA	Latency reversing agent
LTR	Long terminal repeat
MACS	Magnetic activated cell sorting
MOTIVATE	Maraviroc versus Optimized Therapy in Viremic Antiretroviral Treatment-Experienced Patients
MSM	Men who have sex with men
NA	Not available
ND	Not detectable
NGS	Next Generation Sequencing
NRTI	Nucleoside reverse transcriptase inhibitor
NSI	Non-syncytium inducing
PBMC	Peripheral Blood Mononuclear cell
PBS	Phosphor-buffered Saline
PCR	Polymerase chain reaction
PD1	Programmed cell death protein 1
PEP	Post-exposure prophylaxis
PHA	Phytohaemagglutinin
poly-A	HIV poly-adenylated transcripts
PrEP	Pre-exposure prophylaxis

Q	Quadrant
QVOA	Quantitative Viral Outgrowth Assay
R5	Chemokine receptor CCR5
RM	Rhesus Macaque
RNA	Ribonucleic acid
RT-PCR	One-step reverse transcriptase PCR
SD	Standard deviation
SHCS	Swiss HIV Cohort Study
SI	Syncytium inducing
SHIV	Simian-Human immunodeficiency virus
SIV	Simian immunodeficiency virus
T	Time point
T_{CM}	Central memory T-cell
TCR	T cell receptor
T_{EM}	Effector memory T-cell
TF	Transmitted/Founder virus
T_N	naïve T-cells
t-SNE	t-distributed stochastic neighbor embedding
T_{TM}	Transitional memory T-cell
V3	Variable loop 3
VL	Viral load

X-Gal	5-bromo-4-chloro-3-indolyl-β-D-galactopyranoside
X4	Chemokine receptor CXCR4
%X4	Frequency of X4-tropic HIV variants

V. Abstract

After an infection event, the Human immunodeficiency virus (HIV) can rapidly seed at its initial contact zone within few days leading to systemic spread in the whole body. It is the combination of high propagation rates and the error-prone viral replication that drives a rapid viral evolution and evasion of an effective immune response. Modern combination HIV therapy can impede such a continuous adaptation of the virus through sustained virus suppression. However, the very rapid return of replicating virus in the blood upon stop of therapy, is a most obvious indicator of active or activatable “sanctuaries”. Lymphoid tissues and especially the gut associated lymphatic tissue (GALT) play key roles in viral persistence. In order to infect the main target, CD4-positive cells, HIV needs to bind a chemokine receptor, either CCR5 or CXCR4, prior to fusing with its target cell. During early periods of the infection, the virus predominantly uses CCR5. In the untreated host, about 50% of patients experience a shift to a dominance of CXCR4-tropic (X4) viruses, associated with higher CD4 depletion rates and an accelerated disease progression. In contrast, under successful therapy CXCR4 tropism does not increase over time but rather seems to become actively eliminated. To address this somewhat unexpected observation, peripheral blood mononuclear cells (PBMCs) were used to assess their contribution to the viral reservoir. The aim was to identify predictive properties of those “circulating cells”, which have the capacity to carry (viral) information from the periphery to distant site of persistence for understanding the dynamics of HIV infections during early treatment periods. For single cell immune characterization, a new methodology called GERDA (Gag and Envelope Reactivation Detection Assay) was established and validated by genetic and functional reservoir assays to find potential infectious cells. To dissect the contribution of cellular reservoirs, viral activity was measured on the level of DNA, RNA and protein. It confirmed that intracellular viral activity quickly declines after initiation of ART. Furthermore, most peripheral cells did not show high viral gene activity in the cytoplasm despite detectable plasma viral load and even when sampling right after diagnosis. This strongly suggests that the main active reservoir remains outside the periphery. In all patients of the study, the dominating virus variant at time of diagnosis was also found inside cells in the form of integrated viral genomes and did not change in the first months of therapy. For individuals with signs of ongoing viral activity, most actively replicating viruses were found in central memory cells, i.e. lymphoid homing cells and not in gut homing cells.

Overall, this study introduces a new concept of reservoir characterization using PBMCs in circulating blood for identifying by use of “homing markers” crucial body compartments and

actively infected cell populations that will help to explain residing viral activity and potential obstacles for the eradication of HIV and towards a cure.

VI. Introduction

VI.1. Introduction to the study: Viral control of CXCR4 under suppressive Therapy

HIV viruses can be categorized in two groups based on which co-receptor they use to fuse with their CD4 target cells: either CCR5 binding (R5-tropic) [1–3] or CXCR4 binding (X4-tropic) [4]. In the acute phase of an infection HIV positive individuals have predominantly R5 tropic viruses in their circulation [5,6]. It is also in the acute infection phase where the virus spreads in the whole body to establish its viral reservoir especially in lymphoid tissues like lymph nodes (LNs) [7] or the gut associated lymphoid tissue (GALT) [8,9], where the virus deprives CD4 populations that cannot be fully replenished. In 50% of therapy naïve HIV positive individuals X4 tropic viruses arise later in disease, concomitantly with dropping CD4+ cells and progression to AIDS [10,11]. Thus X4 tropic viruses were associated with faster disease progression, along with higher replication rates and higher cytopathic effects [12–14]. However, a direct causal link could not be established, so that it remained largely unclear if the X4-tropic viruses in untreated individuals caused the immunological deterioration or if they were rather the result of a broken immune response. Today modern effective antiretroviral therapy (ART) can effectively restore immune competence by repressing viral replication. (more details are specified in VI.3. Background).

A study by Kaufmann and co-workers observed for a group of HIV positive individuals only a slow and partial CD4 cell recovery despite suppressive ART, suggesting incomplete response. The only predictive clinical parameters for these findings were higher age at time of infection and advanced disease status at diagnosis [15]. Since X4 tropism is associated with faster disease progression Bader et al found that 60% of these incomplete responders were X4-tropic at therapy initiation. Moreover 71.4% of the study group had unexpectedly changed their proviral tropism from baseline X4- to R5-tropic, after 5 years on suppressive therapy [16]. These results were further supported by a subsequent Next Generation Sequencing (NGS) study of HIV positive individuals with fully suppressive ART and continuous recovering CD4 counts showing that 80% of individuals had no increasing but rather diminished levels of X4 tropic proviral populations [17]. So are X4-tropic viruses really the herald of faster disease progression? Another line of evidence against this statement came from the MOTIVATE study, that evaluated the efficacy of Maraviroc, a CCR5 antagonizing drug, in patients with a failing selvage therapy that presented at the beginning as CCR5 tropic [18,19]. For most patients the drug outperformed the optimized backbone therapy, but a minor proportion of patients failed reflected by increasing viral loads. It turned out that for all failing patients the rebounding virus was dual- or mixed (DM) tropic. [20,21] Maraviroc patients defined as “failing” as per the

study protocol were shifted back to the optimized backbone therapy, which led to the tropism again changing back from DM-tropic to R5-tropic, indicative for a superior role of R5-tropic viruses. The predominance of CCR5 was also described in case studies during early infection after needle stick accidents and vertical transmission, reporting that an initial dominating X4-tropic infection reverted back to a R5-tropic dominated population [22–24].

Putting all these results into perspective these findings suggest that the persistence of X4-tropic viruses must be inferior to R5-tropic viruses as most patient present as R5-tropic, while X4-tropic virus can only arise under immunocompromised condition. Further X4 seems to be readily detected and cleared in recovering patients. The central question is, what is the eliminating pressure? Are X4-tropic selectively cleared by the immune system or are these cells found in different compartments compared to R5 tropic counterparts?

VI.2. Aim of the study

Most diagnostic work on HIV utilizes blood as the most accessible and relevant compartment providing information about ongoing disease parameters or the dynamics and stability of the virus. It is evident that transiently circulating cells do not at all constitute a “homogeneous cell population” of cells from a single compartment or in permanent circulation but a rather complex mix of cells with distinct properties and different homing characteristics that are dynamically changing. Recent work by Bader et al found that Envelope properties of HIV correlate with immunologic recovery and disease outcome. In particular, effective combination therapy appears to facilitate a predominant control of CXCR4-tropic HIV [17]. Based on this rather unexpected activity, this study aims at a detailed characterization of HIV inside the key T-cell populations during ART to identify critical lymphoid compartments responsible for the selective elimination of X4-tropic proviruses and cells.

VI.3. Background on HIV

VI.3.1. HIV epidemiology

"…the arrow of funds, medical expertise, research and experimentation with the Department of Health and Human Services, and its allies around the world, have aimed and fired at the disease AIDS, and has hit the target only two or three rings away from the bullseye itself. Here are the specifics:

First, the probable cause of AIDS has been found --…

Second, not only has the agent been identified, but a new process has been developed to mass produce this virus…Finally, we also believe that the new process will enable us to develop a vaccine to prevent AIDS in the future. We hope to have such a vaccine ready for testing in approximately two years." – Margareth Heckler, U.S. Health and Human Services Secretary, Press conference 1984 April 23rd. [25]

Today almost 40 years later, there is still no vaccine available to conquer the global spread of HIV. Since the start of the epidemic, approximately 75.7 million people became infected with HIV and 32.7 million have died from AIDS related illnesses. To date 38 million people globally are living with HIV, with 1.7 million new infections annually and 690´000 AIDS related deaths [26]. However, with the discovery of antiretroviral (ARV) drugs against HIV, the former deadly disease is becoming controllable. The ambitious 90-90-90 goal of UNAIDS, which became effective after 2015 [27], stating that by 2020, 90% of people living with HIV know their status, 90% of diagnosed people are under antiretroviral therapy (ART), and 90% of treated individuals have a suppressed viral load (VL), was not achieved. The current global status is 81-67-59, with 25.4 million people having had access to ART in 2019, a number which has more than tripled since 2010. Furthermore, countries like Switzerland or Eswatini have even surpassed the 95-95-95 goals. But despite of these success stories, there is still a long way to go in order to achieve the set targets, and a big discrepancy in the success of HIV prevention between countries must be noted, especially for countries of Sub-Saharan Africa compared to e.g. Europe [28]. Therefore, as long as no effective vaccine is available, the current best remedy against new infections remains to be the concept of Treatment as prevention, that encompasses pre-exposure prophylaxis (PREP), post-exposure prophylaxis (PEP) or ART for HIV treatment for protecting the HIV negative population from vertical and horizontal

transmission. In order to prevent further spread of HIV and to keep the viral reservoir for each infected individual as limited as possible, initiating ART right after diagnosis ("Test and Treat") is highly recommended [29,30].

VI.3.2. HIV-1 essentials and tropism

To achieve viral suppression, i.e. the last 90 of the UNAIDS 2020 goal, a lot of potent drugs have been developed in the last decades. For the development it was thus essential to understand a) how the virus infects target cells, b) how it replicates and c) which role the respective viral proteins have in the viral life cycle.

HIV-1 is a 9.2 kb positive oriented single strand RNA ((+)ssRNA) Lentivirus that belongs to the family of *Retroviridae*. Its genome encodes for the structural proteins Gag (Matrix p17 , Capsid p24 and Nucleocapsid p7 and P6), Pol (Protease p12, Reverse Transcriptase p66/51 and Integrase p32) and Env (Envelope glycoprotein gp120 and gp41), and 2 additional regulatory proteins being Tat (transactivator of transcription p14), Rev (regulator of expression of virion proteins p19) as well as 4 accessory proteins Nef (negative factor p27), Vif (viral infectivity factor p23), Vpr (virus protein r p15) and Vpu (viral protein U p16) as depicted in Figure 1. After viral entrance the (+)ssRNA is reverse transcribed into double stranded DNA , which is integrated by Integrase into the host genome. These integrated viral genomes are called proviruses. Viral transcription regulation is promoted by Tat and Rev, leading to temporal production of viral regulatory proteins, followed by viral accessory proteins, and finally viral structural and enzymatic precursor proteins. At the cellular surface, viral proteins are assembled, the nascent viral particle buds off and as a last step HIV Protease cleaves all structural proteins to have a fully mature and infectious virus [31].

FIGURE 1 HIV-1 proviral genome organization

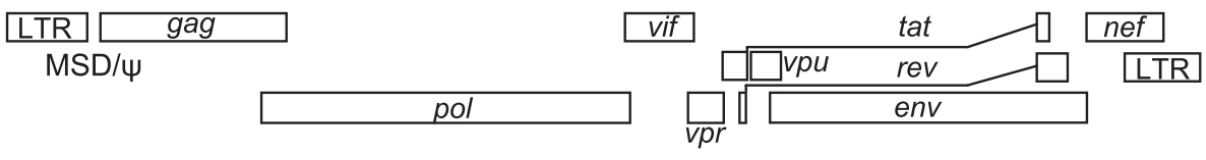

Figure 1. HIV-1 proviral genome map. All genes are organized according to the respective open reading frame. LTR: Long terminal repeat. MSD: major splice donor. Ψ: packaging signal. Adapted from R. Pollack et al 2017 [32]

To infect a target cell HIV needs to bind to the CD4 receptor [33–35] and a co-receptor being either CCR5 (R5)[1–3] or CXCR4 (X4) [4] in order to fuse with its target cell. Main target cells are primarily CD4+ T-cells [33,34], Macrophages [36,37] and Dendritic cells[38,39]. CCR5 as well as CXCR4 are so called chemokine receptors that belong to the family of seven-transmembrane G-protein coupled receptors (GPCR) and have important functions in cell migration [40]. R5-tropic viruses are rather macrophage tropic with a non-syncytium inducing (NSI) [41] phenotype, whereas X4-tropic viruses mainly infect T-cells and are of syncytium inducing (SI) nature [42,43]. Some viruses even have the ability to infect cells via both co-receptors being dual tropic [44] or come in a mix of different tropic viruses (mixed tropic). Embedded within the unbound viral Envelope Glycoprotein 120 (gp120) is the variable V3 loop, which is about 35 amino acids in length. Upon CD4 binding V3 is exposed and interacts with the co-receptor making it the major tropism determining factor [45]. Especially positively charged residues at positions 11, 24 and 25 are critical for X4 tropism assignment as well as loss of N-linked glycosylation sites [46,47]. Currently the FDA has approved only one CCR5 antagonist called Maraviroc (Selzentry® Pfizer) [48]. The drug is only approved for patients that present as R5-tropic. Early phenotypical tropism determining assays, like the TROFILE assay [49], had the disadvantage of being very time consuming and labor intensive. Thus genotypic tropism algorithms like Geno2Pheno, which decide by a hierarchical decision tree if the circulating virus is rather R5 or X4 tropic based on the V3 sequence [50], have advanced tropism determination.

VI.3.3. HIV-1 latency and the viral reservoir

After the primary infection event in a newly infected person and the establishment of a founding population of viruses and virus-infected cells in various immune compartments, the proviral landscape begins to be dynamically shaped. It is formed by a number of critical contributors such as cell elimination driven by viral cytopathic effects [51,52] , a clonal expansion of HIV-target cells [53–56], homeostatic proliferation [57–59] or antigenic proliferation [60,61], and simultaneous selection pressure[32,62–64] . Later, once a chronic infection situation is established, the main viral reservoir is primarily found in T-cell memory compartments harboring the highest percentage of intact proviral genomes with a mean half-life of 44 months [65,66]. For T-cell memory formation naïve T-cells (T_N) need to encounter a cognate antigen to differentiate into effector cells that migrate to inflamed sites to clear the encountered pathogen. After antigen clearance a small proportion of these effector cells further differentiate into long-lived

memory cells. These memory cells include, from least to most differentiated, stem-cell-like memory (T_{SCM}), central memory (T_{CM}), transitional memory (T_{TM}), effector memory (T_{EM}), and finally terminal effector memory (T_{TE} or T_{EMRA}) cells as highlighted in Figure 2. Further, special T-cell subset include tissue resident memory cells (T_{RM}) and follicular helper T-cells (T_{FH}) [67]. Many of these T-cell subsets have been proposed to be main viral reservoirs but the superior role of one subset compared to the other is controversial [57,68–73]. These contradicting results are most likely due to the viral and host specific heterogeneities. Nevertheless one general observation is that T_{EM} harbor most HIV integrations due to differentiation and enhanced proliferation rates of precursor subsets [69].

FIGURE 2 T-cell memory compartments

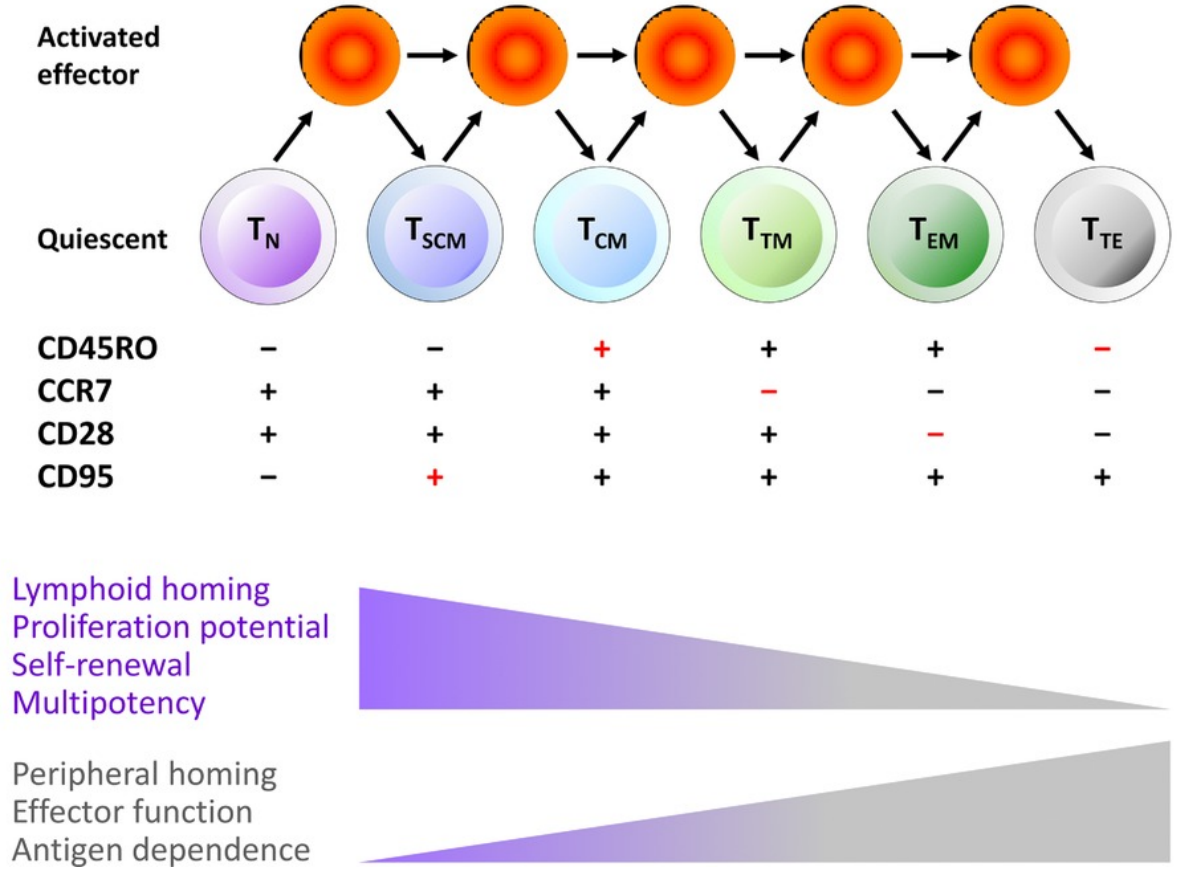

Figure 2. T-cell memory differentiation. Progressive memory T-cell differentiation, from least (left) to most differentiated (right): naïve T-cells (T_N), stem-cell-like memory (T_{SCM}), central memory (T_{CM}), transitional memory (T_{TM}), effector memory (T_{EM}), and finally terminal effector memory (T_{TE} or T_{EMRA}) cells. Each subset can be assigned by a characteristic marker expression profile listed below each subset. Physiological functions lost or gained through progressive differentiation of each memory class are highlighted in gradient bars at the bottom of the graph. Adapted from YD Mahnke et al 2013 [67]

Most studies concerning the viral reservoir in these T-cell compartments have mainly focused on the peripheral blood, which according to most recent studies accounts for only 0.2% of all

virus [74]. A lot of these insights were obtained from monkey infection studies with the simian immunodeficiency virus (SIV), which is a closely related genetic predecessor of HIV that had been transmitted from primates to human. The primary non-human infection model of choice is Rhesus Macaques (RMs) and other Asian non-human primates, which are non-natural SIV hosts that reflect the human pathogenesis with progression to AIDS. In stark contrast is the disease progression in the natural SIV host of African green monkeys (AGMs), which do not develop any AIDS like symptoms despite chronic active viral replication. The ultimate differences are not entirely clear but the main aspect concerns the control over chronic immune activation and inflammation [75]. Thus, new insights of monkey studies revealed that especially tissues of lymphoid origin like Lymph nodes (LNs) or the gut associated lymphatic tissue (GALT) represent the most important sanctuaries for SIV and were also translatable to HIV [7,8,76].

Especially the gut is one of HIV's first targets hit during acute infection [8,9]. Early viral replication disrupts the gut epithelium and causes a dysregulation of epithelial cell homeostasis leading to microbial translocation and consequently to chronic inflammation [77,78]. The gut homing marker Integrin $\alpha_4\beta_7$ (A4B7) [79] plays a central role, as it actively binds HIV with high affinity and makes cells highly susceptible for HIV infection [80,81]. This receptor is also over-proportionately present on membranes of virions during early infection [82] and is furthermore associated with HIV acquisition and disease progression outcome [83]. Blocking of A4B7 in SIV infected monkeys lead to decreased susceptibility [84,85] or even viral control if combined with ART [86].

An important role for homing to secondary lymphoid organs has been described for the receptors CD62L and CCR7 expressed on peripheral immune cells. Their expression permit these cells to bind to receptors of the high endothelial venules, where different Integrin families are also expressed and involved in binding of these circulating cells, inducing trans-endothelial migration and eventually homing to Lymph nodes. [87,88]

A whole range of biomarkers has been linked to the persisting viral reservoir, among which CD32a is being discussed as prominent correlate [89], which is, however, still under debate [90–93]. For assessing the biomarker or cellular compartment contribution to "the true" viral reservoir *in vivo*, a plethora of assays that detect HIV DNA or RNA, viral proteins or extracellular viral products after viral outgrowth has been described (Figure 3). [94–98] However, one key limitation seems to be that ≥ 95% of all integrated proviral genomes appear to be

defective [70,99]. Thus the ultimate measure to proof if a cure approach was successful is the controlled analytical treatment interruption (ATI), which nevertheless needs careful considerations to not avertable harm patients.

FIGURE 3 HIV-1 molecular reservoir

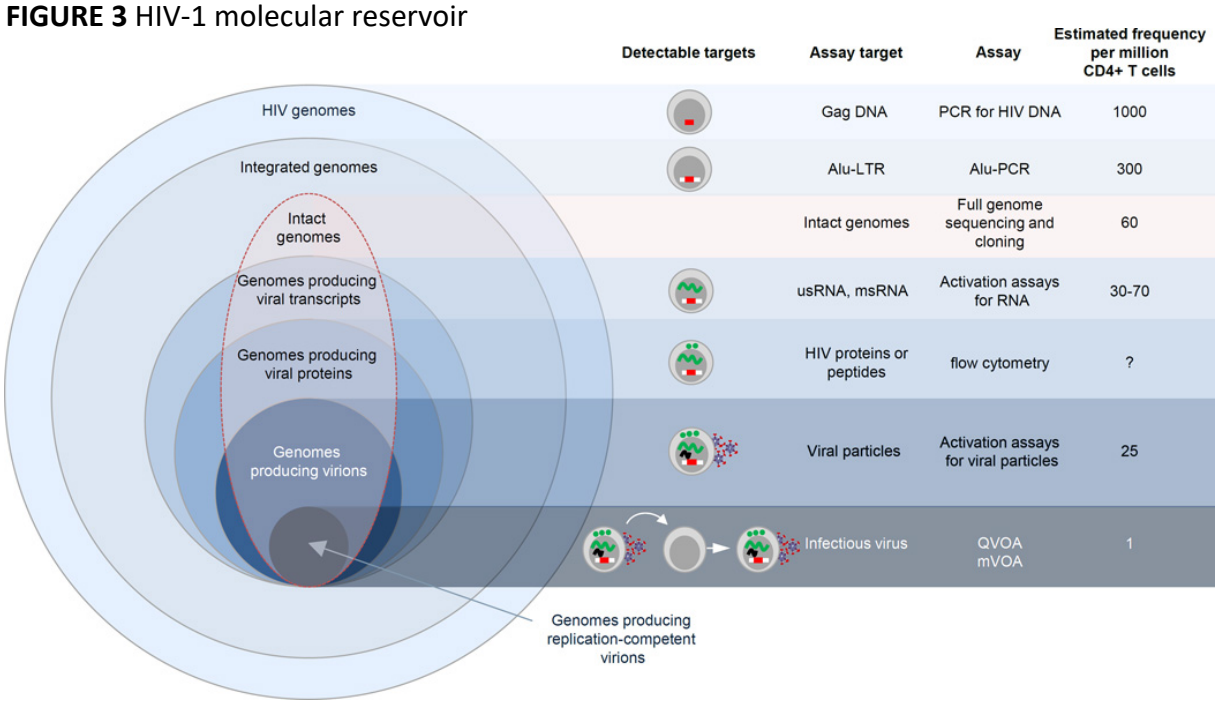

Figure 3. HIV-1 reservoir quantification assays. Hemispheric representation of each molecular level of HIV reservoir detection. Each assay is highlighted in individual colors with respective detectable target, assay target, name of assay and estimated frequency detected per million CD4+ T cells. Adapted from SG Deeks at el 2016 [165]

VI.3.4. New concepts of HIV treatment and cure approaches

In 2008 the Swiss statement [100] was released, which claimed that if HIV viral load (VL) durably remains below the detection limit in peripheral blood there is no risk of transmitting it to another HIV negative person by sexual intercourse. Until today this statement never got disproven [101,102]. Based on these findings, four years later the approval of PREP, with a combination of nucleoside reverse-transcriptase inhibitors (NRTIs) called TRUVADA® [103] paved the way for a new era of HIV prevention. High risk groups have now a greatly reduced hazard to contract HIV if PREP is taken as recommended prior to high risk exposures [104]. Even after risk exposure individuals have the option to use PEP within 72 h after potential exposition to HIV [105]. One innovative new concept of PREP or ART is becoming the usage of long-acting injectables using a combination of a very potent integrase strand transfer inhibitor (INSTI) and a NRTI that have the benefit of a single injection every 2 months opposed to the daily intake of ARV pills. It is non-inferior as PREP (HIV Prevention Trial Network (HPTN) 083 [106]) and has

special implications for settings, where people do not have easy access to treatments like in rural areas of developing countries.

Since 2009 another milestone in HIV treatment was set by the discovery of highly potent broadly neutralizing antibodies (bNAbs) [62,63,107–109]. These bNAbs are found in 1% of HIV positive individuals, referred to as “elite neutralizer”, and possess the ability to recognize a wide range of viral strains and binding these viruses with very high potency [110]. There are basically 5 epitopes for bNAbs to bind HIVs Envelope (Env) illustrated in Figure 4: the CD4 binding site, V1/V2 variable loop (Apex), V3 stem (high mannose patch), gp41-gp120 interface and membrane proximal external region of gp41 (MPER). In comparison to conventional ARVs, bNAbs can not only bind and neutralize viruses, but due to their antibody structure, they possess an Fc (fragment crystallizable) region that can be bound by other Fc receptor (FcR) expressing immune cells like phagocytes or natural killer cells (NKCs). Once the Fc part is bound by these immune cells, they can elicit active killing on cells expressing HIV Env antigens [111]. What still remains very challenging though is that most infectious proviruses remain latent and their host cells will thus not be recognized and cleared by bNAbs.

FIGURE 4 bNAb epitope mapping

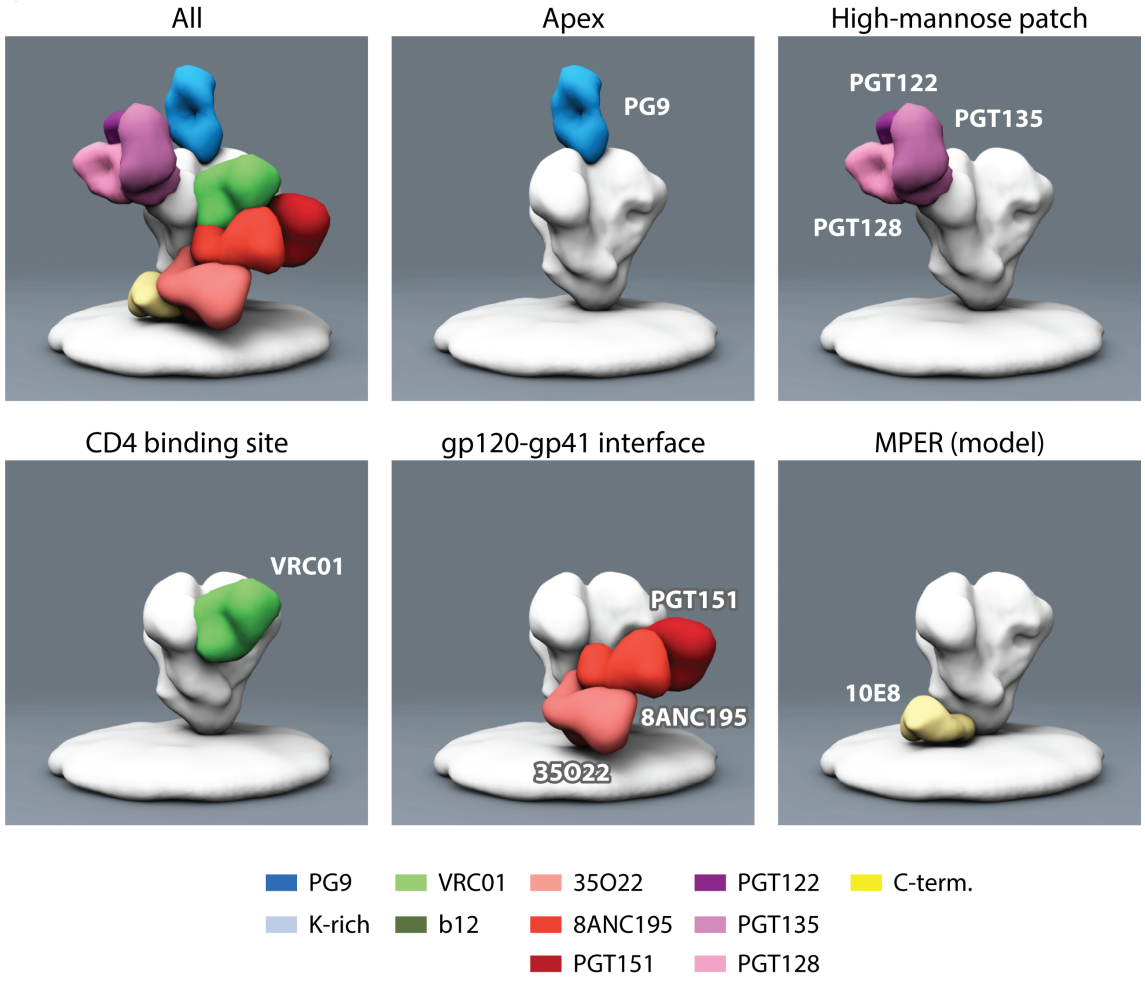

Figure 4. bNAb epitopes of HIV Envelope: Electron microscope illustration of individual bNAb epitopes and respective binding sites on the HIV Envelope trimer. Binding domains of exemplified bNabs are highlighted in respective colors. Adapted from DR Burton et al 2016 [112]

HIV latency is governed by multiple mechanisms like the site of proviral DNA integration [53,54], epigenetic modifications such as histone acetylation/ methylation and chromatin remodeling [113–115], cell intrinsic silencing responses [116] , impaired RNA transcription/splicing [117] or nuclear export [118].

A plethora of different latency reverting agents (LRAs) have been studied, like epigenetic modifiers, NFκB Agonists or T-cell receptor (TCR) activators to name only a few [119]. All efforts to reactivate virus and quantitatively clear infected cells in a so called “kick and kill” approach have nevertheless failed up to now [120].

Since the outbreak of the HIV endemic two successful cure approaches have been achieved by allogeneic hematopoietic stem-cell transplantation (HSCT) for the “Berlin” [121] and the “London” [122] patient, with the Dusseldorf patient likely becoming the third case [123]. All patients were HIV positive and suffered from hematological malignancies. For the “Berlin” and “London” patient, two main features were observed that might be responsible for the cure success: a) both had a donor homozygous for CCR5-Δ32, a very rare 32 base pair deletion in the CCR5 gene, causing the absence of CCR5 on the cell surface due to a protein truncation which is found in ~1% of the Caucasian population [124–126] (the Berlin patient had been heterozygous for the deletion) and b) both underwent graft versus host disease, indicating that the donor cells might have actively eliminated all remaining host cells [127]. Newest insights of a cohort of transplanted HIV positive individuals showed that especially after transplantation enhanced CD4 activation and anti-HIV CD8 responses can be detected, suggesting that it is very important to maintain ART after HSCT to avoid reseeding of the viral reservoir [128].

However, this intervention will not be an option for HIV positive individuals that harbor X4- or dual-tropic viruses, which do not exclusively rely on CCR5 co-receptor for cell fusion [129,130], as it was the case for the Essen patient [131]. Further, the manipulation is of high risk for a person’s health and can thus only be performed for HIV positive individuals suffering from malignancies that strictly require a HSCT.

Thus, future cure approaches need to address, where to find intact virus and how to target both R5- and X4-tropic viruses.

VII. Results

VII.1. Patient characteristics

Overall, 25 patients were enrolled for all experiments. Most of the participants were male (88 %), most of them being MSM (48 %), with a median age of 53 years, and 88 % were of white ethnicity. The median age at infection was 41 years with a median infection duration of 165 months. Baseline CD4 count was 433 cells/µL, corresponding to a median of 23% CD4+ Lymphocytes and a median ΔCD4 of 449, with a median HIV VL of 4.5 $\log_{10}$ copies/mL. Baseline CD8 count was 892 cells/µL, corresponding to a median of 53% CD8+ Lymphocytes. Baseline characteristics and characteristics for each individual experimental group are summarized in Table 1.

Table 1. Characteristics of patients at Baseline. Data are shown for all relevant experiments done for this project, wih subdivision for each approach. Delta CD4 is the absolute difference between lowest CD4 count and current CD4 count. Other encompasses all risk groups which are not separately defined like transgender or bisexuality. SD: standard deviation, IQR: interquartile range, MSM: men who have sex with men

Characteristic	**All patients (n=25)**	**Cell expansion (n=4)**	**pre-ART (n=4)**	**MACS (n=8)**	**GERDA (n=9)**
Sex					
Male	22 (88)	4 (100)	2 (50)	7 (87.5)	9 (100)
Female	3 (12)		2 (50)	1 (12.5)	
Age, median years ± SD	53 ± 13.4	53 ± 7.4	68.5 ± 9.9	55 ± 10.6	44 ± 8.9
Ethnicity					
White	22 (88)	4 (100)	3 (75)	6 (75)	9 (100)
Black	1 (4)			1 (12.5)	
Hispanic	2 (8)		1 (25)	1 (12.5)	
Risk group					
MSM	12 (48)	2 (50)	1 (25)	5 (62.5)	4 (44.4)
Heterosexual	8 (32)		3 (75)	3 (37.5)	2 (22.2)
Unknown	2 (8)				2 (22.2)
Other	3 (12)	2 (50)			1 (11.1)
Age at Infection, median years ± SD	41 ± 9.8	36.5 ± 4.7	54 ± 12.6	39 ± 8.4	42.0 ± 9.5
Duration of Infection, median months ± SD	165 ± 117.4	224.5 ± 82.0	185.5 ± 39.3	270 ± 107.5	9 ± 71.1
Baseline HIV RNA load (IQR) log_{10} copies/mL	4.5 (4.2-4.8)	4.2 (3.8-4.5)	4.3(4.2-4.4)	4.7(4.3-5.0)	4.5(4.3-5.0)
Delta CD4 T-cell count Cells/µL	449 (258-644)	451 (401-673)	523 (387-798)	647 (568-1132)	183 (46-274)
Baseline CD4 T-cell count (IQR), cells/µL	433 (304-523)	515 (397.5-594.3)	425 (297.3-521.5)	395 (292.5-580.8)	412 (304-511)
Baseline % CD4+ Lymphocytes (IQR)	23 (16-28)	27 (21.3-31.5)	24.7 (21.5-29.8)	20.5 (11.3-24.8)	23.2 (16-27)
Baseline CD8 T-cell count (IQR), cells/µL	892 (740-1156)	777 (660-858)	743.5 (533.8-958)	933.5 (725-1183.8)	1019 (772-1203)
Baseline % CD8+ Lymphocytes (IQR)	53 (45.3-64)	53 (42.8-63.3)	53.2 (41.7-62.3)	52 (45.5-64.5)	53 (46.6-64)

VII.2. MACS sorts on chronically infected SHCS samples

To get a first impression which lymphoid homing cells are more enriched for HIV DNA, arbitrarily chosen HIV-positive patient samples of peripheral blood from the Swiss HIV Cohort Study (SHCS) were separated by magnetic activated cell sorting (MACS). Cells were sorted in 3 subsequent selection steps: first irrelevant cytotoxic T-cells (CD8) and B-cells (CD19) were depleted and CD8-CD19- fractions were subdivided in CD4+ and CD4- cells. Both subdivided fractions were either selected for Integrin β_7 (gut homing) or CCR7 (lymph node homing). As shown in Supp. Figure 1 most fractions expressed the intended markers after enrichment. CD4+ cells were eliminated with an efficiency of 96% so that the CD8+CD19+ fractions only contained traces of CD4+ cells. This is also reflected in lower proviral loads compared to pre-sort conditions on the group and individual levels (Figure 5, 6). Integrin β_7 (gut homing) was chosen as surrogate antibody for Integrin $\alpha_4\beta_7$ since Integrin $\alpha_4\beta_E$ is mainly expressed in tissues and not in the periphery [132]. Only fraction β_7+CD4+CD8-CD19- yielded for all examined HIV positive individuals a proviral readout. This reading was for all tested candidates higher than the pre-separation condition, on an individual as well as fraction level (Figure 5, median 7897, vs 1219 p= 0.065, 95% CI [-0.066, 1.219]). Looking at CCR7 (Lymphoid/Lymph node homing) selected fractions the conditions with CCR7+CD4+CD8-CD19- (Figure 6, median 3664.5, p = 0.028, 95% CI [0.232, 2.071]) and CCR7-CD4+CD8-CD19- (Figure 6, median 6686, p= 0.173, 95% CI [-7382.253, 26028.753]) phenotypes demonstrate increased proviral levels compared to pre-sort conditions (median 341.5). For CCR7 as well as for Integrin β_7 no individual major fraction with highest proviral loads could be identified for any of the tested individuals. Furthermore, CD4 positive fractions have increased proviral loads compared to CD4 negative fractions, where proviruses can hardly be detected. Of note: The CD4-negative fraction should also include those cells, in which the HIV infection had led to a down-modulation of the CD4-receptor, which can be linked to the action of viral regulatory proteins Vpu [133] and Nef [134].

FIGURE 5 Proviral load of Integrin β_7+ PBMCS

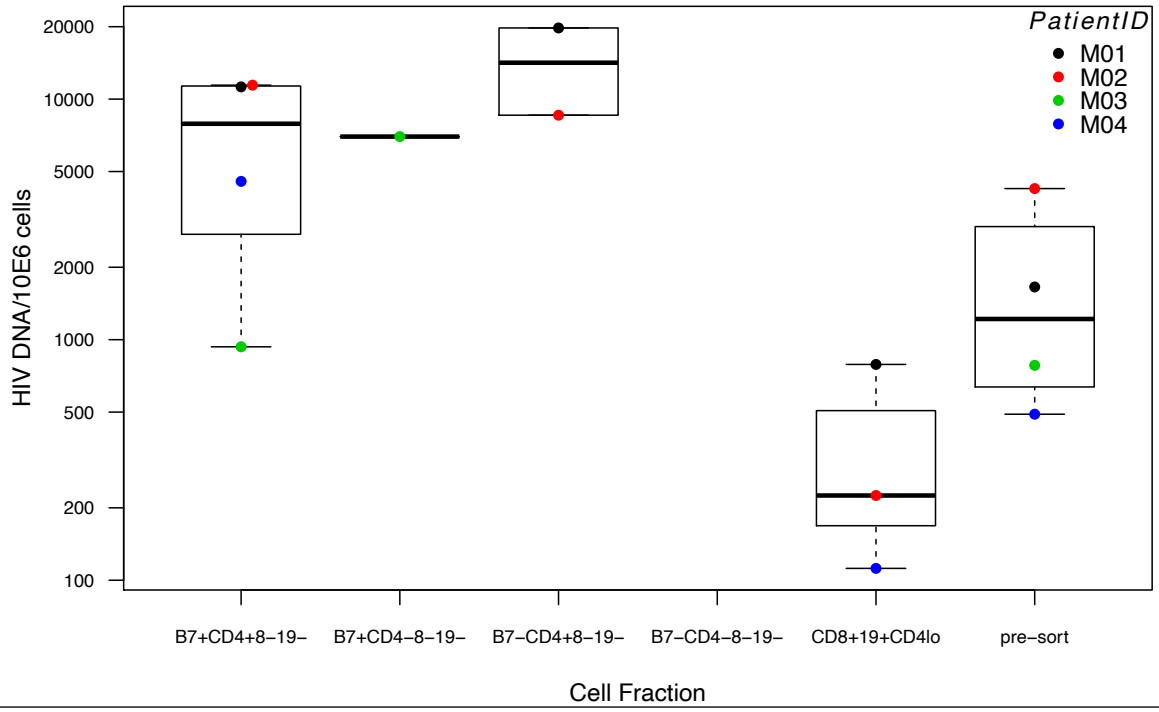

Figure 5. Proviral load of Integrin β_7 MACS selected PBMCs. Proviral loads are given as HIV DNA per 10E6 cells on the Y-axis. X-axis depicts identifier for each tested fraction. For comparison pre-sorted and CD4 depleted fractions are included. Patient IDs are given in Legend next to box plots

FIGURE 6 Proviral load of CCR7+ PBMCs

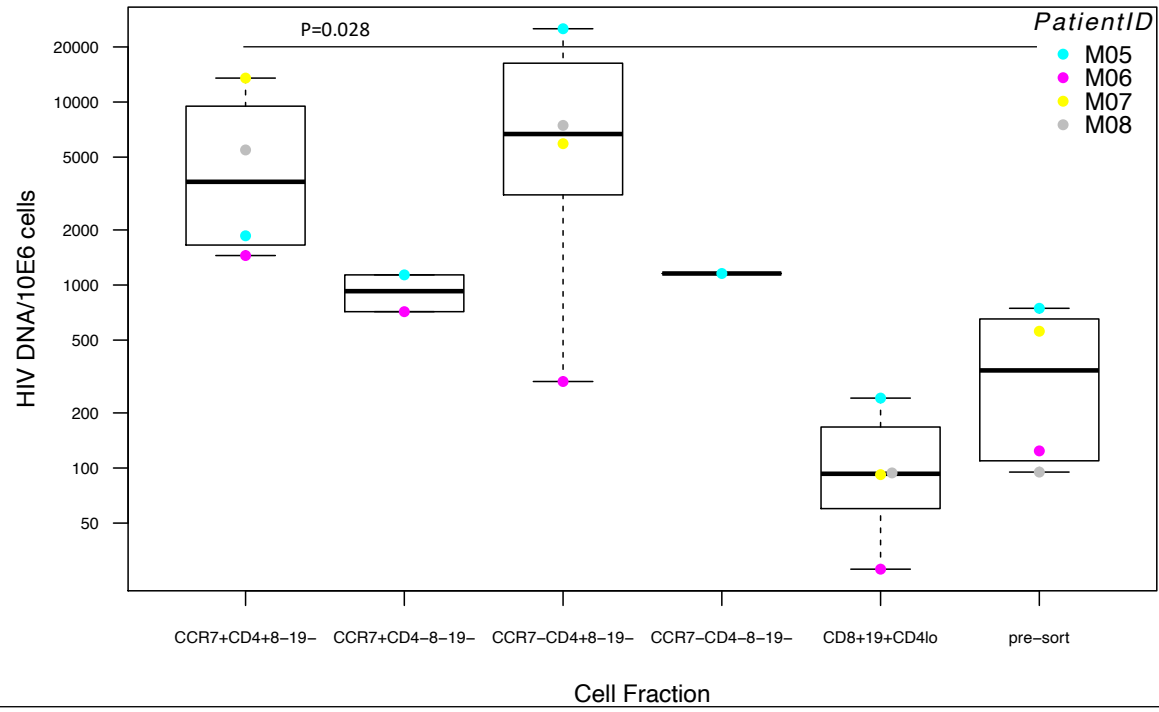

Figure 6. Proviral load of CCR7 MACS selected PBMCs. Proviral loads are given as HIV DNA per 10E6 cells on the Y-axis. X-axis depicts identifier for each tested fraction. For comparison pre-sorted and CD4 depleted fractions are included. Patient IDs are given in Legend next to box plots. Significant difference between fractions are indicated with p-value.

VII.3. FACS on fixed chronically infected SHCS samples

As the possible application range of consecutive selection steps for MACS was exhausted, further analysis were done by fluorescence-activated cell sorting/scanning (FACS) to widen the marker repertoire and to deepen the complexity and quality of the cell analysis.

Cell sorts of fixed PBMCs from chronically infected HIV positive individuals failed to retain representative proviral loads of distinct cell compartments like Integrin β_7+ memory cells or CCR7+ central memory cells (T_{CM}). This is linked to DNA shearing and loss of genetic material by fixative that needed to be added for Biosafety reasons (data not shown). Nevertheless, further analyses revealed that on average 95% of CD4+ Integrinβ_7+ memory cells also co-express CCR7 (n=4, data not shown). Vice versa only 18% co-express Integrin β_7 on TCM (n=4, data not shown). FACS sorts also unveiled that only 5% of CD4+ T-cells from peripheral blood are Integrin β_7+ memory cells which was also reported by others [83]. Hence further analysis would need higher volumes of blood to have a representative number of gut homing (memory) cells. Thus, to test if cell numbers can be propagated to a sufficient extent while retaining the original cell properties, bulk HIV neg PBMCs were stimulated for cellular expansion. Table 2 A-C highlights the marker alterations over 7 days. Elevated expression levels of the activation marker CD25 and diluted detection of the cell division marker Carboxyfluorescein succinimidyl ester (CFSE) corroborate successful expansion of bulk PBMCs. In comparison to the baseline FACS profile some markers, like CD3 or CD127 kept their relative contribution, whereas most other markers changed quite drastically, like CD45RA (important for naïve/memory compartment allocation) or Integrin β_7 (gut homing).

Table 2. Marker expression after cell expansion for HIV negative PBMCs. A: Day 1 post stimulation marker profile. B: Day 3 post stimulation marker profile. C: Day 7 post stimulation marker profile (note: CD28 was not stained here). For all timepoints baseline marker profile was included for comparison (CD8 stain was not examined here). All markers are shown as percentage of Live Lymphocytes. To see individual differences among stimulation conditions, rows were highlighted with heatmap colors ranging from low (blue) to high (yellow) expression. Group mean and SD (standard deviation) are depicted at the bottom of each column.

A

	%CCR6+ Live	%CCR7+ Live	%CD3+ Live	%CD4+ Live	%CD8+ Live	%CD25+ Live	%CD28+ Live	%CD45RA+ Live	%CD127+ Live	%CFSE- Live	%B7+ Live
HIV neg PBMC_Miltenyi_018.fcs	29.3	34.6	49.0	33.7	13.3	31.9	43.2	32.7	23.7	36.3	19.5
HIV neg PBMC_PHA_017.fcs	29.8	66.9	80.4	57.7	17.5	67.3	73.8	49.7	34.0	2.25	26.5
HIV neg PBMC_SCT 25_019.fcs	25.5	58.5	2.37	44.2	30.7	63.8	2.13	45.4	30.7	0.70	27.2
HIV neg PBMC_SCT 50_020.fcs	27.7	58.2	4.80	43.8	30.3	67.4	2.32	48.7	31.9	1.02	29.3
HIV neg PBMC_baseline_015.fcs	24.3	43.7	74.5	38.4	0.64	0.94	58.5	48.8	54.4	0.40	31.5
HIV neg PBMC_unstimulated_016.fcs	32.0	59.4	79.3	57.1	15.3	15.6	68.5	51.4	40.2	0.76	38.2
Mean	*28.3*	*53.3*	*48.5*	*45.7*	*18.2*	*41.0*	*41.2*	*46.3*	*35.8*	*6.89*	*28.7*
SD	*2.68*	*10.9*	*33.4*	*8.92*	*10.4*	*26.6*	*29.3*	*6.29*	*9.63*	*13.2*	*5.63*

B

	%CCR6+ Live	%CCR7+ Live	%CD3+ Live	%CD4+ Live	%CD8+ Live	%CD25+ Live	%CD28+ Live	%CD45RA+ Live	%CD127+ Live	%CFSE- Live	%B7+ Live
HIV neg PBMC_Miltenyi_019.fcs	18.0	52.9	51.2	30.0	18.6	42.5	44.2	25.7	42.7	84.0	35.1
HIV neg PBMC_PHA_018.fcs	24.5	81.4	79.4	46.6	23.8	73.5	69.6	36.0	55.3	75.4	61.1
HIV neg PBMC_SCT 33_020.fcs	18.5	76.1	3.86	35.3	29.5	71.4	12.3	23.8	47.7	66.1	55.5
HIV neg PBMC_SCT 66_021.fcs	20.5	66.8	16.5	30.7	32.1	65.9	19.5	26.2	42.2	63.6	49.2
HIV neg PBMC_baseline_015.fcs	24.3	43.7	74.5	38.4	0.64	0.94	58.5	48.8	54.4	0.40	31.5
HIV neg PBMC_unstimulated_017.fcs	20.9	65.0	76.5	51.4	21.7	9.95	63.8	55.2	45.8	20.1	49.1
Mean	*21.1*	*64.3*	*50.5*	*39.8*	*21.0*	*43.4*	*45.6*	*36.1*	*47.9*	*51.1*	*47.3*
SD	*2.54*	*12.9*	*30.1*	*8.43*	*10.2*	*29.3*	*22.0*	*12.1*	*5.18*	*30.5*	*10.6*

C

	%CCR6+ Live	%CCR7+ Live	%CD3+ Live	%CD4+ Live	%CD8+ Live	%CD25+ Live	%CD28+ Live	% CD45RA+ Live	% CD127+ Live	%CFSE- Live	%B7+ Live
HIV neg PBMC_Miltenyi_016.fcs	17.9	66.5	81.7	32.3	42.0	71.5	0.12	7.12	39.0	98.0	85.9
HIV neg PBMC_PHA_015.fcs	18.2	69.3	90.0	54.7	30.8	71.4	0.11	14.2	46.9	99.4	90.1
HIV neg PBMC_SCT 33_017.fcs	17.0	86.8	83.2	56.6	28.1	90.5	0.22	14.8	51.5	98.3	94.4
HIV neg PBMC_SCT 66_018.fcs	19.3	88.2	86.6	60.6	27.9	91.0	0.25	11.1	57.7	98.8	94.6
HIV neg PBMC_baseline_015.fcs	24.3	43.7	74.5	38.4	0.64	0.94	58.5	48.8	54.4	0.40	31.5
HIV neg PBMC_unstimulated_014.fcs	24.9	34.5	75.3	38.6	33.4	37.7	0.093	25.2	38.8	90.9	71.5
Mean	*20.3*	*63.3*	*82.5*	*47.3*	*27.3*	*60.5*	*9.96*	*20.1*	*48.1*	*80.9*	*78.0*
SD	*3.14*	*20.5*	*5.81*	*10.8*	*12.8*	*32.0*	*21.7*	*13.9*	*7.24*	*36.1*	*22.2*

Moreover, the stimulation potency of PHA versus T-cell receptor stimulating antibodies (CD3, CD28 and CD2) could be directly compared. PHA and the antibody cocktail of STEMCELL® Technologies had the fastest activation kinetics based on CD25 upregulation and CFSE dilution. However, it should be noted that excessive CD3/CD28 activation antibodies occupy CD3/CD28 epitopes, which cannot be bound by fluorescent CD3/CD28 staining antibodies as seen for Table 2 A, B and Table 3 A, B. The antibody system of Miltenyi Biotec had a distorted CFSE stain and only moderate activation kinetics. Therefore, the Miltenyi system was excluded for further experiments.

To rule out that HIV reactivation might have an impact on marker expression, PBMCs of 4 HIV positive individuals were also expanded for 7 days. Like for HIV negative samples baseline

and day 3 samples were almost identical. But for expansions for up to one week, markers like CD4, CD8, CD127, Integrin B7 and CCR7 had changed significantly.

Table 3. Marker expression after cell expansion for HIV positive PBMCs. A: Baseline marker profile. B: Day 3 post stimulation marker profile. C: Day 7 post stimulation marker profile. All markers are shown as percentage of Live Lymphocytes. To see individual differences among stimulation conditions, rows were highlighted with heatmap colors ranging from blue (low) to yellow (high) expression. Group mean and SD (standard deviation) are depicted at the bottom of each column.

A

	% CD3+	% CCR6+	% CCR7 +	% CD4+	% CD8+	% CD25+	% CD45RA+	% CD127+	% CD28+	% Integrin B7 +
Pat_251	83.0	5.54	61.2	45.1	31.1	9.69	41.7	63.4	66.7	57.1
Pat_252	82.0	6.33	56.3	55.8	16.9	7.98	42.1	71.1	7.72E−3	27.1
Pat_269	76.7	11.9	51.2	58.6	12.0	9.91	46.5	58.4	58.0	9.01
Pat_271	68.3	11.6	51.1	49.1	23.0	8.15	53.3	60.0	57.4	22.0
Mean	***77.5***	***8.84***	***54.9***	***52.1***	***20.8***	***8.93***	***45.9***	***63.2***	***45.5***	***28.8***
SD	***6.73***	***3.37***	***4.82***	***6.16***	***8.24***	***1.01***	***5.39***	***5.65***	***30.6***	***20.3***

B

	% CD3+	% CCR6+	% CCR7+	% CD4+	% CD8+	% CD25+	% CD45RA+	% CD127+	% CD28+	% Integrin B7+
day 3_251	92.2	9.12	59.8	32.4	45.1	66.9	59.4	68.4	55.1	78.0
day 3_252	87.4	6.27	57.1	43.3	37.6	52.7	58.2	69.8	61.4	48.4
day 3_269	82.1	13.7	63.9	48.2	20.8	61.5	65.8	67.2	56.8	39.4
day 3_271	82.7	10.8	71.0	35.1	50.0	69.3	62.9	74.5	56.7	59.9
Mean	***86.1***	***9.97***	***63.0***	***39.8***	***38.4***	***62.6***	***61.6***	***70.0***	***57.5***	***56.4***
SD	***4.71***	***3.11***	***6.05***	***7.29***	***12.8***	***7.36***	***3.45***	***3.20***	***2.71***	***16.7***

C

	% CD3+	% CCR6+	% CCR7+	% CD4+	% CD8+	% CD25	% CD45RA+	% CD127+	% CD28+	% Integrin B7+
day7_251	93.9	9.54	28.9	16.9	74.9	72.7	31.7	30.4	59.0	97.9
day7_252	95.0	17.2	33.2	27.8	65.3	79.4	25.5	40.3	62.7	94.3
day7_269	94.9	13.3	42.4	27.6	66.1	77.6	34.9	47.7	66.3	90.7
day7_271	95.7	10.4	57.3	18.6	76.1	77.8	38.2	23.3	38.2	94.0
Mean	***94.9***	***12.6***	***40.5***	***22.7***	***70.6***	***76.9***	***32.6***	***35.4***	***56.5***	***94.2***
SD	***0.74***	***3.46***	***12.6***	***5.79***	***5.69***	***2.90***	***5.41***	***10.8***	***12.6***	***2.94***

The FACS profiles of the expanded cell cultures provided fundamental information about receptor kinetics during cellular stimulation and further allowed to clarify which stimulant to use to optimize culture conditions for upcoming cell stimulation experiments.

VII.4. Establishment of the GERDA methodology

Extensive expansion (≥ 7 days) showed for some markers quite drastic changes, while short stimulation intervals (< 2 days) of cells did not significantly affect the marker landscape too much. Based on the issues with viral reservoir detection methods mentioned in IV.3.3. introductory Figure 3, a method termed GERDA (Gag and Envelope Reactivation Detection Assay) able to precisely detect what is referred to as "the real viral reservoir" was established by assessing immunological, viral and lymphoid homing markers of circulating blood cells (Supp. Fig. 2). Most currently available assay systems detect either viral transcription products or a single HIV-1 protein (mostly p24 Gag), which leads to the sensitive determination of cells that might contain intact proviruses while these assays also lack the ability to exclude defective proviruses, i.e. those carrying besides others large internal deletions, inversions or APOBEC3G/F-mediated hypermutations. The objective of the newly established GERDA approach described here, is to shortly (36h) stimulate CD4 pre-selected cells, which subsequently reactivates dormant proviruses that can than start to produce viral proteins. To allow for an accurate approximation of "the real viral reservoir" in PBMCs detection of intracellular (IC) HIV-1 Gag expression was combined with extracellular (EC) HIV-1 Envelope presentation by using highly potent and broadly neutralizing antibodies. Herein the Gag detection allows to judge if cells are able to produce particles, while Envelope will further allow to address if these released virions possess the viral Env-spikes as indicator for infectivity.

Supp. Fig. 2 highlights the principal workflow. It requires a lower number of input cells and less hands-on time compared to other FACS techniques [97,135]. Furthermore, a semi-automated computational analysis approach was used to minimize the bias in data interpretation. For validating the staining procedure, it was first tested if in a mix of HIV-positive and -negative cells each population can be identified. For this, chronically infected (HUT4-3 [136]) cells were serial diluted in uninfected Lymphocytes (SupT1) at predefined concentrations in log steps. Cells were co-stained with CD4, gating the CD4-negative HUT4-3 and CD4-positive SupT1 cells (depicted in Supp. Fig. 3 A, B, Supp. Fig. 4 D, E). As shown in Figure 7 A, cells gated as HUT4-3 localized as distinct, HIV Gag and Env double positive (DP) population in green in the second quadrant (Q2) of the Contour plot, while uninfected SupT1 cells located to the double negative (DN) quadrant Q4, in cyan. Gag and Envelope expression showed a high correlation ($R=0.66$, $p<2.2X10^{-16}$, Supp. Fig. 3 C).

FIGURE 7 GERDA establishment

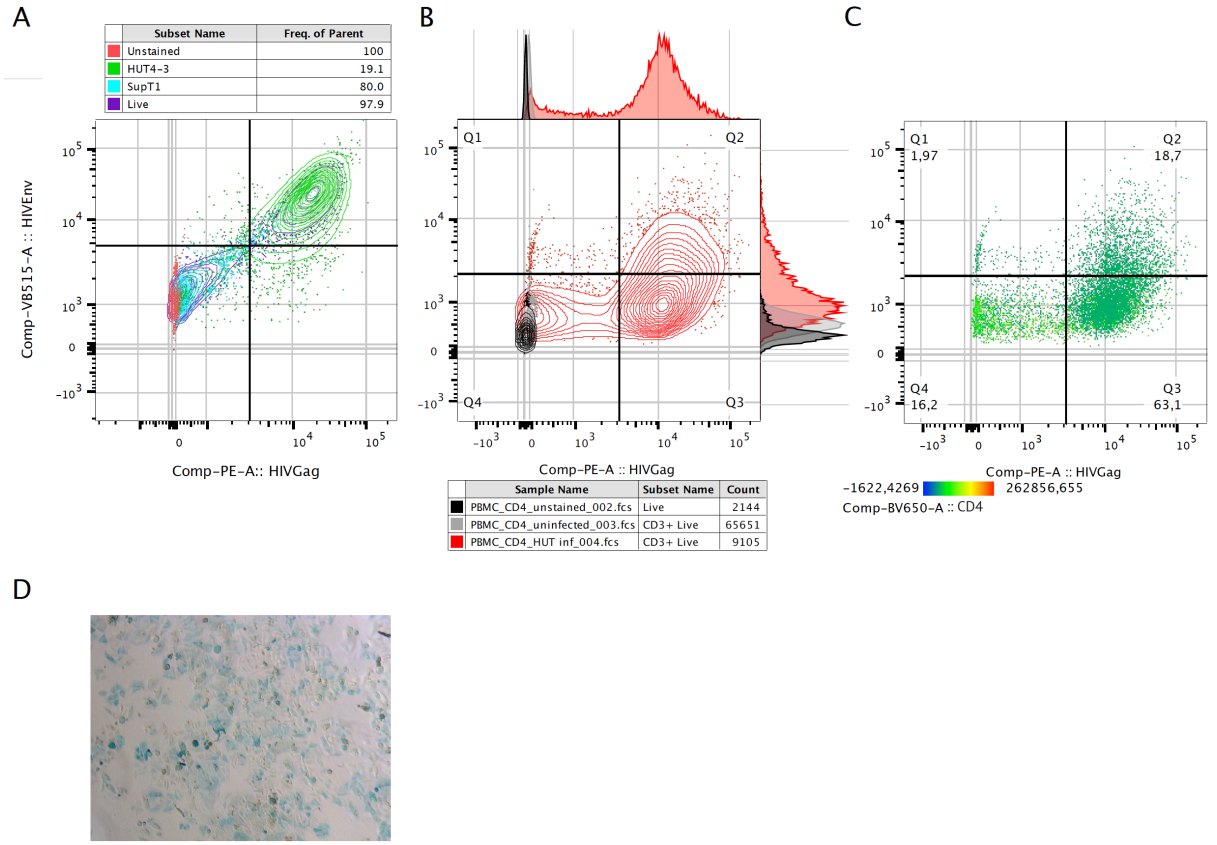

Figure 7. GERDA staining establishment. A: HIV Gag / Env staining on a mixed pool of infected (HUT4-3: green) and uninfected (SupT1: cyan) cells. B: HIV Gag/Env staining of infected CD4+ T-cells (red) in comparison to unstained (black) and uninfected (grey) controls. C: CD4 expression heatmap of HUT4-3 virus infected CD4+ T-cells. D: X-Gal assay of viral supernatant from infectious CD4+ PBMCs 6 dpi examined in Fig.7 B. Blue cells show individual infection events.

Next either SupT1 cells or PHA-pre-stimulated, HIV negative PBMCs were used for infection with several cell-free HIV-1 strains: NL4-3_X4, LAI_X4, Ala-1_X4, Mal-2_R5 to cover various HIV-1 subtypes and tropisms as indicated. To verify that DP cells permit the production of infectious viral particles, culture supernatant containing maturated viruses from infected cells, was then applied to SX-R5 [137] indicator cells with a highly sensitive HIV LTR promoter-dependent X-Gal readout. As illustrated in Figure 7 B and Supp. Fig. 5 A, the infections of either cell type yielded the expected levels of double positive cells for all HIV subtypes and of X4- or R5-tropism (Supp figures 5 M-R). The LTR-driven blue staining of cells in the X-Gal assay confirms the presence of intact and infectious virus particle progeny (Fig 7 D; Supp Fig. 5 E, J, O, Q, R). Of note, in all DP cells CD4 expression became downmodulated (Fig. 7 C; Supp. Fig. 5B), in contrast to the uninfected controls (Supp. Fig. 5 I, N), attributable e.g. to the action of viral Vpu [133] and Nef [134].

FIGURE 8 Sensitivity of the GERDA system

A

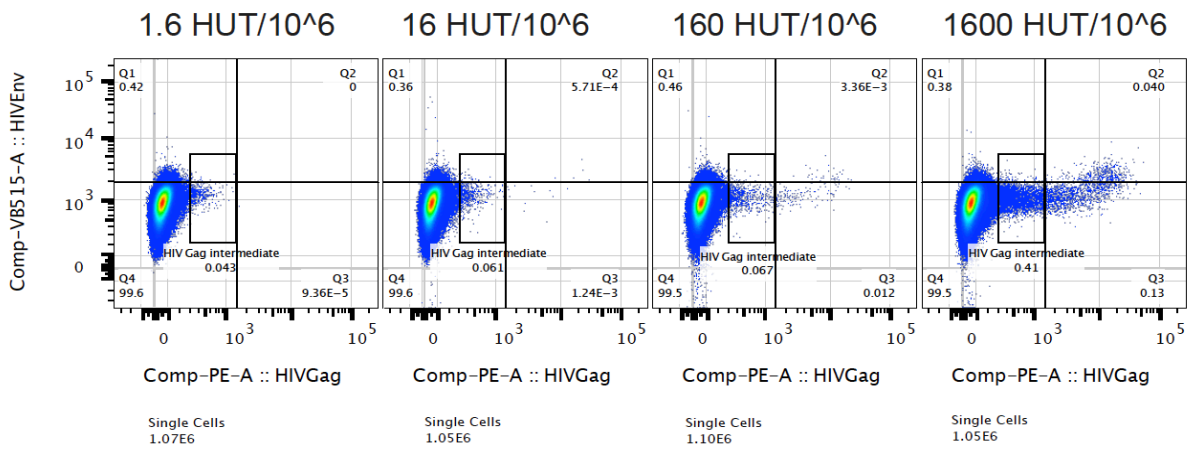

B

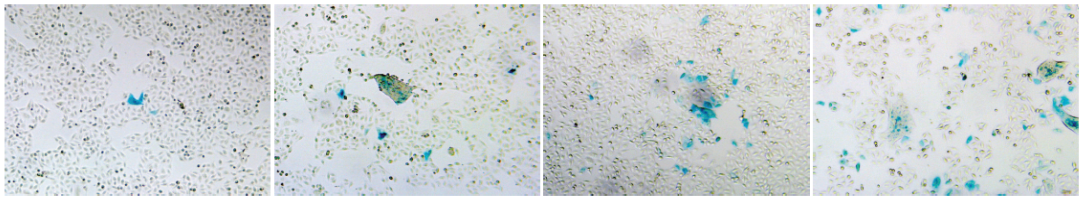

C

	# HIV Gag+/ Env+	HIV Gag+/ Env+ [%]	# HIV Gag+/ Env-	HIV Gag+/ Env- [%]	# HIV Gag+	HIV Gag+ [%]
HUT-SupR5_1.6in10E6_024.fcs	0	0	1.00	9.36E-5	1.00	9.36E-5
HUT-SupR5_16in10E6_024.fcs	6.00	5.71E-4	13.0	1.24E-3	19.0	1.81E-3
HUT-SupR5_160in10E6_025.fcs	37.0	3.36E-3	129	0.012	166	0.015
HUT-SupR5_1600in10E6_026.fcs	421	0.040	1324	0.13	1745	0.17

D

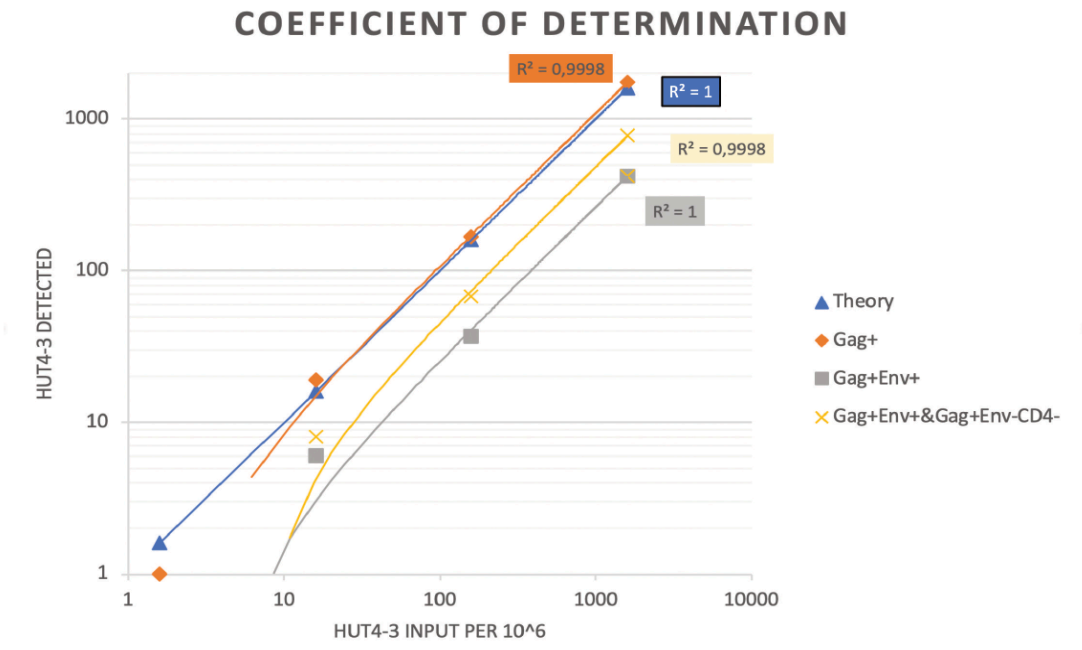

Figure 8. GERDA sensitivity. Titration of infected HUT4-3 cells into uninfected SupT1 cells. A: Gag vs Env expression plots of log dilutions. Intermediate Gag events are boxed. Respective conditions are labelled on top of graph. B: X-Gal staining of respective titration steps. Blue cells show individual infection events. C: Table of quantities and percentage of HIV Gag+, HIV Gag+Env+ or HIV Gag+Env- events detected. D: Linearity of detection for HIV Gag+, HIV Gag+Env+ or combination of HIV Gag+Env+ and HIV Gag+Env-CD4- (potential HUT4-3) events.

As further demonstration of the robustness of the SXR5 readout system, a comparison with the international standard TZM-bl cell line (Tranzyme Inc., Birmingham, Ala. (X. Wu et al., unpublished data)) revealed an excellent correlation (Supp Fig. 5 F, K). For evaluating assay sensitivity and specificity, a precisely defined number of infected HUT4-3 cells was spiked into uninfected SupT1 cells (Fig 8 A, B). Half of the cells were either used for GERDA or for X-Gal staining. Co-staining demonstrated a very consistent detection down to 16 copies shown in Figure 8 C (Gag+Env+ detected $6/10^6$, R^2 0.998; Gag+ detected $19/10^6$, R^2 1), confirming high sensitivity of the GERDA system ready to be tested on HIV positive samples.

VII.4.1. Immune characterization of recently diagnosed HIV patients

It has been shown that cells circulating in the peripheral blood possess different properties and can transiently originate from distant compartments and immunological organs [67,74,79,87,88]. To examine the viral reservoir in peripheral blood, it was aimed at determining the identity of infected cells by determining immunological, viral and lymphoid homing markers of circulating cells in venous blood. For clearer presentation of multi-dimensional data sets t-distributed stochastic neighbor embedding (t-SNE) [138,139] and Density-Based Spatial Clustering of Applications with Noise (DBSCAN) [140] were introduced for DP infectious cell cluster identification. t-SNE reduces high dimensional data into two-dimensional t-SNE space and clusters all cells that have very similar properties, i.e marker composition, close to each other in reduced 2D space. For more refined clustering DBSCAN identifies further sub clusters inside 2D t-SNE space. To compare the validity of the GERDA system, it was compared to proviral loads as a crude estimate of the viral reservoir as well as HIV poly-adenylated transcripts (poly-A) as proxy for completion of transcription/protein translation.

Utilizing the sensitive GERDA method cryo-preserved PBMC of pre-ART samples from HIV-infected individuals were analyzed. Control experiments with Isotype controls (Supp. Fig. 6 A, B) and uninfected controls (Supp. Fig. 6 M) were used to set Gag/Env thresholds. Due to low cell counts, samples were pooled and barcoded from several individuals who presented with high proviral loads at an early time point during therapy [17,141] to have a more comprehensive analysis. As illustrated in Fig. 9 A, as little as ~70 infected cells per 10E6 CD3+ viable CD4 T-cells were detectable, with significant correlation of Gag and Env signals (R=0.34, p=0.017, Supp Fig. 6 D). Marker profiles of biologically relevant identified clusters are shown in Supp. Figure 7 H-K, summarized by a heatmap in Supp Fig 6 L. DBSCAN identified DP clusters of

different differentiation status (cluster 386: T_{CM}, cluster 189, 153 & 97: T_N, cluster 141: T_{EM}) with differential CD4 expression levels, higher degrees of exhaustion (PD1+) and gut homing potential (Integrin β_7+). This finding is well in line with classical gating (Supp Fig. 6 C). Due to lower cell recovery from cyro-preserved specimens, the starting material was at first scaled up and higher volumes of fresh blood from patients diagnosed within 6-18 months were examined but did not show any viral activities after stimulation (see Patient P01 in Table 4 as example). Thus, sample selection was shifted to recently diagnosed (1-4 weeks), consenting individuals, anticipating a higher proportion of circulating cells with enhanced viral activity in this patient group. In line with proviral load and poly-A HIV transcripts (4'412 /10E6 PBMCs and 85'033/10E6 PBMCs, respectively, Table 4) the highest number of Gag+ (480/10E6 CD3+ viable CD4 T-cells) and Gag+Env+ DP cells (140/10E6 CD3+ viable CD4 T-cells) was found for individual P03, as shown in Figure 9 B, and DP cells show a close correlation for both markers ($R=0.44$, $p=0.14X10^{-11}$, Supp. Fig. 6 P). Using dimension reduction and unbiased clustering (Fig 9 D, E; Supp Fig. 6 Q), major contribution of T_{CM} pools was observed (Fig. 9 F-H, clusters 100, 160, 166) as the main viral reservoir in this individual. The harvested infected cells were mainly CD4+, had high levels of cell exhaustion (PD1+) and no or very little gut homing potential (Integrin β_7+).

While for most individuals, virus was detectable in the periphery, only a small number of Gag/Env DP events were detected in the respective samples (median 6/10E6 CD3+ viable CD4 T-cells), which is also in line with proviral (median 276/10E6 PBMCs) and HIV transcription data (median 1'379/10E6 PBMCs) (see also Table 4). Using very early sampling time-points, the findings corroborated that viral activity rapidly declines after initiation of ART as demonstrated for individual P03 by GERDA (HIV Gag+Env+ 2/10E6 CD3+ viable CD4 T-cells), proviral load (1'297/10E6 PBMCs) and HIV transcript load (418/10E6 PBMCs) over time (Fig 9 C, Table 4). Same dynamics are seen for most individuals when looking at proviral loads over time (Figure 6). The only exceptions are P05 and P07, which are both late presenters and might therefore have fluctuating proviral loads. For P02 only one timepoint was available for HIV DNA load determination after therapy drop-out, which was also the case for individuals P06 and P09.

Proviral load dynamics show a trend of decreasing numbers of integrated HIV DNA (Figure 10), which is in line with decreased HIV poly-A transcripts and decreasing DP events. These data are also consistent with the approximations shown in Figure 3 stating that the deeper

these assays measure the less activity is found, indicating that sample selection is very relevant to find especially for the GERDA system viral productive cells.

FIGURE 9 GERDA applied on recent HIV-1 diagnosed individuals

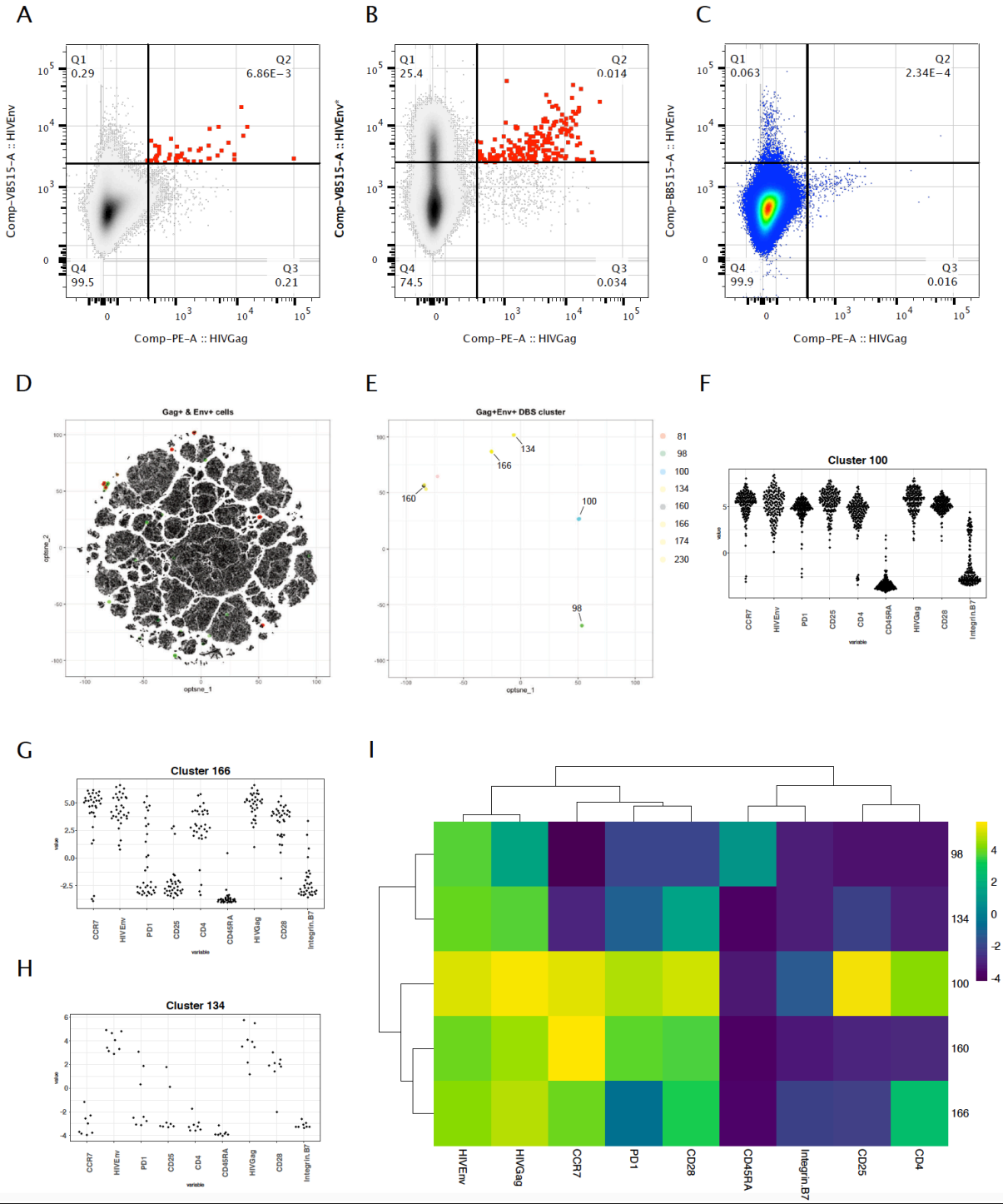

Figure 9. GERDA staining on PBMCs of HIV-1 infected individuals. Cells were pre-gated on CD3+CD19-CD8- viable cells. A,B: Gag vs Env expression of cryo-preserved PBMCs from infected individuals before ART initiation (A) or from one recently diagnosed ART naïve individual (P03) (B). DP-stained cells are highlighted in red. C: Gag vs Env expression of 53-day follow-up sample of recently diagnosed individual P03. D, E: t-SNE plots of first timepoint of individual P03. Each dot represents one cell as single data point (1.41E106 cells in total). Highlighted are all Gag+ (green) and Gag+Env+ (red) populations (D) or only DBSCAN clusters of just Gag+Env+ cells (E). F-H Individual cell marker expression profiles of representative DBSCAN cluster as indicated in Figure 4 E. I: Marker expression heatmap of all identified biologically relevant clusters. X-axis shows examined marker, y-axis depicts cluster ID. Scale next to plot highlights heatmap gradient color of low (blue) to high (yellow) marker expression.

FIGURE 10 Proviral dynamics after diagnosis

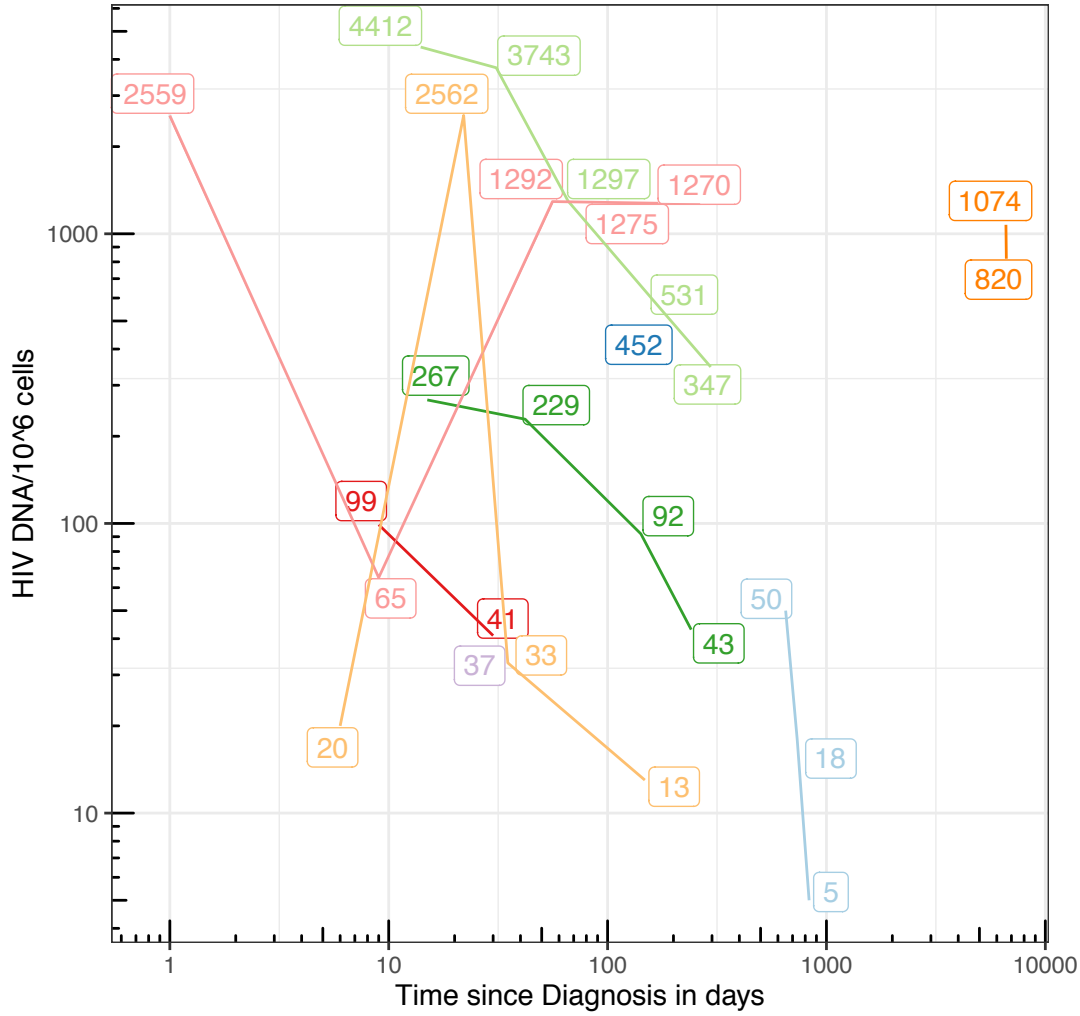

Figure 10. Proviral dynamics over time. Proviral loads of different timepoint after diagnoses were determined. X-axis depicts time in days since diagnosis (log), y-axis corresponds to HIV DNA per 10E6 cells (log). Each individual proviral measurement is indicated next to curves. Patient ID is given in legend next to plot.

Table 4. Summary table of Patient related clinical data. RNA VL, CD4 cell count, % CD4 of Lymphocytes and recency were provided by the SHCS databank. All other data were obtained from own experiments. [a] not performed; [b] no sample available; [c] re-initiation of ART; [d] first ART initiation

Patient ID	Timepoint	Days since ART start	RNA VL (c/mL)	CD4 (cells per µL)	% CD4+ of Lymphocytes	HIV DNA/ 10E6	HIV DNA/10E6 CD4	HIV Poly-A/10E6	HIV Poly-A /HIV DNA	GERDA Gag+Env+ events (%)	Recency/ History
P01	TP1	531	0	506	32	ND	-	ND	-	0	> 1 year, delayed sampling
	TP2	629	NA[a]	NA[a]	NA[a]	50	-	NA[a]	NA[a]	0	
	TP3	713	0	513	27	18	67	NA[a]	NA[a]	NA[a]	
	TP4	811	NA[a]	NA[a]	NA[a]	5	-	ND	-	NA[a]	
P02	T1	0	15'665	412	28	452	1'614	169	0.37	7 (3.45E-4)	NA
P03	TP0	-11	867‘496	NA[a]	NA[a]	NA[b]	-	NA[b]	NA[b]	NA[b]	1st year of infection
	TP1	0	143‘033	511	16	4'414	27'588	85'033	19.26	204 (0.014)	
	TP2	17	2‘553	NA[a]	NA[a]	3'743	-	NA[a]	-	NA[a]	
	TP3	52	142	807	32	1'297	4'053	418	0.32	4 (2.34E-4)	
	TP4	168	84	761	40	531	1'328	ND	-	NA[a]	
	TP5	296	NA[a]	NA[a]	NA[a]	347	-	ND	-	NA[a]	
P04	TP0	-1	28‘427	1‘310	40	NA[b]	-	NA[b]	NA[b]	NA[b]	Acute
	TP1	12	90	1‘928	50	276	552	ND	-	3 (1.8E-4)	
	TP2	39	0	1‘224	42	229	545	ND	-	9 (5.24E-4)	
	TP3	139	0	1‘901	43	92	214	NA[a]	NA[a]	NA[a]	
	TP4	241	NA[a]	NA[a]	NA[a]	43	-	NA[a]	-	NA[a]	
P05	TP0	0	43‘064	65	4	2'559	63'975	22'631	8.84	NA[b]	Late presenter
	TP1	8	NA[a]	NA[a]	NA[a]	65	-	ND	-	6 (0.041)	
	TP2	14	150	NA[a]	NA[a]	NA[b]	-	NA[b]	NA[b]	NA[b]	
	TP3	55	0	123	6	1'983	33'050	ND	-	19 (0.057)	
	TP4	170	0	103	8	1'275	15'938	1'129	0.89	NA[a]	
	TP5	261	NA[a]	NA[a]	NA[a]	1270	-	-	NA[a]	NA[a]	
P06	TP0	-9	113‘370	599	23	NA[b]	-	NA[b]	NA[b]	NA[b]	1st year of infection
	TP1	0	50‘666	472	21	99	471	ND	-	3 (6.43E-4)	
	TP2	21	NA[a]	NA[a]	NA[a]	41	-	NA[a]	NA[a]	0	
P07	TP0	-21	7'670	433	26	NA[b]	-	NA[b]	NA[b]	NA[b]	Late presenter
	TP1	-15	4'808	322	25	20	80	ND	-	5 (1.78E-3)	
	TP2	1	NA[a]	NA[a]	NA[a]	2'562	-	NA[a]	NA[a]	4 (2.02E-2)	
	TP3	14	0	NA[a]	NA[a]	33	-	ND	NA[a]	NA[a]	
	TP4	127	0	630	28	13	46	ND	-	NA[a]	
P08	TP0	0[c] (6'604)[d]	555‘625	20	4	NA[b]	-	NA[b]	NA[b]	NA[b]	Diagnosed 2002, 2020 555‘625 VL
	TP1	12[c] (6'616) [d]	9‘450	53	6	1'074	17'900	1'628	1.52	19 (0.21)	
	TP2	39[c] (6'643) [d]	NA[a]	NA[a]	NA[a]	820	-	4'368	5.33	10 (8.7E-4)	
P09	TP0	14	305	649	23	NA[b]	-	NA[b]	NA[b]	NA[b]	> 1 year
	TP1	42	NA[a]	NA[a]	NA[a]	37	-	670	18.11	NA[a]	

VII.4.2. GERDA applied to viral outgrowth assay

To demonstrate the capability of the GERDA system to detect traces of viral infectivity during viral outgrowth with high sensitivity, the new method was tested in combination with the X-Gal assay [137] in a viral outgrowth format. Cells from the blood of HIV-infected individuals were CD4 preselected and sorted into their respective memory compartment to separate cells of different origin. Cell fractions were then stimulated with a cocktail of antibodies directed against CD3, CD28 and CD2 to reactivate putative latent viral genomes. After 14 days of cultural expansion, the GERDA system solidly detected viral replication events (Fig. 11 A), which were confirmed by LTR-X-Gal-reactive events in parallel cultures (Fig. 11 B), indicating induced viral propagation over time (Supp Fig. 7 C).

FIGURE 11 GERDA vs QVOA

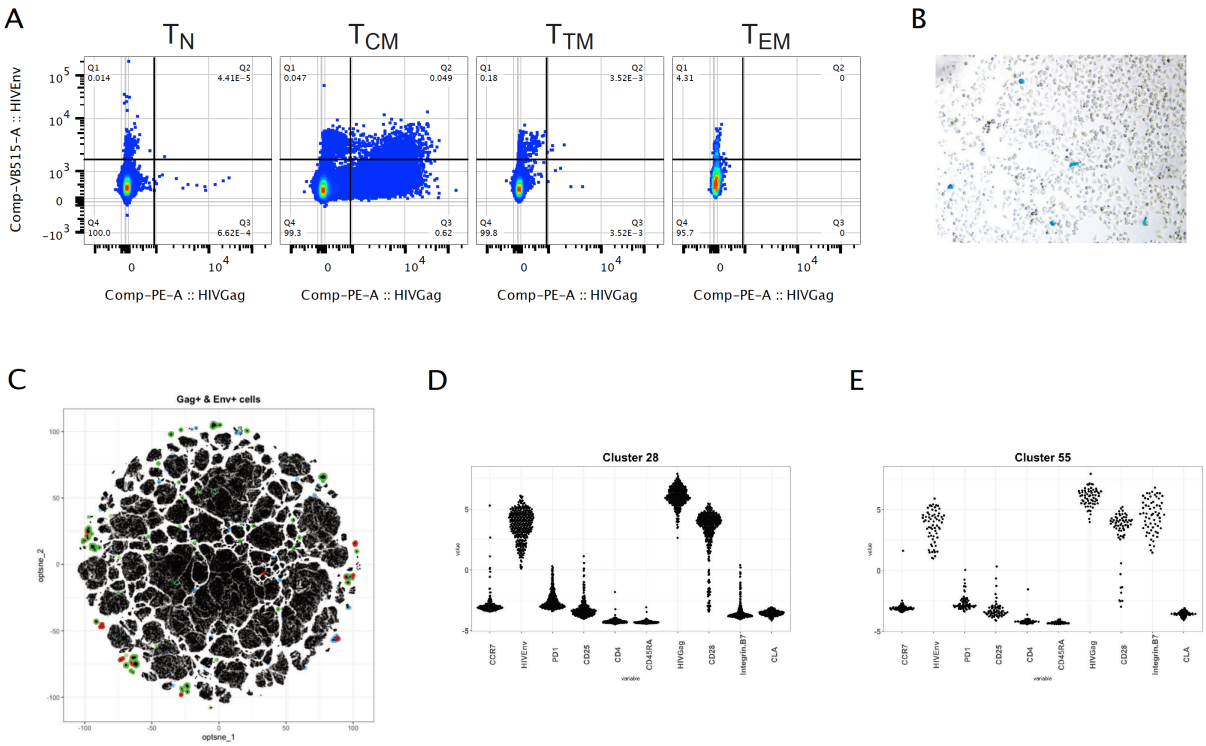

Figure 11. GERDA performance during viral outgrowth. Representative data of individual P03. A: Gag vs Env expression events in sorted fractions (from left to right: Naïve (T_N), central memory (T_{CM}), transitional memory (T_{TM}) and effector memory (T_{EM})) 14 days post stimulation. B: X-Gal staining of T_{CM} fraction 14 days post stimulation. C: t-SNE plots of TCM culture on day 14. Each dot represents one cell as single data point (2.07E106 cells in total). Highlighted are all HIV Gag+ (green), HIV Env+ (blue) and HIV Gag+Env+ (red) populations (C). D, E: Marker expression profile of a selection of identified clusters.

For clinical sample P03, the viral reservoir was almost exclusively assigned to T_{CM} with 12.04 IUPM (95% CI [5.48, 26.43]) in the tested format, which was in line with data from earlier

timepoints sampled from the same individual as mentioned above (Fig.9 F, G, I). Again, this data was validated by the determination of the proviral load in cell lysates and by quantification of HIV-1 poly-A transcripts (Table 5): T_{CM} had the highest poly-A transcript load as well as the highest RNA/DNA ratio. As shown in the t-SNE analysis highlighted in Figure 11 D+E, expanded cells further differentiate into T_{TM}. This strongly supports the notion that most cells are differentiating ex vivo over the course of repetitive stimulation. Patients P01 (delayed sampling) and P04 (diagnosed in acute infection phase) were also sorted and expanded for quantitative viral outgrowth assay (QVOA). For P01 only proviral loads were determined on day 10 which already revealed very low viral integration events inside memory T-cell compartments. This was also reflected in no Gag/Env detection for GERDA and no blue events in the X-Gal readouts (data not shown). After 9 days of expansion P04 showed little poly-A activity in the T_{CM} compartment, supported by increased proviral loads of day 9 and GERDA activity on day 14 (although only single positive events were detected for Gag and Env, see Supp. Table 1). Eventually no blue cells were detectable for X-Gal even after three weeks and three rounds of T-cell receptor stimulation (data not shown), which is consistent with the GERDA results.

Table 5. HIV-1 reservoir in T-cell subsets. Representative data of individual P03. All readouts were done after 14 days of expansion except proviral load (day 7). Results are normalized to 10E6 cells. GERDA: Gag and Envelope Reactivation Detection Assay. IUPM: infectious units per million. ND: not detectable. QVOA: Quantitative Viral Outgrowth Assay. Poly-A: HIV poly-A transcripts

	Provirus (QVOA d 7)	Poly A (QVOA d14)		GERDA		QVOA
ID	HIV DNA/10E6	Poly-A/10E6	HIV RNA/HIV DNA	Gag+ per 10E6	Gag+Env+ per 10E6	IUPM
P03_T4_TN	250	85‘297	341	7	0.4	ND
P03_T4_TCM	155‘113	85‘513‘919	551	6690	490	12.04
P03_T4_TTM	6‘433	10‘158	2	70	35	ND
P03_T4_TEM	ND	ND	ND	ND	ND	ND

For all cell sorts, the individual molecular layers measured by proviral load, poly-A, GERDA and QVOA show consistent results with most activity in T_{CM}.

VII.5. V3 dynamics during early therapy

To see how viral dynamics change during early ART periods the tropism determining V3 stretch was sequenced by NGS and analyzed by Geno2Pheno454 to detect circulating viral strains in cell free plasma as well as cell associated proviral sequences. To rule out that remaining DNA traces might distract the analysis, RNA samples were DNaseI treated. Both the dominating virus as well as the dominating provirus were for all individuals studied identical and were never overgrown by another sequence during the study visits of each individual (exemplified for P03 in Table 6). Most strains found in HIV RNA were also present in HIV DNA reflecting that most viruses were replication competent and not the result of a clonal expansion of a defective provirus.

3 patients presented as X4-tropic and 4 patients as R5-tropic at diagnosis applying a FPR (False positive rate: probability of classifying an R5-virus falsely as X4) cut-off of 10 % for Geno2Pheno454 and a cut-off of 2% relative abundance, assigning populations with X4 abundance below 2% as R5-tropic as suggested by Swenson et al. [50,142] 5/7 did not change their tropism between the first and last sampled timepoint. For both late presenters a tropism shift became apparent. P05 switched from R5 to X4-tropic. Over the follow-up time P05 had in contrast to P03 increased V3 dynamics (Supp. Table 2 A, B). For P07 a switch from X4 to R5 occurred, concurrent with loss of high abundant X4 variants (data not shown). However, V3 comparison showed that individuals P05 and P07 had identical viruses as majorities in their viral pool suggesting a sample mix up, which was evident after sequence alignment of the clearly variable viral genomic regions of Protease-Reverse Transcriptase (PR-RT, Supp. Fig. 8 A) and Integrase (INT, Supp. Fig. 8 B). Thus, long term follow-up V3 results were only considered from P05, who had more consistent follow-up timepoints.

Table 6. V3 loop NGS. Representative NGS data of first 10 most detected V3 variants of Patient P03. Individual aligned V3 variants of time point 1 descending by relative abundance with amino acid changes highlighted in red. To highlight the fate of each listed V3 variant from timepoint 1, all consecutive timepoints for proviral (DNA) and viral (RNA) V3 variants are listed in comparison to each V3 variant of timepoint 1 with indication of V3 rank and its relative abundance. FPR: False positive rate (Geno2Pheno$_{coreceptor}$), rel.ab: relative abundance. Count: absolute number of same variants detected.

Timepoint 1 (T1) DNA					T2 DNA	T3 DNA	T5 DNA	T1 RNA	T2 RNA
Rank	**V3.LOOP**	**COUNT**	**FPR**	**Rel.ab.**	**(Rank; Rel.ab.)**	**(Rank; Rel.ab.)**	**(Rank; Rel.ab.)**	**(Rank; Rel.ab.)**	**(Rank; Rel.ab.)**
1	CTRPNNNTRKSIHMGFGKTFYATGEIIGDIRQAHC	32711	49.27	96.3 %	1; 94.5 %	1; 96.5 %	1; 95.7 %	1; 95.1 %	1; 97.3 %
2	CTRPNNNTRKSIHIGFRKTFYATGEIIGDIRQAHC	103	64.39	0.30 %	-	-	-	-	-
3	RQRPNNNTRKSIHMGFGKTFYATGEIIGDIRQAHC	91	38.08	0.27 %	5; 0.22 %	2; 0.18 %	3; 0.28 %	12; 0.17 %	2; 0.29 %
4	KRQPNNNTRKSIHMGFGKTFYATGEIIGDIRQAHC	66	45.2	0.19 %	7; 0.16 %	6; 0.13 %	5; 0.15%	8; 0.19 %	4; 0.14 %
5	CTRPNNNTRKRIHMGFGKTFYATGEIIGDIRQAHC	60	1.74	0.18 %	8; 0.14%	3; 0.16%	6; 0.13 %	17; 0.09 %	6; 0.12%
6	CTRPNNNTRKSIHMGFGKTFYATGEIIGDIRPVSY	49	95.35	0.14 %	12; 0.07 %	4; 0.15 %	2; 0.31 %	13; 0.13 %	5; 0.13 %
7	GTRPNNNTRKSIHMGFGKTFYATGEIIGDIRQAHC	43	64.24	0.13 %	6; 0.20 %	9; 0.06 %	11; 0.08 %	14; 0.10 %	3; 0.17 %
8	CTRANNNTRKSIHMGFGKTFYATGEIIGDIRQAHC	42	67.15	0.12%	11; 0.09 %	5; 0.14 %	7; 0.11 %	20; 0.06%	20; 0.10 %
9	CTRHNNNTRKSIHMGFGKTFYATGEIIGDIRQAHC	22	68.75	0.06%	9; 0.11 %	7; 0.13 %	16; 0.06%	18; 0.08 %	11; 0.04 %
10	CIRDSNNTRKSIHMGFGKTFYATGEIIGDIRQAHC	20	70.93	0.06%	13; 0.06 %	16; 0.04 %	19; 0.06 %	22; 0.04 %	17; 0.04 %

Table 7. V3 dynamics over time. Tropism shift of earliest timepoint compared to last sampled timepoint. NGS data were evaluated by applying Geno2Pheno$_{coreceptor}$ FPR of 3.5%, 5%, 10%, 15% or 20%. CRF: circulating recombinant form. NA: not available, T: timepoint, %X4: Frequency of X4-tropic HIV variants.

			Earliest timepoint	Last timepoint
ID	**Recency**	**Subtype**	**%X4 at FPR 10% (FPR3.5%, 5%,15%, 20%)**	**%X4 at FPR 10% (FPR3.5%, 5%,15%, 20%)**
P01	NA	CRF01B	T1: 100% (1.04%, 99.31%, 100%, 100%)	T2: 99.98% (1.0%, 99.49%, 100%, 100%)
P03	1st year	B	T1: 0.27% (0.18%, 0.23%, 0.33%, 0.48%)	T5: 0.2% (0.13%, 0.15%, 0.22%, 0.41%)
P04	Acute	B	T1: 0.19% (0.18%, 0.19%, 0.24%, 0.24%)	T2: 1 variant: 0% (0%, 0%, 0%, 0%) 92.9
P05	late presenter	B	T1: 0.62% (0.07%, 0.13%, 1.05%, 97.7%)	T5: 6.58% (6.1%, 6.26%, 29.88%, 92.68%)
P06	1st year	CRF01-AB	T1: 99.9% (90.9%, 99.6%, 99.9%, 99.9%)	T2: 100% (95.8%, 100%, 100%, 100%)
P07	late presenter	NA	T2: 6.1% (4.2%, 4.2%, 13.8% 83.7%)	T4: 0.7% (0.2%, 0.3%, 4.6%, 88.9%)
P08	Unsuppressed	B	T1: 0.07% (0.03%, 0.03%, 0.19%, 0.37%)	T2: 0.2% (0.1%, 0.1%, 0.23%, 0.44%)

This section highlighted that it is important to measure on different layers of complexity to make conclusive statements on viral reservoirs in circulating blood cells. These data also imply that samples are very heterogeneous when it comes to viral activity in cells and that there is much more beyond VL and CD4 clinically relevant to understand the viral and cellular reservoirs of HIV positive individuals. Combining the characteristics of cellular reservoirs with the features of circulating viruses or proviruses will further illuminate the relation of viral and cellular properties for viral persistence.

VIII. Discussion

A lot of anatomical sanctuaries have been discussed in the past for HIV. Studies in RMs (Rhesus macaques) showed that sexual transmission of SIV results in very few local infection foci inside the genital tract during the first 1-3 days of viral challenge, rapidly spreading to draining lymph nodes the next days and eventually to distal LNs and other tissues in about 1-2 weeks [143–145]. Thus LNs are one of the first targets of viral encounter and the GALT, encompassing approximately 70% of all immune cells [146], was shown to be attacked as early as from Fiebig stage I (first detection of viral RNA) with no or only partial recovery of CD4 cells under suppressive ART [9,83]. Depletion is mainly associated with highly active cell proliferation [9] making these cells even more susceptible to SIV/HIV infection [8,147]. Most viral reservoirs remain in 98% of the lymphatic tissues according to studies in RM, with GALT as highest prevalent organ (62.3%) followed by LNs (35.9%) and residual organs [76].

VIII.1. HIV enrichment in Lymphoid and gut homing cells and their peripheral contribution

In order to precisely define the viral reservoir in an HIV positive individual for future cure approaches, new reservoir assays need to fulfill certain criteria, like using low quantities of easily accessible specimen and having a conclusive and reliable readout. The specimen of choice is blood, since all clinical parameters to evaluate a patient's physical condition are deduced from venipunctures. Considering that PBMCs present a "homing signature" derived by their surface expression of homing markers, this study tried to characterize infected cells of the periphery, their relative contribution to the viral reservoir and the genetic aspect of the containing proviruses. The reservoir inside PBMCs was studied based on immunological and secondary lymphoid homing aspects to extrapolate the extent of the viral reservoir beyond the periphery. Pilot experiment using MACS gave already a first approximation that Lymphoid or gut homing CD4+ T-cells are enriched for HIV proviruses compared to pre-sort condition with an increased HIV DNA load on the individual as well as on the group level (Fig 5, 6). However, a clear representation of all cell fraction was not achieved in the tested patients. For some individuals proviral loads were quite high like for β_7+CD4-CD8-CD19- cells, whereas for other individuals these fractions did not have any HIV DNA detection at all, suggesting inter-patient heterogeneity. Especially for β_7+CD4-CD8-CD19- cells with a proviral readout cell recoveries were quite low (data not shown), which might cause a bias in data interpretation when quantifying HIV DNA per 10E6 cells. Further subsequent FACS control experiments of all selected fractions revealed that individual fractions were not highly pure, particularly the

aforementioned β_7+CD4-CD8-CD19- cells (Supp. Fig. 1 A). One potential reason for this is that all lymphocytes that have Integrin β_7 expression, like CD4+, CD8+ or CD19+ cells are depleted and thus no cells are left with sufficient levels of Integrin β_7 expression. In addition, all patients used for MACS were long time chronically infected (median 270 months). Although most patients have decreasing proviral loads over time, Bachmann and colleagues found for 26.6% of participants over a 1.5 to 10 year period a relative increase in proviral loads [141]. Thus periods of low level viremia in combination with clonal expansion, which is already apparent after 4 weeks after infection [99,148], are a substantial confounder that might detect a lot of largely defective clonal proviruses that will only reflect an clonal enrichment in certain cell compartments.

Initial sorts with fixed cells further showed that cells of interest, i.e. Integrin β_7+ memory cells are only present at a mean of 5% of all CD4+ T-cells, which was also shown by others [83]. As an aside, the repository of the SHCS cyto-bank stores bulk PBMC aliquots in the range of 2X10E6-10E7 cells. Thus, CD4 pre-selection and sorts would not allow to have enough cells for adequate and representative analysis. Further expansion for longer than three days, to yield higher cell quantities, altered the cellular receptor repertoire and would not reflect the *in vivo* situation anymore. This was demonstrated by expansion experiments (Table 2, 3), the viral outgrowth data (Fig 11 D,E) and described by others using cell differentiation for HIV-1 reactivation modeling [149].

VIII.2. Novel GERDA system detects productively infected cells

Here, a novel and innovative flow-based method was established to evaluate the infectivity of HIV-1 infected circulating blood cells to comprehend the *in vivo* viral reservoir (Supp Fig. 2). With the simultaneous detection of HIV-1 Gag and Envelope proteins, exact and conclusive predictions can be made, if infected cells can give rise to viral particles using Gag as surrogate marker and if these particles are potentially infectious derived by Env detection. Furthermore, GERDA combines the benefit of a high sensitivity, enabling detection of as few as 16 infected cells per million with less hands on time compared to other comparable assays [97,135]. In addition, the power of single cell characterization represents another unique feature. GERDA performed equally well when using fresh or cryo-preserved cells and is suitable for small cell sample sizes. The assay has been validated further by comparing it to the separate detection

and quantification of intracellular HIV DNA/RNA in bulk PBMCs and the gold standard QVOA for benchmarking, to yield the full picture of all key reservoir levels in the viral life cycle.

In comparison to recently described techniques, the assay considers almost the entire viral genome length, by assessing Gag and Env protein production, thus avoiding a 5' or 3' constrained bias (see Fig. 1). This appears critical as recent studies found that Env expression is much more affected by genetic defects than the expression of functional Gag [150,151]. Thus, an assay format relying only on Gag as a viral reservoir marker seems unsuitable for assessing the true viral reservoir, since some reactivity might also overestimate Gag cells as seen for early time point of late presenting patients (Table 4, P05). Moreover recently described genetic reservoir determining methods only assess the viral "intactness" based on the absence of indels, inversions, hypermutations leading to premature Stop codons, packaging signal or major splice donor site defects [55,70]. However a recent study found that although a lot of Envelope sequence would be classified as genetically intact, are actually functionally impaired due to defective Env protein expression [152]. This is also supported by other studies showing that defective and non-defective cells are able to produce viral transcripts as well as proteins [32,153–155] which would mistakenly be anticipated as active viral reservoirs.

Of note, not all cells in Quadrant 2 of Figure 8A (1600 HUT/10E6 cells condition) were detected as DP events, indicated in Figure 8D, which may be attributed to the fact that the number of Gag molecules exceeds by far (about 2000 [156]) per nascent particles compared to Env trimers (about 7-10 per virion [157]). However, the semi-quantitative depiction of expressed HIV Gag is sufficient to reliably identify translation-competent cells. Overall, a strong correlation between Gag and Envelope DP expressing cells was observed indicating a high principal congruence between Gag- and Env synthesis (Supp Fig. 3 C and Supp. Fig. 6 D, P). In addition, when single Gag-positive FACS-events were analyzed in mixed cell populations containing HIV-infected HUT4-3 cells and uninfected SupT1 cells, CD4 expression served as a reliable guide for identifying uninfected cells in the mixed population (see Supp. Fig 3 A, B; Supp Fig. 4 D: HUT4-3 cells = CD4 negative; Supp Fig. 4 E: uninfected SupT1 = CD4 positive). One potential experimental limitation may come from the fact that, prior to analysis, HUT4-3 - and SupT1 cells had been co-incubated for ≥4 h. It can therefore not be excluded that during this period individual SupT1 cells might have already fused with chronically infected HUT4-3 cells or free virions in the supernatant, which can be observed already after ~1 h of co-incubation [137], giving rise to a low Gag+ signal and/or increased size, highlighted by bigger

scattering (Supp Fig 4 F-H). Furthermore, all CD4 negative, i.e. potentially HUT4-3 cells, of Q3 in Figure 8 A (1600 HUT/10E6 cells condition) show a tendency of higher Gag and Envelope expression compared to CD4 positive SupT1 cells (Supp Fig 4 A-C). Thus, Env detection for these cells might be below the detection threshold, due to low Env expression or Env shedding. To increase the sensitivity of Env detection, sophisticated signal amplification techniques like Immuno SABER could improve detectability of low Env expressing cells [158]. Ramos B-cells (added as carrier cells) did not contribute any significant Gag/Env background signal (Supp. Fig. 4 I, J).

To grasp the multidimensional data in the most effective and unbiased way, the dimensional reduction tool t-SNE [138,139] and the clustering algorithm DBSCAN [140] were utilized. This allowed the analysis of all data in an identical manner using the same analytical pipeline. All final clusters were double-checked with classical gating, which in all cases supported the findings. Cluster Beeplots also showed that each marker has a clear pattern of being either positive or negative for each cluster (Fig. 9 F-H; Fig. 11 D, E; Supp. Fig. 6 H-K), further highlighting good cluster mapping by t-SNE and DBCAN. The pipeline will beyond this work allow the expansion of new reservoir markers of interest, using more sophisticated techniques like CyTOF (cytometry by time of flight) or Cytek® Flowcytometry that allow to look at 40+ marker simultaneously and will thus be fundamental to understand multi-dimensional datasets.

The high background Env signal shown for cells of individual P03 (Fig. 9 B) was due to a technical staining issue. Accordingly, the respective data were adjusted for this issue. (as shown in Supp. Fig. 6 O). As result, no false DP signals remained for the corresponding HIV neg control stain (Supp Fig. 6 M) or for an independently same day tested clinical sample (P02) with low viral activity (Supp. Fig. 6 N; Table 4). This provided proof that the DP events of P03 in Figure 9 B were indeed *bona fide* Gag+Env+ cells. It should nevertheless be noted that due to the correction only very few T_N could be considered for Gag+Env+ assignment. However, these cells had only a marginal positive signal for IC Gag (data not shown).

The analysis revealed that most DP cells have more lymphoid homing potential based on the expression of CCR7 compared to Integrin β_7 (gut) (or cutaneous leukocyte antigen (CLA, skin). Most obvious was this observation for P03, who had most DP events for CCR7+ (central) memory cells at the first sampled timepoint and who had most provirus, poly-A transcripts, poly-A per HIV DNA, most DP cells and clear outgrowth events in the central memory cell

fraction after 6 months follow-up (Figure 11 A; Table 5). Although for P04 no viral outgrowth was detectable, possibly due to very early ART initiation in acute infection phase which limits reservoir dissemination, proviral load and poly-A quantification showed elevated signals in the T_{CM} fraction (Supp. Table 1). It should nonetheless be considered, that T_{TM} and T_{EM} fractions had only very few cells for QVOA in comparison to T_N or T_{CM} fractions and are thus less adequately represented. Of note, we had sampled primarily patients who had very recently started ART. It is known that especially Integrin $\alpha_4\beta_7$ expressing cells are predominantly infected and depleted during the early infection phase, with an only insufficient recovery under ART [9,83]. This observation is exemplified for the acute Patient P04, who was diagnosed earliest in Fiebig stage III (first detection of HIV IgM) and had only 1% Integrin β_7+ memory cells of peripheral CD4+ T-cells (data not shown). A very recent trial that evaluated the use of Vedoluzimab, a monoclonal antibody directed against Integrin $\alpha_4\beta_7$, as potential treatment to control viral infection as recently reported for RMs [86], did not proof to show high efficacies in the human setting[159], questioning the role of Integrin $\alpha_4\beta_7$ late in the chronic stage of the disease.

One essential aspect of this study was that, although most patients had detectable free virus present in the plasma, in 4/7 individuals with detectable viral load (90-50'666 copies/mL) no viral activity was found in the circulating cells based on transcriptional (HIV poly-A) and translational (GERDA) levels. This supports the assumption that most circulating virus stemmed from resident cells in (distant) tissues, which will not be detected in the pool of circulating peripheral cells, supported by a study in RM [76].

However, for most patients no or only minor viral activities were measurable with poly-A quantification and GERDA staining (Table 4; Supp. Fig 10). Although most of our patient samples were collected in the first month of diagnosis (see Table 4), other parameters are also likely to be more relevant including viral setpoint, CD4 count, recency of infection or active immune responses by e.g. primary infections. Individual P03, who had the highest viral activity, had reasonably high viral load (867'496 copies/mL at diagnosis), intermediate CD4 counts (511 cells/µL) and was in the first year of infection, emphasizing that high viral activity and a still intact immune system are elementary. However, although ART can rapidly shut down detection of HIV poly-A transcripts, these can nevertheless be detected at later time points like for individual P05 (Table 4), who had a surgery just before timepoint 5. This introduces a potential stimulatory influence on inflammatory responses and has as a

consequence influence on the viral reactivation. Since patient characteristics need further evaluation for selection criteria, cell samples right at diagnosis (2nd validation with PCR and Western blot, see Supp Fig. 9) could be used for proviral as well as HIV poly-A quantification to consider further cellular characterization by GERDA. As illustrated in Figure 6 proviral load monitoring will serve as crude estimation of the reservoir status, complemented by HIV poly-A quantification as proxy for protein translation. Although all individuals evaluated with GERDA were white males, patients had a diversified clinical background with late presenters, one acute infection, and two infections in the first year.

A key focus of this study was to consider exclusively those CD4 T-cells circulating in the peripheral blood, which are known to incorporate most proviruses of infected cells. Very recent studies seem to propose that for some anatomical sites, macrophages could play a more essential role for the viral reservoir compared to CD4+ T-cells. [37] The format of this assay can easily be adapted by including also aspects of such tissue-resident macrophages or any other type of cells should they be identified as to being involved in crucial viral reservoirs.

While many past studies identified virus in essentially every 'corner' of the body that was carefully studied with no obvious major hot spots, the highest degree of viral replicative activity appears to localize to lymphatic tissue and lymph nodes [160–162], supporting the findings of this study. Nevertheless most anatomically separated viruses cannot be attributed to be genetically very distant to each other indicating that continuous cell trafficking and lymphoid homing is indeed essential for spreading of the virus throughout the body [160,161]. Thus, techniques like GERDA that examine the reservoir in peripheral blood can give us a first hint where most viral active sites are.

Lastly the reactivation potential of latent proviruses are limited a) by the use of mitogens, which are not exceptionally HIV specific for viral reactivation, and b) by the stochastic nature of the intact proviral reservoir [163]. Recent studies using the viral outgrowth format (QVOA) had revealed that one single round of stimulation will stimulate viral replication in only 60% of cultures compared to the effect after 4 consecutive stimulations [73,164], which is still heavily underestimating the assumed entire intact viral reservoir as illustrated in Fig. 3 [70,73,99,163,165]. However using PHA or selective antibodies directed against CD2, CD3 and CD28 proof to be currently the most potent reactivation agents reported in literature [166].

VIII.3. V3 dynamics during early therapy

Most patients get infected with a single so called Transmitted/Founder virus (TF), although cases of up to 5 different TFs are reported, causing a genetic transmission bottle neck. TFs favor CCR5 usage, despite the presence of X4 variants in the index patient and are more closely related to the index patients ancestral viral sequences [6,167–170]. Recent work showed that especially the time near therapy initiation builds the base for the established replication competent HIV-1 reservoir [171,172]. With the early sampling in this work, the primarily archived viral founder populations from Plasma and cells could be characterized. All dominating viruses of Plasma were also found in the proviral cell pool, which persisted for periods of a median of 9 months. But also smaller minorities did not change significantly in the first weeks (exemplified in Table 6) for all patients except P05, who showed already after timepoint 2 rearrangements in the abundance of viral variants that proceeded to timepoint 5, despite viral suppression (Supp. Table 2 A, B; Table 4). Recent data of Bader et al showed that over the years a single pre-treatment proviral minority gets almost exclusively selected for outgrowth after up to 4 years of therapy most likely due to clonal expansion [17]. However Wang and colleagues found that proviral clones arise and disappear again over time [60]. For all individuals enrolled during early treatment periods there was no selection in favor of a minority with therapy initiation during the observed time interval. Instead the actively replicating majority will also be found later as latent majority under therapy. However only 2/7 patients were examined for longer periods, since patients with very low proviral load failed for V3 amplification, which is supported by the observation that timepoints with lower proviral loads consequently resulted also in lower NGS reads (Fig. 10, Table 7 individual P04). Ought to the relative short sampling interval it remains therefore open how the proviral landscape of all enrolled individuals will change over years since >50 % of replication competent proviruses are comprised of proviral clones [173,174]. Moreover especially defective clones predominantly expand over time due to lack of cytotoxic T-Lymphocyte (CTL) selection pressure, overgrowing variants that dominated at the beginning of therapy [32]. Therefore, more patients need to be recruited and followed up for longer time periods to make a conclusive statement.

We found in seven patients just after diagnosis four R5-tropic and three X4-tropic dominating viral pools. One X4 tropic individual can be linked to late clinical presentation (P07), a known feature of advanced disease progression without treatment [10,11]. X4-tropism was also apparent for one individual (P06), which was in the first year of infection. However,

this patient had recombinant Subtype CRF01-AB, which might not be assigned by Geno2Pheno with high reliability since the algorithm is optimized on Subtype B.

The aspect that the differences in viral tropism leads to district compartmentalization, which is assessable by homing properties of the CD4 T cells could not be addressed in the frame of this study. One early observation in the field of HIV was that R5-tropic viruses rather infect Macrophages whereas X4-tropic viruses infect T-cells [41,42,175]. A study by S. Zhou et al could show that X4 and R5 do have very limited recombination products indicating that these viruses might not be found inside the same cells subsets [176]. It is also well known that X4 can infect T_N, contrary to R5-viruses, which is linked to higher CXCR4 expression on these cell subsets [177,178]. Studies in monkeys showed that X4-tropic SIV rapidly depletes naïve T-cells during acute phase [179]. Further studies in humans showed that although T_N have the lowest viral contribution when looking at HIV integrations, T_N show equal contribution of replication competent/ genetically intact viruses when corrected for difference in HIV DNA [180,181]. CCR5 on the other side predominantly infects activated memory T-cells [8,147]. It will be of further interest in which T-cell memory compartment the initial established viruses will be found since a recent study obtained contradicting results stating that ancestral sequences are found in more differentiated subsets for some individuals, but for others the opposite was the case [182]. Here the combination of GERDA and QVOA can contribute to break down the viral compartmentalization.

Although CXCR4 utilizing viruses can infect naïve as well as memory T-cells [178,183], the GALT, as the biggest immune organ and major HIV target, comprises abundant expression of CCR5 on CD4+ lymphocytes, while CXCR4 is sparse, favoring R5 tropic dominance [8].

Beside reservoir aspects, there are fundamental differences among CXCR4 and CCR5, i.e. CXCR4 strains have a higher replication capacity and are also linked to higher inflammation and immune activation rates [13,184]. If a competent immune response still can be mounted, i.e. during primary infection, especially the more active and less glycosylated X4 tropic Env [46,47] expressing cells can be detected by humoral immune responses and will be more easily cleared as their “silent” CCR5 counterparts [185–187].

Work of JM Harouse et al could show that coinfection of RM with CCR5- and CXR4-tropic SIV complemented with HIV Envs (SHIVs) led to transmission and replication of both tropic viruses without dissemination of either strain. Like in human infection R5 tropic predominance

ensued. Following CD8 depletion, CXCR4 viruses re-emerged emphasizing the potential role of CTL mediated control over CXCR4 viruses [188].

CXCR4 also show a higher degree of diversification inside the Env gene compared to CCR5 counterparts, meaning X4 is either under constant pressure to diversify to evade humoral and/or cellular immune responses or to adapt the differential cellular reservoirs [189,190].

To conclude, the simplifying GERDA system described here has a performance equivalent to the current gold standard of QVOA and could be validated by other approved quantifying DNA- and RNA-reservoir assays. Future cure and reservoir approaches may thus benefit from considering when to sample (time point in relation to ART initiation), what to sample (in order to include relevant specimen like blood or tissues) and how to measure the reservoir, i.e. integrating in parallel several complementing methods for reservoir determination instead of choosing only one. Future studies will need to address the role and dynamics of resident tissue reservoirs of HIV and how to eliminate these.

IX. Outlook and Conclusion

To understand the viral dynamics before and after therapy initiation for future cure approaches, this study tried to shed light on the HIV reservoir in transiently circulating blood cells to uncover the role of tissue sanctuaries beyond the periphery.

This work has validated the novel GERDA cell profiling system for HIV-1 by sensitive genetic and functional methods; GERDA provides the following advantages over existing methods:

i) it allows for an accurate approximation of the "real viral reservoir" in PBMCs by simultaneously integrating intracellular Gag and extracellular Envelope protein as proxies for released infectious virions from host cells;
ii) it allows for the characterization of the reservoir, including cellular homing, down to the single-cell level; and
iii) it requires smaller sample volumes than most comparable assays, making it the method of choice

Furthermore, this study revealed that:

i) it is fundamental to integrate different reservoir assays measuring on all key molecular levels to make conclusive statement on the "real viral reservoir"
ii) there is evidence for an active viral reservoir contribution beyond the periphery
iii) the dominating virus at treatment initiation keeps majority of established founder population throughout the first months of therapy
iv) lymphoid homing plays major role for viral infectious cells during early therapy, whereas Gut homing has only minor contribution

To further evaluate HIV reservoir dynamics, additional individuals need to be continuously enrolled to follow-up on cellular and viral reservoir aspects to study shifts in clonal expansion and viral populations inside target cells. Furthermore, newly recruited patients need to be enrolled at an earlier timepoint after diagnosis to test for proviral loads and HIV poly-A loads preferably only a few days after a 1st HIV positive test (see Supp. Fig. 9). This will allow to pre-screen patients for viral activity, assessing the feasibility for additional GERDA evaluation to look for cellular reservoirs in these patients. It will further enable to determine which molecular and clinical parameters are substantial for observing high viral activity inside cells.

For a more comprehensive analysis, scaling up the amount of blood, e.g. using buffy coats, would further help to have more relevant cells in final fractions for VOA and for the detection of individual viral sequences. Moreover, for already implemented and following viral outgrowth approaches, viruses from reactivated sorted cell fractions will be analyzed by single genome sequencing (SGS) [168] to characterize individual reactivated viruses and their compartmentalization, to also link these data to the V3 sequences obtained from earlier time points. Along those lines, additional sorts of candidates with higher viral active cells will help to understand the difference of X4 and R5 populations and their cellular origin. If applicable, a recently described method called full length individual proviral (FLIP) sequencing [70] would further help to characterize which cells are genetically intact and can unravel mutation rates inside different HIV genes like Env to see differences in viral evolution between X4 vs R5 viruses over time.

With accumulating data on peripheral cells and the evidence of reservoir contribution beyond peripheral cells, an intuitive next step will be to look inside lymphoid tissues of LN or GALT to characterize which cells are infected and can give rise to infectious virus. Several studies pinpoint, that infected cells in tissues still can give rise to viral RNA+ cells despite "suppressive" ART, suggesting that drug penetration might not be optimal for some drug classes [191,192]. For this purpose, extension of the marker repertoire is essential to also look at tissue resident memory cells, which have been reported to have elevated HIV activity [72,193].

Finally to complement the work on differential dynamics of X4 and R5 over time, experiments in RM monkey models would further allow to address a) if there are any tropism dependent cell or lymphoid organ restrictions and b) what is the role of differential immune pressure on X4 vs R5 tropic viruses over the course of infection.

These foreseen future studies will eventually help:

i) to analyze the "cellular infection landscape" using new diagnostic tools like GERDA, which may influence the design of treatment strategies for an early clinical intervention.
ii) to extrapolate the potential for viral re-emergence and cellular spread and thus have clinical implications

iii) to understand the variation between individual patients and the association with e.g. primary infection or situations of high vs. low immune competence that might also have consequences for clinical therapy strategies
iv) to provide evidence for specific tissues and organ sites critically involved in HIV infection and persistence
v) to follow proviral history and intactness over time, to understand the molecular decay and also the capacity to re-establish reservoirs with intact viral genomes, e.g. after treatment cessation.

In conclusion, all aspects discussed here will contribute to identifying essential body compartments and actively infected cell populations that help to explain residing viral activity and which can pose critical obstacles for the eradication of HIV and an eventual cure.

X. Materials & Methods

X.1. Materials

X.1.1. Chemicals, Enzymes and Consumables

Name	Supplier
Gel electrophoresis	
Agarose	Promega
TAE Buffer 10x	Roth
SYBR™ Safe DNA Gel Stain	Invitrogen
Gel loading dye, purple	New England Biolabs
100 bp DNA ladder (500 µg/mL)	New England Biolabs
1 kb DNA ladder (500 µg/mL)	New England Biolabs
Sanger Sequencing	
BrightDye Terminator	Nimagen
BrilliantDye® v1.1/3.1 Sequencing Buffer (5x)	Thermo Fisher
Next Generation Sequencing	
Agencourt AMPure XP	Beckman Coulter
Quant-iT PicoGreen dsDNA Assay Kit	Invitrogen
Nextera XT DNA Library Preparation Kit	Illumina
Flow Cytometry	
Intracellular Staining Permeabilization Wash Buffer (10X)	Biolegend
Rainbow Calibration Particles, 6 peaks (3.0-3.4 µm)	Biolegend
UltraComp eBeads™ Compensation Beads	Thermo Fisher
Drugs	
Maraviroc	Selleckchem
AMD 3100	Selleckchem
Efavirenz	Selleckchem
Z-VAD-FMK	Selleckchem
qPCR/qRT-PCR	
Luna® Universal Probe qPCR Master Mix	New England Biolabs
Brilliant III Ultra-Fast qRT-PCR Master Mix	Agilent
Quantifluor® ONE dsDNA Sysem	Promega
PCR	
Herculase II Fusion DNA Polymerase	Agilent

Name	Supplier
Cell culture Medium	
ImmunoCult™-XF T cell expansion medium	STEMCELL Technologies
RPMI-1640 Medium	Sigma
Dulbecco's Modified Eagle's Medium	Sigma
Medium supplement	
Immunocult™ Human CD3/CD28/CD2 T cell activator	STEMCELL Technologies
Human IL-2 IS, premium grade	Miltenyi Biotec
PHA-L	Sigma
DNase I recombinant grade I	Roche
T-cell Activation/Expansion kit, human	Miltenyi Biotec

X.1.2. Commercial kits

Name	Supplier
RNA isolation	
Maxwell® RSC miRNA Plasma and Serum Kit	Promega
Maxwell® RSC simplyRNA Cells Kit	Promega
DNA isolation	
Maxwell® RSC Cultured Cells DNA Kit	Promega
DNA purification	
NucleoSpin® Gel and PCR Clean-up	Macherey Nagel
Biotinylation	
EZ-Link™ Micro Sulfo-NHS-LC-Biotinylation Kit	Thermo Fisher
Zeba Spin Desalting Columns (7K MWCO), 2 mL, 25 columns	Thermo Fisher
Flow Cytometry	
CFSE Cell Division Tracker Kit	Biolegend
Zombie NIR™ Fixable Viability Kit	Biolegend
Transfection	
Transfection jetPRIME®	Polyplus Transfection

X.1.3. Antibodies

FACS Anitbody (Clone)-Fluorochrome	Isotype	Supplier
CD45RA(HI100)-FITC	Mouse, IgG2b K	Biolegend
Anti-Biotin-Vio®Bright B515, REAfinity™	Recombinant	Miltenyi Biotec
CD4 (RPA-T4) FITC	Mouse IgG1, κ	Biolegend
CD45 (HI30)-PerCp/Cy5.5	Mouse IgG1, κ	Biolegend
CLA (HECA-452)-PerCP-Cyanine5.5	Rat, IgM, K	Biolegend
HIV core antigen(KC57)-PE	Mouse IgG1 K	Beckman Coulter
Mouse IgG1 k-PE (Iso ctrl HIV Gag)	Mouse IgG1 K	Biolegend
CD28.2 -PE/Dazzle594	Mouse IgG1, κ	Biolegend
Integrinß7(FIB504)-PE-Cy7	Rat, IgG2a K	Thermo Fisher
CCR7(G043H7)-APC	Mouse IgG2a K	Biolegend
CD45(HI30)-A700	Mouse IgG1, κ	Biolegend
CD8(RPA-T8)-Alexa700	Mouse IgG1 K	Biolegend
CD8(RPA-T8)-APC-Cy7	Mouse IgG1 K	Beckton Dickinson
CD19(HIB19)-APC/Cyanine7	Mouse IgG1 K	Biolegend
CD14-APC/Cyanine7	Mouse IgG1 K	Biolegend
CD45 (HI30)-BV421	Mouse IgG1, κ	Biolegend
PD-1(EHA12.2H7)-BV421	Mouse IgG1 K	Biolegend
CD103(Ber-ACT8)-Bv421	Mouse IgG1 K	Biolegend
CD3(UCHt1)-BV510	Mouse IgG1 K	Biolegend
CD25(BC96)-BV605	Mouse IgG1 K	Biolegend
CD45 (HI30)-BV605	Mouse IgG1 K	Biolegend
CD4(RPA-T4)-BV650	Mouse IgG1 K	Biolegend
CD45RA(HI100)-BV711	Mouse IgG2b K	Biolegend
CD45 (HI30)-BV785	Mouse IgG1, κ	Biolegend
CD45(HI30)-BUV395	Mouse IgG1, κ	Beckton Dickinson
HIV broadly neutralizing Antibodies	**Isotype**	**Supplier**
3BNC117 (CD4bs)	human IgG1	Prof. Florian Klein
10-1074 (V3-loop)	human IgG1	Prof. Florian Klein
PG16 (V1V2-loop)	human IgG1	Prof. Florian Klein
35O22 (gp120-gp41 interface)	human IgG1	Prof. Florian Klein
10E8 (MPER gp41)	human IgG1	Prof. Florian Klein
MGO (human IgG1 Isotype control)	human IgG1	Prof. Florian Klein

MACS Anitbody (Clone)-Fluorochrome	Isotype	Supplier
CCR7, REAfinity™-Biotin	Recombinant	Miltenyi Biotec
CD4, REAfinity™-Biotin	Recombinant	Miltenyi Biotec
CD8, REAfinity™-Biotin	Recombinant	Miltenyi Biotec
CD19, REAfinity™-Biotin	Recombinant	Miltenyi Biotec
Integrin ß7, REAfinity™-Biotin	Recombinant	Miltenyi Biotec
FcR Blocking reagent	IgG1	Miltenyi Biotec
Anti-Biotin MicroBeads kit		Miltenyi Biotec
CD4+ T-cell isolation kit, human		Miltenyi Biotec
MACSxpress® Whole Blood CD4 Isolation kit		Miltenyi Biotec
REAlease® CD4 Micobeads kit, human		Miltenyi Biotec

X.1.5. Equipment

Name	Supplier
MACS	
QuadroMACS Separator	Miltenyi Biotec
MACSxpress Separator	Miltenyi Biotec
FACS	
LSR Fortessa Flow Cytometer	Beckton Dickinson
FACSAria III Cell sorter	Beckton Dickinson
PCR-Cycler	
Biometra Trio 48 PCR Cycler	Analytik Jena
7500 Fast Real-Time PCR System	Applied Biosystems
Sequencer	
3130 Genetic Analyzer Sequencer	Applied Biosystems
MiSeq Benchtop Sequencer	Illumina
Nucleic acid extraction/quantification	
Maxwell® RSC	Promega
Quantus™ Fluorometer	Promega
Microscopy	
LEICA DMi1	Leica

X.1.6. Plasmids

Name	Appliaction
pNL-NF	HIV-1 reference plasmid (derivative of pNL4-3)
pMVQA	Standard for HIV-1 poly-A quantification (Supp. Fig. 11)
pBRU2	HIV-1 Subtype B, X4-tropic
pMal2	HIV-1 Subtype D, R5-tropic
pADIc Cl-13	HIV-1 Subtype B, X4-tropic (Ala-1)

X.1.7. Buffers

FACS staining/MACS separation Buffer
PBS + 2 mM EDTA + 1% (v/v) human Serum

Paraformaldehyde Fixation Buffer
PBS + 4% (m/v) Paraformaldehyde

X-Gal Buffer
5 mM $K_4[Fe(CN)_6]$ * $3H_2O$ + 5 mM mM $K_3[Fe(CN)_6]$ + 2 mM $MgCl_2$ * $6H_2O$

Density gradient medium (Histopaque® Sigma)
Density: 1.077 g/mol

X.1.8. Primer

Names	Comment	Sequence 5' - 3'
F-522	Forward LTR-Primer; provirus qPCR (Liszevski et al Methods 2009)	GCC TCA ATA AAG CTT GCC TTG A
R-643	Reverse LTR-Primer; provirus qPCR (Liszevski et al Methods 2009)	GGG CGC CAC TGC TAG AGA
HIV LTR-Probe	LTR- Probe 5; FAM; 3`BHQ-1; provirus qPCR (Liszevski et al Methods 2009)	CCA GAG TCA CAC AAC AGA CGG GCA CA
F-9501 (VQA)	Forward primer to quantify poly-A HIV transcripts (VQA: Shan et al 2013 JVI))	CAG ATG CTG CAT ATA AGC AGC TG
R_10T20 (VQA)	R+everse primer to quantify poly-A HIV transcripts (VQA: Shan et al 2013 JVI)	TTT TTT TTT TTT TTT TTT GAA GCA CTC
VQA-Probe	Probe to quantify poly-A HIV transcripts (VQA: Shan et al 2013 JVI)	CCT GTA CTG GGT CTC TCT GG
F-CCR5	Forward primer for cellular internal control with CCR5 gene; provirus qPCR	ATG ATT CCT GGG AGA GAC GC
R-CCR5	Reverse primer for cellular internal control with CCR5 gene; provirus qPCR	AGC CAG GAC GGT CAC CTT
Probe CCR5	Probe CCR5 gene 5' Fakima Yellow; 3' BHQ-1; provirus qPCR (Malnati et al 2008 Nature Protocols	AAC ACA GCC ACC ACC CAA GTG ATC A
F-6553	V3_Foward primer 1st PCR for Illumina NGS	ATG GGA TCA AAG CCT AAA GCC ATG TG
F-6848	V3_Foward primer 2nd PCR for Illumina NGS	CCA ATT CCC ATA CAT TAT TGT GCC CCG GCT GG
R-7371	V3_Reverse primer 1st PCR for Illumina NGS	AGT TAC AGT AGA AAA ATT CCC CTC CAC AAT TAA A
R-7801	V3_Reverse primer 2nd PCR for Illumina NGS	AGT GCT TCC TGC TGC TCC CAA GAA CCC AAG
M13 forward	sequencing primer (TOPO-TA vector)	GTA AAA CGA CGG CCA G
M13 reverse	sequencing primer (TOPO-TA vector)	CAG GAA ACA GCT ATG AC
F_HXB2_9045	Forward primer just before HXB2 5`-end LTR, used for pMVQA cloning	AGC TGT AGA TCT TAG CCA CT

X.2. Methods

X.2.1. Nucleic acids

X.2.1.1. Nucleic Acid Extraction

RNA and gDNA extraction were performed with Maxwell RSC (Promega, Madison, Wisconsin, USA) using the "miRNA Plasma and Serum" (for viral RNA), "Cultured cells" (for gDNA) or "Simply RNA cells" (for intracellular RNA) Kit according to the manufacturers protocol.

X.2.1.2. Proviral load determination

Proviral loads were measured as described earlier [94] using a singleplex real time PCR approach with a VIC labeled CCR5 probe and a FAM labeled HIV LTR probe (see X.1.8. for details). 15 µL of Master Mix were mixed with 5 µL of extracted patient gDNA. For qPCR standards pre-determined amounts of HUT4-3 cells (chronically infected cell line with two HIV DNA integrations per genome) were used. For one reaction the Master Mix was composed of 0.8 µL of 10 µM forward primer (CCR5/LTR), 0.8 µL of 10 µM reverse primer (CCR5/LTR), 0.5µL of 10 µM CCR5/LTR probe and 10 µL of 2x Luna® Universal qPCR Master Mix (New England Biolabs) in a final volume of 20 µL. Cycling conditions were as follows: one minute at 95°C, 45 cycles of alternating 15 seconds at 95°C and one minute at 60°C.

X.2.1.3. Total/Completed HIV RNA transcript quantification

Intracellular poly-A HIV transcripts were measured as described earlier [95]. In brief intracellular nucleic acids from frozen PBMC were isolated (Promega Maxwell RSC simply RNA cells) either used directly or frozen at -80°C. HIV poly-A transcripts were quantified by One-step RT qPCR using standards of inhouse plasmid pMVQA (Supp. Fig. 11) and reads were normalized to cell counts using CCR5 as described elsewhere [94]

X.2.1.4. Cloning of pMVQA plasmid

To quantify poly-A HIV transcripts the HIV reference plasmid pNL-NF was cloned from position 9045-9625 with addition of 20 mer poly-A using primers F-9045 and 10T20 (see X.1.8.). The amplicon was cloned into a TOPO-TA vector (Invitrogen) and the sequence was confirmed by

Sanger sequencing. Plasmid concentration was measured by Quantus (Promega) and serial dilutions of pMVQA were used to generate a standard curve to quantify HIV-1 poly-A transcripts.

X.2.1.5. DNA integrity and PCR product visualization

To visualize the integrity and size of the obtained PCR products each PCR reaction was loaded on a 1.5 % TAE buffered agarose gel. 1.5 g of agarose was dissolved in 100 mL TAE buffer by initial heating and cooling to ambient temperature, whereupon 10 µL SYBR® Safe (Thermo Fisher) DNA gel stain was added. 5µL of PCR reaction was mixed with 3 µL Gel loading dye Purple (6x, no DMSO), 10 µL MilliQ H_2O and loaded onto the 1.5 % gel. The Gel was run for 30 min at 100 Volts.

X.2.1.6. DNA quantification

For DNA quantification for qPCR standards the Quantifluor® ONE dsDNA Sysem (Promega) was used according to the protocol.

X.2.2. Sanger Sequencing

Sequencing reaction mix was set up as follows: 1µL Bright Dye Terminator, 4µL Brilliant dye Buffer (5X), 3µL of 1µM forward or reverse primer and 200-500 ng of cleaned plasmid DNA, topped with MilliQ H2O to a final volume of 20µL. Sequencing conditions were carried out in 40 cycles of denaturing at 96°C for 20 seconds, annealing at 50°C for 20 seconds and elongation for four minutes at 60°C. The reaction was cleaned through a Sephadex G-50 superfine column. The pure PCR product was sequenced with an ABI 3130 Genetic Analyzer with the five seconds injection protocol.

X.2.3. V3 Next Generation Sequencing

X.2.3.1. V3 amplification for Next generation sequencing

For amplification a nested PCR approach was chosen. The Herculase II Fusion DNA Polymerase Kit (Agilent Technologies) was used in a 25 µL reaction volume. 24 µL of Master Mix were mixed with 1 µL of extracted patient gDNA or purified first PCR. Each PCR was carried out in triplicates to normalize for PCR amplification bias. The Master Mix was composed of 17 µL MilliQ H_2O, 0.625 µL of 10 µM F-6848 (1st PCR) or F-6553 (2nd PCR), 0.625µL of 10 µM R-

7371 (1st PCR) or R-7801 (2nd PCR), 0.25 µL Herculase II dNTP, 5 µL of 5x Herculase II Reaction Buffer and 0.5 µL of Herculase II fusion DNA Polymerase.
First PCR cycling conditions were as follows: initial three minutes at 95°C, 30 cycles of denaturation for 15 seconds at 95°C, annealing for 20 seconds at 60°C and extension for 45 seconds at 72°C. Final extension was done for three minutes at 72°C. Cycling conditions for the second PCR were the same as for the first PCR except an annealing temperature of 56°C for 20 sec.

X.2.3.2. 1st PCR V3 amplicon

Each replicate of the first PCR of the V3 amplicon was pooled (6 µL each) and treated with 2 µL of Illustra™ ExoProStar™ to get rid of excessive primers. Reaction was digested for 15 min at 37°C followed by a denaturation step at 80°C for 15 min.

X.2.3.3. 2nd PCR V3 amplicon

Each replicate of the second PCR of the V3 amplicon was pooled (~60 µL). Purification of the final PCR product was done according to the protocol of NucleoSpin ® Gel and PCR Clean-Up kit (Macherey Nagel). DNA was eluted in 2X 15 µL elution buffer.

X.2.3.4. Purification of PCR product

After PCR the DNA product was cleaned with Agencourt AMPour XP beads (Beckmann Coulter) according to protocol.

X.2.3.5. DNA quantification

For DNA quantification of NGS samples the Quant-iT PicoGreen dsDNA Assay Kit (Invitrogen) was used according to protocol.

X.2.3.6. Library preparation

DNA concentration was adjusted to 0.2 ng/µL and the Nextera XT DNA Library Preparation Kit (Illumina) was used to prepare the library according manufacturer's protocol.

X.2.3.7. NGS Sequencing

Sequencing was performed with an Illumina MiSeq Benchtop sequencer with 2x250bp reads.

X.2.4. Peripheral blood cell isolation

X.2.4.1. Buffy coat cell isolation of HIV negative blood donors

Initially 5X 50 mL SepMate™ tubes (Stem Cell Technologies) were prepared by adding 15 mL of Histopaque® (Sigma) to the bottom reservoir of the tube. 50 mL of Buffy coat were diluted with 100 mL of PBS 2 mM EDTA 1% (v/v) Human Serum (washing buffer), mixed and distributed to the prepared SepMate™ tubes (30 µL per tube). SepMate™ Tubes were centrifuged for 20 min at 800xg with breaks off. Plasma was discarded and Leucoring was poured into fresh 50 mL tubes and resuspended with washing buffer in a total volume of 50 mL. Cell suspension was centrifuged 2 times for 10 min at 400xg with breaks on, pooling cell pellets first in 2X50 mL and last in one 50 mL tube. Cells were resuspended in 50 ml washing buffer. Cell viability and cell count were evaluated by Trypan Blue (Thermo Fisher) stain. Collected cells in a final centrifugation step at 120xg 15 min at 4°C with breaks off and discarded SN. Cells were resuspended in pre-cooled freezing medium (FBS with 10% (v/v) DMSO) to have a final cell concentration of 10^7 cells/mL. 1 mL of cell suspension was loaded in Nunc Cryo tubes and put in a cryo container and put immediately at -80°C. On the next day cells were transferred to liquid Nitrogen and stored until use.

X.2.4.2. CPT/EDTA tube cell isolation of HIV positive samples

A) CPT tubes with fresh blood were inverted ten times prior to 20 min centrifugation at 1650xg. B) For EDTA tubes blood was mixed 1:2 with PBS 2mM EDTA 1% (v/v) Human Serum (washing buffer) and layered on top of 15 mL Leucoprep into a SepMate™ tube (30 µL per tube). Tubes were centrifuged for 20 minutes at 800xg with breaks off. All subsequent steps were for both types of blood tubes (A/B) the same. Aliquots of the upper phase were taken for early timepoints with a detectable viral load for viral V3 NGS. Residual Plasma was discarded and cells were resuspended with 50 mL washing buffer. Cells were collected for 15 min at 400xg with breaks on. Transferred SN into new tube and resuspended cells in 50 mL washing buffer and centrifuged both tubes for 15 min at 400xg with breaks on. Pooled all cell pellets and repeated washing step again. Resuspended cells in 10 mL washing buffer, counted cells, put 1-3 aliquots of 5X10^6 cells on side for proviral load, V3 NGS or HIV-1 poly-A determination and collected cells for 15 min at 120xg with breaks off. Removed SN and either used cells directly for downstream applications or resuspended cells in freezing medium (FBS

with 10% (v/v) DMSO) to have 10^7 cells/mL and froze 1 mL aliquots in a cryo-container at -80°C. On the next day cells were transferred to liquid nitrogen and stored until use.

X.2.5. Cell culture

X.2.5.1. Conditioned medium

HIV negative bulk PBMCs were isolated as stated in X.2.4.1. and were activated for 2 days in RPMI supplemented with 10% (v/v) FBS, 5 IU/mL Penicillin, 5 µg/mL Streptomycin, 2 µg/mL PHA-L and 100 IU/mL IL-2. Cells were washed thoroughly on day 2 and were transferred into Immuno Cult™-XF T Cell Expansion Medium (Stem Cell Technologies) with supplemented 5 IU/mL Penicillin, 5 µg/mL Streptomycin as well as 100 IU/mL IL-2 and were kept for 3 days in culture at 37°C 5% CO_2. Cells were collected for 10 min at 400xg and Medium was sterile filtered (0.2 µM pore size) and frozen at -80°C in 1.5 mL or 5 mL aliquots.

X.2.5.2. Loading of Anti-Biotin MACSiBead™ Particles (T cell Activation/Expansion system MiltenyiBiotec)

MACSiBeads™ were prepared according to manufacturer's protocol (Miltenyi Biotec). In brief, appropriate amounts of CD2-Biotin, CD3-Biotin, CD28-biotin and anti-Biotin MACSiBead particles were mixed together and volume was adjusted to 1 mL. Mixture was kept for 2 h at 2-8°C while rotating slowly. Antibody loaded MACSiBeads™ were stored at 4°C until use.

X.2.5.3. PBMC Cell thawing

Cells were quickly transferred to 37°C water bath and thawed until 90% of content was liquid. 10 ml of RPMI supplemented with 10% (v/v) FBS, 5 IU/mL Penicillin, 5 µg/mL Streptomycin and 25 IU/mL DNaseI was added slowly (dropwise manner) per 1 mL cryo-preserved cells. Collected cells for 10 min 350xg and used for downstream applications.

X.2.6. Infection experiments

X.2.6.1. Virus stock generation

One day before transfection plated 293T cells in DMEM supplemented with 10% (v/v) FBS, 5 IU/mL Penicillin, 5 µg/mL Streptomycin. At day of transfection medium was exchanged and 10 µg of plasmid were transfected according to protocol of jetPRIME® (Polyplus transfection). Cells were incubated for 6 h at 37°C, 5% CO_2. Subsequently cells were washed 3 times in PBS 1% (v/v) FBS and fresh medium was added to cells for incubation overnight at 37°C, 5% CO_2. The next day cells were once again washed as described above. After 5 h incubation at 37°C cells were washed once more in PBS and fresh medium was added for another overnight incubation at 37°C, 5% CO_2. The next day virus containing SN was harvested, centrifuged, sterile filtered (0.45µm pore size), aliquoted and stored at -80°C for downstream applications.

X.2.6.2. Spinoculation Experiments

1-2 mL of virus containing SN was concentrated by centrifugation at full speed (21130xg) for ≥ 1 h at 4°C. During centrifugation removed as much SN from SXR5 [137] cells. After 1h virus concentration discarded upper 90% of volume. Added to concentrated virus desired Medium volume and added concentrated virus to SXR5 cells. Centrifuged virus at 800xg for 1.5 h onto SXR5 cells. Topped wells with medium needed for cell propagation and incubate cells at 37°C, 5% CO_2.

X.2.6.3. X-Gal assay

X-gal assay was performed as described earlier[137]. SXR5 or TZM-bl cells were used to check infectivity of cells or viral supernatants by HIV LTR dependent β-Galactosidase activity. 2-3X10^6 SXR5 OR TZM-bl cells were plated in 50% DMEM/50% RPMI supplemented with 10% (v/v) FBS, 5 IU/mL Penicillin and 5 µg/mL Streptomycin the day before co-culture. Cells were either co-cultured for 2-3 days with infectious cells or viral supernatants were spinoculated as described in X.2.6.6. and incubated for 2-3 days before cells were fixed and freshly prepared X-Gal buffer with X-Gal substrate was added. Cells were incubated with X-Gal for 3h at 37°C and inspected under the microscope.

X.2.6.4. Quantitative viral outgrowth Assay (QVOA)

Sorted cell fractions were plated in 96-well format. Per well 10^5 patient cells were plated with addition of 10^4 SupT1 hu R5 (SupT1 expressing the CCR5 co receptor) cells for viral propagation in 50% ImmunoCult™-XF T Cell Expansion Medium, 50% conditioned medium, 100 IU IL-2 and anti-human CD3/CD28/CD2 mAb stimulation cocktail (Stem Cell Technologies). After 3 days new medium, 50IU IL-2 was added and every 2-3 days medium was exchanged. On day 7 and 14 cells were restimulated. From the 7th day onwards viral outgrowth was measured by X-Gal stain to see viral propagation over time.

X.2.7. Immunology

X.2.7.1. MACSorting of cells of interest

PBMCs were kept for at least 3-4h in RPMI supplemented with 10% (v/v) FBS, 5 IU/mL Penicillin, 5 µg/mL Streptomycin, 100 IU IL-2, 300 nM EFV, 100 nM RAL if CCR7 selection was done. For selection the Quadro MACS ™ Separator (Miltenyi Biotec) was used. Cells were selected first against CD8 and CD19, followed by CD4 selection (using REAlease® CD4 Microbead Kit, human Miltenyi Biotec) and finally selected for Integrin β7 or CCR7 according to the protocol of Anti-Biotin Microbeads kit (Miltenyi Biotec).
For CD4 untouched selection of PBMCs the CD4+ T-Cell Isolation Kit, human (Miltenyi Biotec) was used according to the manufacturers protocol.

X.2.7.2. Basic FACS staining

PBMC were kept at 37°C during all PBS washing steps. FcR was blocked for 5-10 min at RT, followed by 15 min Live/Dead and CCR7 staining. Subsequently all other surface markers were incubated for additional 20 min at RT. Cells were washed in all subsequent steps in staining buffer (PBS, 2mM EDTA, 1 % human serum). For FACS analysis a basic antibody panel was used: CD3 (UCHT1, BV510, Biolegend), CD4 (RPA-T4, BV650, Biolegend), CD8 (RPA-T8, A700 Biolegend or APC-Cy7 Beckton Dickinson), CD14 (63D3, APC-Cyanine7, Biolegend), CD19 (HIB19, APC-Cyanine7, Biolegend)., CD25(BC96, BV605, Biolegend), CD28 (CD28.2, PE-Dazzle, Biolegend), CD45RA (HI30, BV711, Biolegend), CCR7 (G043H7, APC, Biolegend), CLA (HECA-

452, PerCP-Cyanine5.5, Biolegend), Integrin ß7 (FIB504, PE-Cy7, Thermo Fisher), PD1 (EHA12-2H7, BV421, Biolegend). For pre-ART samples antibodies for barcoding against CD45 (PerCP-Cy5.5, A700, BV421, BV605, BV785, Biolegend or BUV395, Beckton Dickinson) were included. For cell sorting, an alternative antibody against CD4 (FITC, Biolegend) was used. For each antibody titrations were done to determine the best antibody concentration. For compensation UltraComp eBeads™ Compensation Beads (Thermo Fisher) were stained in the same way as cellular samples.

X.2.7.3. FACSorting

Up to 40 mL of whole blood was drawn from HIV positive individuals ≥ 6 months post-ART and CD4 cells were isolated by whole blood untouched MACS selection (Miltenyi). Preselected cells were cultured overnight in ImmunoCult™-XF T Cell Expansion Medium (Stem Cell Technologies), 1 µM AMD, 1 µM MVC, 0.5 µM EFV and 50 IU/mL IL-2 (Miltenyi) at 37°C 5% CO2. The next day cells were harvested, washed and stained as described in X.2.7.2. Cells were kept on ice before sorting on a FACS ARIA III cell sorter (Beckton Dickinson).

X.2.7.4. Biotinylation of HIV Envelope bNAbs

For each Envelope epitope one bNAb was obtained from the lab of Florian Klein (Institute of Virology Cologne): 3BNC117 (CD4 binding site), 10-1074 (V3 stem), PG-16 (V1V2 variable loop), 35O22 (gp120/gp41-interface) and 10E8 (MPER). Biotinylation was done according to the protocol of EZ-Link® Micro Sulfo-NHS-LC-Biotinylation Kit (Thermo Fisher). bNAbs 3BNC117, 10-1074 and PG-16 were combined in one bNAb mix as well as 35O22 and 10E8. Biotinylated bNAb mixes were kept at 4°C until use.

X.2.7.5. GERDA (Gag and Envelope Reactivation Detection Assay)

A CD4 untouched pre-separation step was performed to enrich for cells of interest as described in X.2.7.1. Selected cells were then stimulated in 50% ImmunoCult™-XF T Cell Expansion Medium (Stem Cell Technologies), 50% conditioned medium, 2.5 µg/mL PHA

(Sigma), 5 µM AMD, 5 µM MVC, 1 µM EFV, 5 µM Z-VAD-FMK, 100 IU IL-2 (Miltenyi) for 36-40h to reactivate dormant proviruses. HUT4-3 cells, our positive control, were stimulated with PHA 24h before staining. For optimized conditions ≥ 2.5X10^6 Ramos cells (CD19+CD3-) were added as carrier cells. Subsequently cells were surface stained for immunological characterization as described in X.2.7.2. as well as for Envelope expression. To detect Env we used 5 µg/mL biotinylated bNAb mixes A (35O22, 10E8) and B (3BNC117, 10-1074, PG16) whereof Mix A was used during initial LiveDead/CCR7 stain and Mix B with the residual surface markers. After 2 washes bNAbs were subsequently targeted by an Anti-Biotin-VioBright B515 (Miltenyi Biotec) secondary antibody. Cells were washed once again in washing buffer and were fixed for 30 min at RT in PBS 2% PFA. Cells were permeabilized twice with ICS Permeabilization Wash buffer (Biolegend) prior to intracellular staining with anti-HIV Gag (KC-57, PE, Beckman Coulter) for 30 min at RT. ICS labeled samples were washed twice in perm-wash buffer by keeping samples for each wash 10-15 min at RT before cell collection. Cells were kept on ice before acquisition on a LSRFortessa Flowcytometer (BD Bioscience). To monitor the Flowcytometer detectors over time Rainbow Calibration Particles, 6 Peaks (Biolegend) were run for each new acquisition.

X.2.8. Computational Analysis

X.2.8.1. Geno2Pheno

Geno2Pheno was used for tropism determination based on the V3 sequence. For Next Generation Sequencing the tropism was determined by Geno2Pheno454 with a FPR cut-off value of 3.5%, 5%, 10%, 15% and 20%. For Next Generation Sequencing, an R5-tropism was assigned if the relative amount of X4-variants in the patient pool was below 2%. If the relative abundance of X4-variants changed by less than 1% between different time points it was designated as “stable”.

X.2.8.2. FACS data

Flow cytometry data were analyzed using FlowJo v10.6.2 software (TreeStar). Cell populations of interest (viable CD3+CD4+/-CD8-CD14-CD19-) were exported in CSV format for t-SNE downstream applications.

X.2.8.3. T-SNE (t-distributed stochastic neighbor embedding)

Data were imported to R 3.5.2 “Eggshell Igloo”. FACS data was first normalized using arcsin (inverse hyperbolic sine function) transformation (custom code Julian Spagnuolo). For data dimension reduction thresholds for each channel were set and normalized data was dimensionally reduced by opt-SNE [139] using following features: perplexity = 30, theta = 0.5, maximal iterations = 2000, eta =200, opt-SNE End 5000, Verbosity = 25.

X.2.8.4. DBSCAN (Density-Based Spatial Clustering of Applications with Noise)

For refined clustering of the dimensional reduced data a density based semi-supervised clustering algorithm DBSCAN [194] (optimized custom code by Julian Spagnuolo) was used. Parameters Minimal points and Epsilon for DBSCAN usage were determined by running knndistplot and looking for “first” valley of the sorted k dist graph [140]. Fine tuning was achieved by scanning through 3-6 minimal points and the smallest range of eligible epsilon values, plotting noise points in obtained graphs (optimized DBSCAN code Julian Spagnuolo).

X.2.8.5. Statistics and data visualization

Data were computed by R. Correlation plots were generated with raw FACS data using ggpubr package [195]. T-SNE plots were computed with ggplot2 package [196] and individual marker expression were plotted with ggbeeswarm package [197]. Heatmaps were created by pheatmap [198]. Continuous data were log transformed and compared by paired t-test.

XI. References

1. Deng, H. K. *et al.* Identification of a major co-receptor for primary isolates of HIV-1. *Nature* **381**, 661–666 (1996).
2. Dragic, T. *et al.* HIV-1 entry into CD4+ cells is mediated by the chemokine receptor CC-CKR-5. *Nature ·* **381**, 667-673 (1996).
3. Alkhatib, G. *et al.* CC CKR5: A RANTES, MIP-1α, MIP-1β receptor as a fusion cofactor for macrophage-tropic HIV-1. *Science.* **272**, 1955–1958 (1996).
4. Feng, Y., Broder, C. C., Kennedy, P. E. & Berger, E. A. HIV-1 entry cofactor: Functional cDNA cloning of a seven-transmembrane, G protein-coupled receptor. *Science.* **272**, 872–877 (1996).
5. Zhu, T. *et al.* Genotypic and phenotypic characterization of HIV-1 in patients with primary infection. *Science.* **261**, 1179–1181 (1993).
6. Keele, B. F. *et al.* Identification and characterization of transmitted and early founder virus envelopes in primary HIV-1 infection. *Proc. Natl. Acad. Sci. USA.* **105**, 7552–7557 (2008).
7. Pantaleo, G. *et al.* Lymphoid organs function as major reservoirs for human immunodeficiency virus (viral burden/peripheral blood/polymerase chain reaction). *Proc. Natl. Acad. Sci. USA* **88**, 9838-9842 (1991).
8. Veazey, R. S. *et al.* Gastrointestinal tract as a major site of CD4+ T cell depletion and viral replication in SIV infection. *Science.* **280**, 427–431 (1998).
9. Guadalupe, M. *et al.* Severe CD4+ T-Cell Depletion in Gut Lymphoid Tissue during Primary Human Immunodeficiency Virus Type 1 Infection and Substantial Delay in Restoration following Highly Active Antiretroviral Therapy. *J. Virol.* **77**, 11708–11717 (2003).
10. Scarlatti, G. *et al.* In vivo evolution of HIV-1 co-receptor usage and sensitivity to chemokine-mediated suppression. *Nat. Med.* **3**, 1259–1265 (1997).
11. Berger, E. A., Murphy, P. M. & Farber, J. M. Chemokine receptors as HIV-1 coreceptors:Roles in viral entry, tropism, and disease. *Annu. Rev. Immunol.* **17**, 657–700 (1999).
12. Tersmette, M. *et al.* Association between biological properties of human immunodeficiency virus variants and risk for aids and aids mortality. *Lancet* **333**, 983–985 (1989).
13. Connor, R. I. & Ho, D. D. Human immunodeficiency virus type 1 variants with increased replicative capacity develop during the asymptomatic stage before disease progression. *J. Virol.* **68**, 4400–4408 (1994).
14. Weiser, B. *et al.* HIV-1 coreceptor usage and CXCR4-specific viral load predict clinical disease progression during combination antiretroviral therapy. *AIDS* **22**, 469–479 (2008).
15. Kaufmann, G. R. *et al.* Characteristics, determinants, and clinical relevance of CD4 T cell recovery to. *Clin. Infect. Dis.* **41**, 361–72 (2005).
16. Bader, J. *et al.* Correlating HIV tropism with immunological response under combination antiretroviral therapy. *HIV Med.* **17**, 615–622 (2016).
17. Bader, J. *et al.* Therapeutic immune recovery prevents emergence of CXCR4-tropic HIV-1. *Clin. Infect. Dis.* ***46***, 295-300 (2016)
18. Gulick, R. M. *et al.* Maraviroc for Previously Treated Patients with R5 HIV-1 Infection. *N. Engl. J. Med.* **35914359**, 1429–41 (2008).
19. Fätkenheuer, G. *et al.* Subgroup Analyses of Maraviroc in Previously Treated R5 HIV-1 Infection for the MOTIVATE 1 and MOTIVATE 2 Study Teams*. *N. Engl. J. Med.* **35914**, (2008).

20. Westby, M. *et al.* Emergence of CXCR4-Using Human Immunodeficiency Virus Type 1 (HIV-1) Variants in a Minority of HIV-1-Infected Patients following Treatment with the CCR5 Antagonist Maraviroc Is from a Pretreatment CXCR4-Using Virus Reservoir. *J. Virol.* **80**, 4909–4920 (2006).
21. Lewis, M. *et al.* Clonal analysis of HIV-1 genotype and function associated with virologic failure in treatment-experienced persons receiving maraviroc: Results from the MOTIVATE phase 3 randomized, placebo-controlled trials. *PLoS One* **13**, e0204099 (2018).
22. Baur, A. *et al.* Continuous clearance of HIV in a vertically infected child. *The Lancet* **334**, 1045 (1989).
23. Pratt, R. D., Shapiro, J. F., Mc Kinney, N., Kwok, S. & Spector, S. A. Virologic characterization of primary human immunodeficiency virus type 1 infection in a health care worker following needlestick injury. *J. Infect. Dis.* **172**, 851–854 (1995).
24. Cornelissen, M. *et al.* Syncytium-inducing (SI) phenotype suppression at seroconversion after intramuscular inoculation of a non-syncytium-inducing/SI phenotypically mixed human immunodeficiency virus population. *J. Virol.* **69**, 1810–1818 (1995).
25. Services, U. S. D. of H. and H. & Heckler, M. Press Conference: Secretary Margaret Heckler. (1984). Available at: https://quod.lib.umich.edu/c/cohenaids/5571095.0488.004/4?page=root;rgn=full+text;size=100;view=image. (Accessed: 22nd August 2020)
26. UNAIDS. UNAIDS fact sheet - Latest statistics on the status of the AIDS epidemic. *End. Aids Epidermics* 8 (2020). doi:2017
27. UNAIDS. 90-90-90: treatment for all | UNAIDS. *Miles To Go - Unaids Data 2018* (2018). Available at: https://www.unaids.org/en/resources/909090. (Accessed: 26th August 2020)
28. HIV/AIDS (UNAIDS), J. U. N. P. on. 2020 Global AIDS Update — Seizing the moment — Tackling entrenched inequalities to end epidemics. (2020).
29. WHO. Prevent HIV,test and treat all - who support for country impact. WHO 2016 survey. **WHO**, 64 (2016).
30. Lundgren, J. D. *et al.* Initiation of antiretroviral therapy in early asymptomatic HIV infection. *N. Engl. J. Med.* **373**, 795–807 (2015).
31. Seitz, R. et al. Human Immunodeficiency Virus (HIV). *Transfus. Med. Hemotherapy* **43**, 203–222 (2016).
32. Pollack, R. A. *et al.* Defective HIV-1 Proviruses Are Expressed and Can Be Recognized by Cytotoxic T Lymphocytes, which Shape the Proviral Landscape. *Cell Host Microbe* **21**, 494-506 (2017).
33. Klatzmann, D. *et al.* Selective tropism of lymphadenopathy associated virus (LAV) for helper-inducer T lymphocytes. *Science.* **225**, 59–63 (1984).
34. Maddon, P. J. *et al.* The T4 gene encodes the AIDS virus receptor and is expressed in the immune system and the brain. *Cell* **47**, 333–348 (1986).
35. Schnittman, S. M. *et al.* The reservoir for HIV-1 in human peripheral blood is a T cell that maintains expression of CD4. *Science.* **245**, 305–308 (1989).
36. Gartner, S. *et al.* The role of mononuclear phagocytes in HTLV-III/LAV infection. *Science.* **233**, 215–219 (1986).
37. Ganor, Y. *et al.* HIV-1 reservoirs in urethral macrophages of patients under suppressive antiretroviral therapy. *Nat. Microbiol.* **4**, 633–644 (2019).
38. Geijtenbeek, T. B. H. *et al.* DC-SIGN, a dendritic cell-specific HIV-1-binding protein that

enhances trans-infection of T cells. *Cell* **100**, 587–597 (2000).
39. McDonald, D. *et al.* Recruitment of HIV and its receptors to dendritic cell-T cell junctions. *Science.* **300**, 1295–1297 (2003).
40. Alkhatib, G. The biology of CCR5 and CXCR4. *Current Opinion in HIV and AIDS* **4**, 96–103 (2009).
41. Schuitemaker, H. *et al.* Monocytotropic human immunodeficiency virus type 1 (HIV-1) variants detectable in all stages of HIV-1 infection lack T-cell line tropism and syncytium-inducing ability in primary T-cell culture. *J. Virol.* **65**, 356–363 (1991).
42. Popovic, M., Sarngadharan, M. G., Read, E. & Gallo, R. C. Detection, isolation, and continuous production of cytopathic retroviruses (HTLV-III) from patients with AIDS and pre-AIDS. *Science.* **224**, 497–500 (1984).
43. S Broder, R. C. G. *A pathogenic retrovirus (HTLV-III) linked to AIDS*. (1984). *N. Engl. J. Med.* **311**, 1292-1297 (1984)
44. Collman, R. *et al.* An Infectious Molecular Clone of an Unusual Macrophage-Tropic and Highly Cytopathic Strain of Human Immunodeficiency Virus Type 1. *J. Virol.* **66**, 7517-7521 (1992).
45. Cocchi, F. *et al.* The V3 domain of the HIV-1 gp120 envelope glycoprotein is critical for chemokine-mediated blockade of infection. *Nature Med* **2**, (1996).
46. Jong, J. DE *et al.* Minimal Requirements for the Human Immunodeficiency Virus Type 1 V3 Domain To Support the Syncytium-Inducing Phenotype: Analysis by Single Amino Acid Substitution minimaly required for production of SI viruses. In addition, naturaly occurring mutations at residue 324 also modulate the virus phenotype. *J. Virol.* **66**, 6777-6780 (1992).
47. Fouchier, R. A. *et al.* Phenotype-associated sequence variation in the third variable domain of the human immunodeficiency virus type 1 gp120 molecule. *J. Virol.* **66**, 3183–3187 (1992).
48. Pfizer. Pfizer's Selzentry TM (Maraviroc) Tablets, Novel Treatment for HIV, Approved by FDA. (2007). Available at: https://www.drugs.com/newdrugs/pfizer-s-selzentry-maraviroc-novel-hiv-approved-fda-595.html. (Accessed: 22nd August 2020)
49. Whitcomb, J. M. *et al.* Development and characterization of a novel single-cycle recombinant-virus assay to determine human immunodeficiency virus type 1 coreceptor tropism. *Antimicrob. Agents Chemother.* **51**, 566–575 (2007).
50. Lengauer, T., Sander, O., Sierra, S., Thielen, A. & Kaiser, R. Bioinformatics prediction of HIV coreceptor usage. *Nature Biotechnology* **25**, 1407–1410 (2007).
51. Perelson, A. S., Neumann, A. U., Markowitz, M., Leonard, J. M. & Ho, D. D. HIV-1 dynamics in vivo: Virion clearance rate, infected cell life-span, and viral generation time. *Science.* **271**, 1582–1586 (1996).
52. Doitsh, G. & Greene, W. C. Dissecting How CD4 T Cells Are Lost During HIV Infection. *Cell Host Microbe* **19**, 280–291 (2016).
53. Maldarelli, F. *et al.* HIV latency. Specific HIV integration sites are linked to clonal expansion and persistence of infected cells. *Science* **345**, 179–83 (2014).
54. Wagner, T. A. *et al.* Proliferation of cells with HIV integrated into cancer genes contributes to persistent infection. *Science.* **345**, 570 LP – 573 (2014).
55. Einkauf, K. B. *et al.* Intact HIV-1 proviruses accumulate at distinct chromosomal positions during prolonged antiretroviral therapy. *J. Clin. Invest.* **129**, 988–998 (2019).
56. Pinzone, M. R. *et al.* Longitudinal HIV sequencing reveals reservoir expression leading to decay which is obscured by clonal expansion. *Nat. Commun.* **10**, 728 (2019).
57. Chomont, N. *et al.* HIV reservoir size and persistence are driven by T cell survival and

homeostatic proliferation. *Nat. Med.* **15**, 893–900 (2009).
58. Bosque, A., Famiglietti, M., Weyrich, A. S., Goulston, C. & Planelles, V. Homeostatic Proliferation Fails to Efficiently Reactivate HIV-1 Latently Infected Central Memory CD4+ T Cells. *PLoS Pathog.* **7**, e1002288 (2011).
59. Vandergeeten, C. *et al.* Interleukin-7 promotes HIV persistence during antiretroviral therapy. *Blood* **121**, 4321–4329 (2013).
60. Wang, Z. *et al.* Expanded cellular clones carrying replication-competent HIV-1 persist, wax, and wane. *Proc. Natl. Acad. Sci. USA.* **115**, E2575–E2584 (2018).
61. Mendoza, P. *et al.* Antigen-responsive CD4 + T cell clones contribute to the HIV-1 latent reservoir. JEM 217 (2020)
62. Klein, F. *et al.* Somatic Mutations of the Immunoglobulin Framework Are Generally Required for Broad and Potent HIV-1 Neutralization. *Cell* **153**, 126–138 (2013).
63. Caskey, M. *et al.* Antibody 10-1074 suppresses viremia in HIV-1-infected individuals. *Nat. Med.* **23**, 185–191 (2017).
64. Niessl, J. *et al.* Combination anti-HIV-1 antibody therapy is associated with increased virus-specific T cell immunity. *Nat. Med.* **26**, 222–227 (2020).
65. Finzi, D. *et al.* Identification of a reservoir for HIV-1 in patients on highly active antiretroviral therapy. *Science* **278**, 1295–300 (1997).
66. Siliciano, J. D. *et al.* Long-term follow-up studies confirm the stability of the latent reservoir for HIV-1 in resting CD4+ T cells. *Nat. Med.* **9**, 727–728 (2003).
67. Mahnke, Y. D., Brodie, T. M., Sallusto, F., Roederer, M. & Lugli, E. The who's who of T-cell differentiation: Human memory T-cell subsets. *Eur. J. Immunol.* **43**, 2797–2809 (2013).
68. Buzon, M. J. *et al.* HIV-1 persistence in CD4+ T cells with stem cell-like properties. *Nat. Med.* **20**, 139–142 (2014).
69. Boritz, E. A. *et al.* Multiple Origins of Virus Persistence during Natural Control of HIV Infection. *Cell* **166**, 1004–1015 (2016).
70. Hiener, B. *et al.* Identification of Genetically Intact HIV-1 Proviruses in Specific CD4 + T Cells from Effectively Treated Participants. *Cell Rep.* **21**, 813–822 (2017).
71. Banga, R *et al*. PD-1+ and follicular helper T cells are responsible for persistent HIV-1 transcription in treated aviremic individuals. *Nat. Med.* **22**, 754-761 (2016).
72. Cantero-Pérez, J. *et al.* Resident memory T cells are a cellular reservoir for HIV in the cervical mucosa. *Nat. Commun.* **10**, (2019).
73. Kwon, K. J. *et al.* Different human resting memory CD4 + T cell subsets show similar low inducibility of latent HIV-1 proviruses. *Sci. Transl. Med* **12**, 6795 (2020).
74. Buggert, M., Japp, A. S. & Betts, M. R. Everything in its right place: resident memory CD8: +: T cell immunosurveillance of HIV infection. *Curr. Opin. HIV AIDS* **14**, (2019).
75. Raehtz, K., Pandrea, I. & Apetrei, C. The well-tempered SIV infection: Pathogenesis of SIV infection in natural hosts in the wild, with emphasis on virus transmission and early events post-infection that may contribute to protection from disease progression. *Infect. Genet. Evol.* **46**, 308–323 (2016).
76. Estes, J. D. *et al.* Defining total-body AIDS-virus burden with implications for curative strategies. *Nat. Med.* **23**, 1271–1276 (2017).
77. Mohan, M. *et al.* Focused Examination of the Intestinal Epithelium Reveals Transcriptional Signatures Consistent with Disturbances in Enterocyte Maturation and Differentiation during the Course of SIV Infection. *PLoS One* **8**, e60122 (2013).
78. Hunt, P. W. *et al.* Gut Epithelial Barrier Dysfunction and Innate Immune Activation Predict Mortality in Treated HIV Infection. JID **210**, 1228-1238 (2014).

79. Berlin, C. *et al.* α4β7 lntegrin Mediates Lymphocyte Binding to the Mucosal Vascular Addressin MAdCAM. *Cell* **74**, 185-195 (1993).
80. Arthos, J. *et al.* HIV-1 envelope protein binds to and signals through integrin α4β7, the gut mucosal homing receptor for peripheral T cells. *Nat. Immunol.* **9**, 301–309 (2008).
81. Cicala, C. *et al.* The integrin α4β7 forms a complex with cell-surface CD4 and defines a T-cell subset that is highly susceptible to infection by HIV-1. *Proc. Natl. Acad. Sci. USA* **106**, 20877–20882 (2009).
82. Guzzo, C. *et al.* Virion incorporation of integrin α4β7 facilitates HIV-1 infection and intestinal homing. *Sci. Immunol* **2**, (2017).
83. Sivro, A. *et al.* Integrin α4β7 expression on peripheral blood CD4 + T cells predicts HIV acquisition and disease progression outcomes. *Sci. Transl. Med* **10**, (2018).
84. Ansari, A. A. *et al.* Blocking of α4β7 Gut-Homing Integrin during Acute Infection Leads to Decreased Plasma and Gastrointestinal Tissue Viral Loads in Simian Immunodeficiency Virus-Infected Rhesus Macaques. *J. Immunol.* **186**, 1044–1059 (2011).
85. Byrareddy, S. N. *et al.* Targeting α4β7 integrin reduces mucosal transmission of simian immunodeficiency virus and protects gut-associated lymphoid tissue from infection. *Nat. Med.* **20**, 1397–1400 (2014).
86. Byrareddy, S. N. *et al.* Sustained virologic control in SIV+ macaques after antiretroviral and α4β7 antibody therapy. *Science .* **354**, (2016).
87. Förster, R., Davalos-Misslitz, A. C. & Rot, A. CCR7 and its ligands: balancing immunity and tolerance. *Nat. Rev. Immunol.* **8**, 362–371 (2008).
88. Berg, E. L., McEvoy, L. M., Berlin, C., Bargatze, R. F. & Butcher, E. C. L-selectin-mediated lymphocyte rolling on MAdCAM-1. *Nature* **366**, 695–698 (1993).
89. Descours, B. *et al.* CD32a is a marker of a CD4 T-cell HIV reservoir harbouring replication-competent proviruses. *Nature 543, 564-567.* (2017)
90. Noto, A. *et al.* CD32 + and PD-1 + Lymph Node CD4 T Cells Support Persistent HIV-1 Transcription in Treated Aviremic Individuals. *J. Virol.* **92**, 901–919 (2018).
91. Abdel-Mohsen, M. *et al.* CD32 is expressed on cells with transcriptionally active HIV but does not enrich for HIV DNA in resting T cells. *Sci. Transl. Med* **10**, (2018).
92. Bertagnolli, L. N. *et al.* The role of CD32 during HIV-1 infection. *Nature* **561**, E17–E19 (2018).
93. Darcis, G., Kootstra, N. A., Van Lint, C., Berkhout, B. & Pasternak, A. O. CD32 + CD4 + T Cells Are Highly Enriched for HIV DNA and Can Support Transcriptional Latency. *Cell Reports* **30**, 2284-2296 (2020).
94. Malnati, M. S. *et al.* A universal real-time PCR assay for the quantification of group-M HIV-1 proviral load. *Nat. Protoc.* **3**, 1240–1248 (2008).
95. Shan, L. *et al.* A novel PCR assay for quantification of HIV-1 RNA. *J. Virol.* **87**, 6521–6525 (2013).
96. Procopio, F. A. *et al.* A Novel Assay to Measure the Magnitude of the Inducible Viral Reservoir in HIV-infected Individuals. *EBioMedicine* **2**, 874–883 (2015).
97. Baxter, A. E. *et al.* Single-Cell Characterization of Viral Translation-Competent Reservoirs in HIV-Infected Individuals. *Cell Host Microbe* **20**, 368–380 (2016).
98. Siliciano, J. D. & Siliciano, R. F. Enhanced Culture Assay for Detection and Quantitation of Latently Infected, Resting Virus in HIV-1-Infected Individuals. *Methods Mol. Biol.* **304**, 3–15 (2005).
99. Bruner, K. M. *et al.* Defective proviruses rapidly accumulate during acute HIV-1 infection. *Nat Med* **22**, 1043–1049 (2016).

100. Vernazza, P., Hirschel, B., Bernasconi, E. & Flepp, M. Les personnes séropositives ne souffrant d'aucune autre MST et suivant un traitement antirétroviral efficace ne transmettent pas le VIH par voie sexuelle. *Bull. des Médecins Suisses* **89**, 165–169 (2008).
101. Rodger, A. J. *et al.* Sexual Activity Without Condoms and Risk of HIV Transmission in Serodifferent Couples When the HIV-Positive Partner Is Using Suppressive Antiretroviral Therapy. *JAMA* **316**, 171-181 (2016).
102. HIV Prevention Trials Network. HPTN 052 Study Summary. (2010).
103. FDA. Approval for TRUVADA (emtricitabine/tenofovir disoproxil fumarate) as PREP. Available at: www.TRUVADApreprems.com. (Accessed: 10th August 2020)
104. Grant, R. M. *et al.* Preexposure chemoprophylaxis for HIV prevention in men who have sex with men. *N. Engl. J. Med.* **363**, 2587–2599 (2010).
105. Heendeniya, A. & Bogoch, I. I. HIV prevention with post-exposure prophylaxis-in-pocket. *The Lancet Public Health* **4**, e494 (2019).
106. The HIV Prevention Trial Network. HPTN083. (2020). Available at: https://www.hptn.org/research/studies/hptn083#block-views-block-study-related-publications-block-1. (Accessed: 10th August 2020)
107. Scheid, J. F. *et al.* A method for identification of HIV gp140 binding memory B cells in human blood. *J. Immunol. Methods* **343**, 65–67 (2009).
108. Scheid, J. F. *et al.* Broad diversity of neutralizing antibodies isolated from memory B cells in HIV-infected individuals. *Nature* **458**, 636–640 (2009).
109. Bar-On, Y. *et al.* Safety and antiviral activity of combination HIV-1 broadly neutralizing antibodies in viremic individuals. *Nat. Med.* **24**, 1701–1707 (2018).
110. Rusert, P. *et al.* Determinants of HIV-1 broadly neutralizing antibody induction. *Nat Med* **22**, 1260-1267(2016).
111. Caskey, M., Klein, F. & Nussenzweig, M. C. Broadly neutralizing anti-HIV-1 monoclonal antibodies in the clinic. *Nat. Med.* **25**, 547–553 (2019).
112. Burton, D. R. & Hangartner, L. Broadly Neutralizing Antibodies to HIV and Their Role in Vaccine Design. Annu. Rev. Immunol **34**,635-659 (2016)
113. Bednarik, D. P. *et al.* DNA CpG methylation inhibits binding of NF-kappa B proteins to the HIV-1 long terminal repeat cognate DNA motifs. *New Biol.* **3**, 969–976 (1991).
114. Lint, C. Van, Emiliani, S., Ott, M. & Verdin, E. Transcriptional activation and chromatin remodeling of the HIV-I promoter in response to histone acetylation. *EMBO J.* **15**, 1112–1120 (1996).
115. Jiang, C. *et al.* Distinct viral reservoirs in individuals with spontaneous control of HIV-1. *Nature* **585**, 261-267(2020)
116. Cohn, L. B. *et al.* Clonal CD4+ T cells in the HIV-1 latent reservoir display a distinct gene profile upon reactivation. *Nat. Med.* **24**, 604–609 (2018).
117. Yukl, S. A. *et al.* HIV latency in isolated patient CD4+ T cells may be due to blocks in HIV transcriptional elongation, completion, and splicing. *Sci. Transl. Med.* **10**, eaap9927 (2018).
118. Lassen, K. G., Ramyar, K. X., Bailey, J. R., Zhou, Y. & Siliciano, R. F. Nuclear retention of multiply spliced HIV-1 RNA in resting CD4+ T cells. *PLoS Pathog.* **2**, 0650–0661 (2006).
119. Kim, Y., Anderson, J. L. & Lewin, S. R. Getting the "Kill" into "Shock and Kill": Strategies to Eliminate Latent HIV. *Cell Host and Microbe* **23**, 14–26 (2018).
120. Spivak, A. M. *et al.* HIV-1 Eradication: Early Trials (and Tribulations). *Trends Mol. Med.* **22**, 10–27 (2016).
121. Hütter, G. *et al.* Long-Term Control of HIV by CCR5 Delta32/ Delta32 Stem-Cell

Transplantation. *N. Engl. J. Med* 360, 692-698 (2009).
122. Gupta, R. K. *et al.* HIV-1 remission following CCR5Δ32/Δ32 haematopoietic stem-cell transplantation. *Nature* **568**, 244–248 (2019).
123. Bjoern-Erik O. Jensen, Dieter Häussinger, Elena Knops, Annemarie Wensing, Javier Martinez-Picado, Monique Nijhuis, Maria Salgado, Jacob D. Estes, Nadine Lübke, Rolf Kaiser, Thomas Harrer, Johannes Fischer, Julian Schulze zur Wiesch, Johanna M. Eberhard, G. K. CCR5Δ32 SCT-INDUCED HIV REMISSION: TRACES OF HIV DNA BUT FADING IMMUNE REACTIVITY - CROI Conference. *CROI 2020* Available at: https://www.croiconference.org/abstract/ccr5δ32-sct-induced-hiv-remission-traces-of-hiv-dna-but-fading-immune-reactivity/. (Accessed: 10th August 2020)
124. Samson, M. *et al.* Resistance to HIV-1 infection in caucasian individuals bearing mutant alleles of the CCR-5 chemokine receptor gene. *Nature* **382**, 722–726 (1996).
125. Dean, M. *et al.* Genetic restriction of HIV-1 infection and progression to AIDS by a deletion allele of the CKR5 structural gene. *Science (80-.).* **273**, 1856–1862 (1996).
126. Liu, R. *et al.* Homozygous defect in HIV-1 coreceptor accounts for resistance of some multiply-exposed individuals to HIV-1 infection. *Cell* **86**, 367–377 (1996).
127. Peterson, C. W. & Kiem, H. P. Lessons from London and Berlin: Designing A Scalable Gene Therapy Approach for HIV Cure. *Cell Stem Cell* **24**, 685–687 (2019).
128. Eberhard, J. M. *et al.* Vulnerability to reservoir reseeding due to high immune activation after allogeneic hematopoietic stem cell transplantation in individuals with HIV-1. *Sci. Transl. Med.* **12**, 9355 (2020).
129. Michael, N. L. *et al.* Exclusive and Persistent Use of the Entry Coreceptor CXCR4 by Human Immunodeficiency Virus Type 1 from a Subject Homozygous for CCR5 32. *J Virol* **72**, 6040-6047 (1998).
130. Gorry, P. R. *et al.* Persistence of dual-tropic HIV-1 in an individual homozygous for the CCR5Δ32 allele. The *Lancet* **359**, 1832–1834 (2002).
131. Kordelas, L., Verheyen, J. & Esser, S. Shift of HIV tropism in stem-cell transplantation with CCR5 delta32 mutation. *New England Journal of Medicine* **371**, 880–882 (2014).
132. Andrew, D. P., Rott, L. S., Kilshaw, P. J. & Butcher, E. C. Distribution of α4β7 and αEβ7 integrins on thymocytes, intestinal epithelial lymphocytes and peripheral lymphocytes. *Eur. J. Immunol.* **26**, 897–905 (1996).
133. Klimkait, T., Strebel, K., Hoggan, M. D., Martin, M. A. & Orenstein, J. M. The human immunodeficiency virus type 1-specific protein vpu is required for efficient virus maturation and release. *J. Virol.* **64**, 621–629 (1990).
134. Rhee, S. S. & Marsh, J. W. Human immunodeficiency virus type 1 Nef-induced down-modulation of CD4 is due to rapid internalization and degradation of surface CD4. *J. Virol.* **68**, 5156–5163 (1994).
135. Grau-Expósito, J. *et al.* A novel single-cell FISH-flow assay identifies effector memory CD4+ T cells as a major niche for HIV-1 transcription in HIV-infected patients. *MBio* **8**, (2017).
136. Hamy, F. *et al.* An inhibitor of the Tat/TAR RNA interaction that effectively suppresses HIV-1 replication. *Proc. Natl. Acad. Sci. USA.* **94**, 3548–53 (1997).
137. Klimkait, T., Stauffer, F., Lupo, E. & Sonderegger-Rubli, C. Dissecting the mode of action of various HIV-inhibitor classes in a stable cellular system. *Arch Virol* **143**, 2109-2131 (1998).
138. Van Der Maaten, L. & Hinton, G. Visualizing data using t-SNE. *J. Mach. Learn. Res.* **9**, 2579–2625 (2008).
139. Belkina, A. C. *et al.* Automated optimized parameters for T-distributed stochastic

neighbor embedding improve visualization and analysis of large datasets. *Nat. Commun.* **10**, (2019).
140. Ester, M., Kriegel, H.-P., Sander, J. & Xu, X. A Density-Based Algorithm for Discovering Clusters in Large Spatial Databases with Noise.Comprehensive Chemometrics **2**, 635-654 (1996).
141. Bachmann, N. *et al.* Determinants of HIV-1 reservoir size and long-term dynamics during suppressive ART. *Nat. Commun.* **10**, (2019).
142. Swenson, L. C. *et al.* Improved Detection of CXCR4-Using HIV by V3 Genotyping: Application of Population-Based and "Deep" Sequencing to Plasma RNA and Proviral DNA. *JAIDS J. Acquir. Immune Defic. Syndr.* **54**, 506–510 (2010).
143. Spira, A. I. *et al.* Cellular targets of infection and route of viral dissemination after an intravaginal inoculation of simian immunodeficiency virus into rhesus macaques. *J. Exp. Med.* **183**, 215–225 (1996).
144. Miller, C. J. *et al.* Propagation and Dissemination of Infection after Vaginal Transmission of Simian Immunodeficiency Virus. *J. Virol.* **79**, 9217–9227 (2005).
145. Deleage, C. *et al.* Defining early SIV replication and dissemination dynamics following vaginal transmission. *Sci. Adv.* **5**, (2019).
146. M Leung, D. Y. *et al.* Clinical reviews in allergy and immunology The gut microbiota and inflammatory noncommunicable diseases: Associations and potentials for gut microbiota therapies. *J. Allergy Clin. Immunol.* **135**, 3–13 (2015).
147. Shan, L. *et al.* Transcriptional Reprogramming during Effector-to-Memory Transition Renders CD4 + T Cells Permissive for Latent HIV-1 Infection. *Immunity* **47**, 766-775.e3 (2017).
148. Coffin, J. M. *et al.* Clones of infected cells arise early in HIV-infected individuals. *JCI Insight* **4**, (2019).
149. Bosque, A. & Planelles, V. Induction of HIV-1 latency and reactivation in primary memory CD4 T cells. Blood **113**, 58-65 (2009).
150. Lu, C. L. *et al.* Relationship between intact HIV-1 proviruses in circulating CD4+ T cells and rebound viruses emerging during treatment interruption. *Proc. Natl. Acad. Sci. U. S. A.* **115**, E11341–E11348 (2018).
151. Bruner, K. M. *et al.* A quantitative approach for measuring the reservoir of latent HIV-1 proviruses. *Nature* **566**, 120–125 (2019).
152. de Verneuil, A. *et al.* Genetically Intact but Functionally Impaired HIV-1 Env Glycoproteins in the T-Cell Reservoir. *J. Virol.* **92**, e01684-17 (2018).
153. Wiegand, A. *et al.* Single-cell analysis of HIV-1 transcriptional activity reveals expression of proviruses in expanded clones during ART. *Proc. Natl. Acad. Sci.* **114**, E3659-E3668 (2017)
154. Imamichia, H. *et al.* Defective HIV-1 proviruses produce novel proteincoding RNA species in HIV-infected patients on combination antiretroviral therapy. *Proc. Natl. Acad. Sci. U. S. A.* **113**, 8783–8788 (2016).
155. Imamichi, H. *et al.* Defective HIV-1 proviruses produce viral proteins. *Proc. Natl. Acad. Sci.* **117**, 3704–3710 (2020).
156. Sun, W. *et al.* Mathematical determination of the HIV-1 matrix shell structure and its impact on the biology of HIV-1. *PLoS One* **14**, e0224965 (2019).
157. Zhu, P. *et al.* Electron tomography analysis of envelope glycoprotein trimers on HIV and simian immunodeficiency virus virions. *Proc. Natl. Acad. Sci.* **100**, 15812-15817 (2003).
158. Saka, S. K. *et al.* Immuno-SABER enables highly multiplexed and amplified protein

imaging in tissues. *Nat. Biotechnol.* **37**, 1080–1090 (2019).
159. Sneller, M. C. *et al.* An open-label phase 1 clinical trial of the anti- α4β7 monoclonal antibody vedolizumab in HIV-infected individuals. *Sci. Transl. Med* **11**, (2019).
160. Marie-Angé lique De Scheerder, A., Vrancken, B., Dellicour, S., Lemey, P. & Palmer, S. HIV Rebound Is Predominantly Fueled by Genetically Identical Viral Expansions from Diverse Reservoirs. *Cell Host Microbe* **26**, 347–358 (2019).
161. Chaillon, A. *et al.* HIV persists throughout deep tissues with repopulation from multiple anatomical sources. *J. Clin. Invest.* **130**, 1699–1712 (2020).
162. AIDS 2020 virtual. OAA0404, Imamichi H, Abstract Supplement Oral Abstracts from the 23rd International AIDS Conference, 6-10 July 2020. *J. Int. AIDS Soc.* **23**, (2020).
163. Ho, Y.-C. *et al.* Replication-Competent Noninduced Proviruses in the Latent Reservoir Increase Barrier to HIV-1 Cure. *Cell* **155**, 540–551 (2013).
164. Hosmane, N. N. *et al.* Proliferation of latently infected CD4(+) T cells carrying replication-competent HIV-1: Potential role in latent reservoir dynamics. *J. Exp. Med.* **214**, 959-972 (2017)
165. Deeks, S. G. *et al.* International AIDS Society global scientific strategy: Towards an HIV cure 2016. *Nature Medicine* **22**, 839–850 (2016).
166. Spina, C. A. *et al.* An In-Depth Comparison of Latent HIV-1 Reactivation in Multiple Cell Model Systems and Resting CD4+ T Cells from Aviremic Patients. *PLoS Pathog.* **9**, 1–15 (2013).
167. Derdeyn, C. A. *et al.* Envelope-Constrained Neutralization-Sensitive HIV-1 After Heterosexual Transmission. *Science (80-.).* **303**, 2019–2022 (2004).
168. Salazar-Gonzalez, J. F. *et al.* Deciphering human immunodeficiency virus type 1 transmission and early envelope diversification by single-genome amplification and sequencing. *J. Virol.* **82**, 3952–70 (2008).
169. Redd, A. D. *et al.* Previously transmitted HIV-1 strains are preferentially selected during subsequent sexual transmissions. *J. Infect. Dis.* **206**, 1433–1442 (2012).
170. Williams-Wietzikoski, C. A. *et al.* Comparisons of Human Immunodeficiency Virus Type 1 Envelope Variants in Blood and Genital Fluids near the Time of Male-to-Female Transmission. *jvi.asm.org 1 J. Virol.* **93**, 1769–1787 (2019).
171. Abrahams, M.-R. *et al.* The replication-competent HIV-1 latent reservoir is primarily established near the time of therapy initiation. *Sci. Transl. Med* **11**, (2019).
172. Brooks, K. *et al.* HIV-1 variants are archived throughout infection and persist in the reservoir. *PLoS Pathog.* **16**, e1008378 (2020).
173. Lorenzi, J. C. C. *et al.* Paired quantitative and qualitative assessment of the replication-competent HIV-1 reservoir and comparison with integrated proviral DNA. *Proc. Natl. Acad. Sci. U. S. A.* **113**, E7908–E7916 (2016).
174. Bui, J. K. *et al.* Proviruses with identical sequences comprise a large fraction of the replication-competent HIV reservoir. *PLOS Pathog.* **13**, e1006283 (2017).
175. Barré-Sinoussi, F. *et al.* Isolation of a T-lymphotropic retrovirus from a patient at risk for acquired immune deficiency syndrome (AIDS). *Science.* **220**, 868–871 (1983).
176. Zhou, S., Bednar, M. M., Sturdevant, C. B., Hauser, B. M. & Swanstrom, R. Deep Sequencing of the HIV-1 env Gene Reveals Discrete X4 Lineages and Linkage Disequilibrium between X4 and R5 Viruses in the V1/V2 and V3 Variable Regions. *J. Virol.* **90**, 7142–58 (2016).
177. Lee, B., Sharron, M., Montaner, L. J., Weissman, D. & Doms, R. W. Quantification of CD4, CCR5, and CXCR4 levels on lymphocyte subsets, dendritic cells, and differentially conditioned monocyte-derived macrophages. *Proc. Natl. Acad. Sci. USA.* **96**, 5215–

5220 (1999).
178. Blaak, H. *et al.* In vivo HIV-1 infection of CD45RA+CD4+ T cells is established primarily by syncytium-inducing variants and correlates with the rate of CD4+ T cell decline. *Proc. Natl. Acad. Sci. USA.* **97**, 1269–1274 (2000).
179. Nishimura, Y. *et al.* Resting naive CD4+ T cells are massively infected and eliminated by X4-tropic simian-human immunodeficiency viruses in macaques. *Proc. Natl. Acad. Sci.* **102**, 8000–8005 (2005).
180. Zerbato, J. M., McMahon, D. K., Sobolewski, M. D., Mellors, J. W. & Sluis-Cremer, N. Naive CD4+ T Cells Harbor a Large Inducible Reservoir of Latent, Replication-competent Human Immunodeficiency Virus Type 1. *Clin. Infect. Dis.* **69**, 1919-1925 (2019)
181. Rullo, E. V. *et al.* Genetic Evidence That Naive T Cells Can Contribute Significantly to the Human Immunodeficiency Virus Intact Reservoir: Time to Re-evaluate Their Role. *Clinical Infectious Diseases* **69**, 2236–2237 (2019).
182. Jones, B. R. *et al.* Genetic Diversity, Compartmentalization, and Age of HIV Proviruses Persisting in CD4 + T Cell Subsets during Long-Term Combination Antiretroviral Therapy. *J. Virol.* **94**, 1786–1805 (2019).
183. Van Rij, R. P. *et al.* Differential coreceptor expression allows for independent evolution of non-syncytium-inducing and syncytium-inducing HIV-1. *J. Clin. Invest.* **106**, 1039–1052 (2000).
184. Hamlyn, E. *et al.* Increased levels of CD4 T-cell activation in individuals with CXCR4 using viruses in primary HIV-1 infection. *AIDS* **26**, 887–890 (2012).
185. Wei, X. *et al.* Antibody neutralization and escape by HIV-1. *Nature* **422**, 307–312 (2003).
186. Bunnik, E. M., Quakkelaar, E. D., Van Nuenen, A. C., Boeser-Nunnink, B. & Schuitemaker, H. Increased Neutralization Sensitivity of Recently Emerged CXCR4-Using Human Immunodeficiency Virus Type 1 Strains Compared to Coexisting CCR5-Using Variants from the Same Patient. *J. Virol.* **81**, 525–531 (2007).
187. Bunnik, E. M. *et al.* Adaptation of HIV-1 envelope gp120 to humoral immunity at a population level. *Nat. Med.* **16**, 995-997 (2010)
188. Harouse, J. M. *et al.* CD8+ T cell-mediated CXC chemokine receptor 4-simian/human immunodeficiency virus suppression in dually infected rhesus macaques. *Proc. Natl. Acad. Sci. U. S. A.* **100**, 10977–10982 (2003).
189. Bonhoeffer, S., Holmes, E. C. & Nowak, M. A. Causes of HIV diversity. *Nature* **376**, 125 (1995).
190. Yamaguchi, Y. & Gojobori, T. Evolutionary mechanisms and population dynamics of the third variable envelope region of HIV within single hosts. *Proc. Natl. Acad. Sci. U. S. A.* **94**, 1264–1269 (1997).
191. Fletcher, C. V *et al.* Persistent HIV-1 replication is associated with lower antiretroviral drug concentrations in lymphatic tissues. *Proc. Natl. Acad. Sci. USA.* **111**, 2307–12 (2014).
192. Thompson, C. G. *et al.* Heterogeneous antiretroviral drug distribution and HIV/SHIV detection in the gut of three species. *Sci. Transl. Med.* **11**, eaap8758 (2019).
193. Hsiao, F. *et al.* Tissue memory CD4+ T cells expressing IL-7 receptor-alpha (CD127) preferentially support latent HIV-1 infection. *PLoS Pathog.* **16**, e1008450 (2020).
194. Hahsler, M., Piekenbrock, M. & Doran, D. dbscan: Density Based Clustering of Applications with Noise (DBSCAN) and Related Algorithms. *Journal of Statistical Software* **91**, (2019).

195. Kassambara, A. ‘ggplot2’ Based Publication Ready Plots [R package ggpubr version 0.4.0].
196. Wickham, H. *ggplot2*. *ggplot2* (2009). doi:10.1007/978-0-387-98141-3
197. Clarke, E. CRAN - Package ggbeeswarm. (2017). Available at: https://cran.r-project.org/web/packages/ggbeeswarm/index.html. (Accessed: 9th September 2020)
198. Kolde, R. & Lizee, A. GitHub - raivokolde/pheatmap: Pretty heatmaps. *GitHub* (2015). Available at: https://github.com/raivokolde/pheatmap. (Accessed: 31st August 2020)

XII. Supplemental Tables

Supplemental Table 1. HIV-1 reservoir in T-cell subsets. Representative data of individual P04. Proviral and Poly-A quantification were done 9 days post stimulation. GERDA was performed on day 14 post stimulation. Results are normalized to 10E6 cells. GERDA: Gag and Envelope Reactivation Detection Assay. IUPM: infectious units per million. ND: not detectable. QVOA: Quantitative Viral Outgrowth Assay. Poly-A: HIV poly-A transcripts

	Provirus Day 9	Poly A (VQA) Day 9		GERDA		QVOA
ID	**HIV DNA/10E6**	**HIV PolyA/10E6**	**HIV RNA/HIV DNA**	**HIV Gag+ /10E6**	**HIV Gag+ Env+/10E6-**	**IUPM**
P04_T4_TN	ND	ND	ND	9	ND	ND
P04_T4_TCM	69	1'103	16	260	1	ND-
P04_T4_TTM	16	ND	ND	110	ND	ND
P04_T4_TEM	ND	ND	ND	ND	ND	ND

Supplemental Table 2 A+B. V3 loop NGS. Representative NGS data of first 10 most detected V3 variants of Patient P05. Individual aligned V3 variants of time point 1 descending by relative abundance with amino changes highlighted in red. A: To highlight the fate of each listed V3 variant from timepoint 1, all consecutive timepoints for proviral (DNA) and viral (RNA) V3 variants are listed in comparison to each V3 variant of timepoint 1 with indication of V3 rank and its relative abundance. Table B: all V3 sequences are compared to the 10 most abundant sequences of timepoint 5. [*CW]: either C or W possible for translation. FPR: False positive rate (Geno2Pheno$_{coreceptor}$), rel.ab: relative abundance. Count: absolute number of same variants detected.

A

Timepoint 1 (T1) DNA					T2 DNA	T5 DNA	T1 RNA
Rank	**V3.LOOP**	**COUNT**	**FPR**	**Rel.ab.**	**(Rank; Rel.ab.)**	**(Rank; Rel.ab.)**	**(Rank; Rel.ab.)**
1	CTRPGNNTRRSIHIGPGKAFYTSEITGDIRQAHC	28991	18.46	96.42	1; 76.6%	1; 52.4%	1; 96.8%
2	CTRPGNNTRRSIHIGPGKAFYTSEITGDIRPVSY	199	78.34	0.66	7; 0.22%	13; 0.15%	2; 0.8%
3	GTRPGNNTRRSIHIGPGKAFYTSEITGDIRQAHC	98	26.45	0.33	9; 0.16%	61; 0.02%	3; 0.62%
4	CTRPGNNTRRSIHIGPGKAFYISEITGDIRQAHC	41	7.27	0.14	-	-	-
5	CTRPDNNTRRSIHIGPGKAFYTSEITGDIRQAHC	31	28.63	0.10	38; 0.03%	-	5; 0.14%
6	KRQPGNNTRRSIHIGPGKAFYTSEITGDIRQAHC	29	17.15	0.10	37; 0.03%	-	4; 0.2%
7	RQRPGNNTRRSIHIGPGKAFYTSEITGDIRQAHC	25	13.37	0.08	-	-	7; 0.08%
8	CTRAGNNTRRSIHIGPGKAFYTSEITGDIRQAHC	21	28.92	0.07	44; 0.03%	71; 0.02%	18; 0.04%
9	CTRPGNNTRRSIHIGAGKAFYTSEITGDIRQAHC	19	8.72	0.06	-	68; 0.02%	10; 0.05%
10	[*CW]TRPGNNTRRSIHIGPGKAFYTSEITGDIRQAHC	17	23.55	0.06	-	34; 0.03%	-

B

Timepoint 5 (T5) DNA					T1 DNA	T2 DNA	T1 RNA
Rank	**V3.LOOP**	**COUNT**	**FPR**	**Rel.ab.**	**(Rank; Rel.ab.)**	**(Rank; Rel.ab.)**	**(Rank; Rel.ab.)**
1	CTRPGNNTRRSIHIGPGKAFYTSEITGDIRQAHC	7612	18.46	52.35	1; 96.4%	1; 76.6%	1; 96.8%
2	CTRPGNNTRRSIHIGPGKAFYTAEITGDIRQAHC	3327	11.63	22.88	43; 0.03%	-	12; 0.04%
3	CTRPGNNTRKSIHIGPGKAFYTSEITGDIRQAHC	725	16.86	4.99	-	4; 5.4%	-
4	CTRPGNNTRRSIHIGPGRAFYTSEITGDIRQAHC	695	15.84	4.78	40; 0.02%	8; 0.18%	-
5	CTRPGNNTRKSIHIGPGKALYTTEITGDIRQAHC	483	33.72	3.32	-	-	-
6	CTRPGNNTRRSINIGPGRAFYTSEITGDIRQAHC	393	27.62	2.70	-	2; 5.7%	-
7	CIRPGIKTRRIIHIGPGKAFYTS-GTGDIRKAHC	357	0.58	2.46	-	-	-
8	CIRPGIKTRRIIHIGPGKAFYTSGITGDIRKAHC	242	0.73	1.66	-	3; 5.5%	-
9	CIRPGIKTRRIIHIGPGKAFYTS--TGDIRKAHC	148	0.29	1.02	-	-	-
10	CTRPGNNTRRSIHIGPGKAFYTTEITGDIRQAHC	46	16.72	0.32	25; 0.03%	-	-

XIII. Supplemental Figures

SUPPLEMENTAL FIGURE 1 MACS fraction purity

A

Sample Name	Subset Name
26449_B7+4+8-19-_007.fcs	Single Cells
26449_B7+4-8-19-_008.fcs	Single Cells
26449_B7-4+8-19-_009.fcs	Single Cells
26449_B7-4-8-19-_010.fcs	Single Cells
26449_8+19+_006.fcs	Single Cells
26449_unstained control_011.fcs	Single Cells

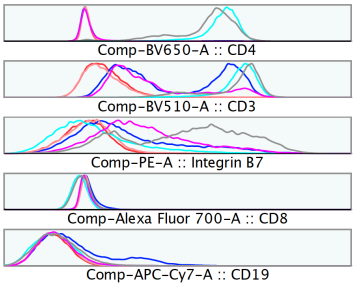

Ancestry Subset Statistic For	CD3+ CD4+	B7+
26449_B7+4+8-19-_007.fcs	88.5	70.3
26449_B7+4-8-19-_008.fcs	0.99	38.4
26449_B7-4+8-19-_009.fcs	98.0	9.92
26449_B7-4-8-19-_010.fcs	0.069	2.03
26449_unstained control_011.fcs	0.016	0.53
26449_8+19+_006.fcs	3.81	27.5

Ancestry Subset Statistic For	CD3- CD19+
26449_B7+4+8-19-_007.fcs	0.050
26449_B7+4-8-19-_008.fcs	0.62
26449_B7-4+8-19-_009.fcs	0.025
26449_B7-4-8-19-_010.fcs	0.15
26449_unstained control_011.fcs	0
26449_8+19+_006.fcs	13.3

B

Sample Name	Subset Name
25832_R7+4+8-19-_002.fcs	Single Cells
25832_R7+4-8-19-_003.fcs	Single Cells
25832_R7-4+8-19-_004.fcs	Single Cells
25832_R7-4-8-19-_005.fcs	Single Cells
25832_8+19+_001.fcs	Single Cells
25832_unstained_006.fcs	Single Cells

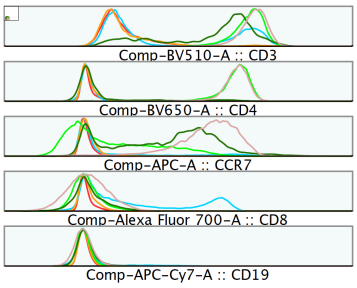

Ancestry Subset Statistic For	CD3+ CD4+	CCR7+
25832_R7+4+8-19-_002.fcs	98.6	94.1
25832_R7+4-8-19-_003.fcs	7.29	62.4
25832_R7-4+8-19-_004.fcs	98.2	22.5
25832_R7-4-8-19-_005.fcs	0.076	2.49
25832_unstained_006.fcs	0	0.016
25832_8+19+_001.fcs	2.34	17.2

Ancestry Subset Statistic For	CD3+ CD4+	CCR7+
25832_R7+4+8-19-_002.fcs	98.6	94.1
25832_R7+4-8-19-_003.fcs	7.29	62.4
25832_R7-4+8-19-_004.fcs	98.2	22.5
25832_R7-4-8-19-_005.fcs	0.076	2.49
25832_unstained_006.fcs	0	0.016
25832_8+19+_001.fcs	2.34	17.2

Supplemental Figure 1 related to Figure 5+6. MACS fraction purity evaluation. A: All fractions separated for Integrin β_7. B: All fractions separated for CCR7. Histoplots show expression of each relevant marker for fraction identification. Tables underneath plots highlight critical marker expression for fraction assignment. To see individual differences among fractions, rows were highlighted with heatmap colors ranging from low (blue) to high (yellow) expression

SUPPLEMENTAL FIGURE 2 GERDA methodology

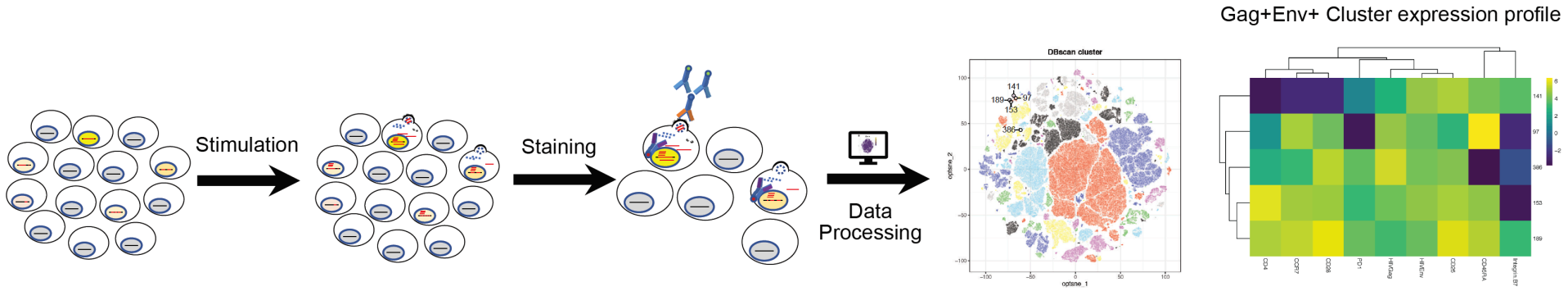

Supplemental Figure 2. GERDA workflow. Preselected CD4 untouched PBMCs, PHA -stimulated, are extracellularly stained for immunological markers and HIV Env, intracellular antibody-stain is used for HIV Gag protein. Dimensional reduction and cluster analysis of acquired FACS data are performed using t-SNE and DBSCAN. T-SNE plot highlighting all clusters identified by DBSCAN (Color palette does not allow to highlight each individual cluster in an individual color). Gag+Env+ events are marked inside plot with individual patient ID. Mean marker expression of each identified cluster is shown by heatmaps.

SUPPLEMENTAL FIGURE 3 GERDA specificity

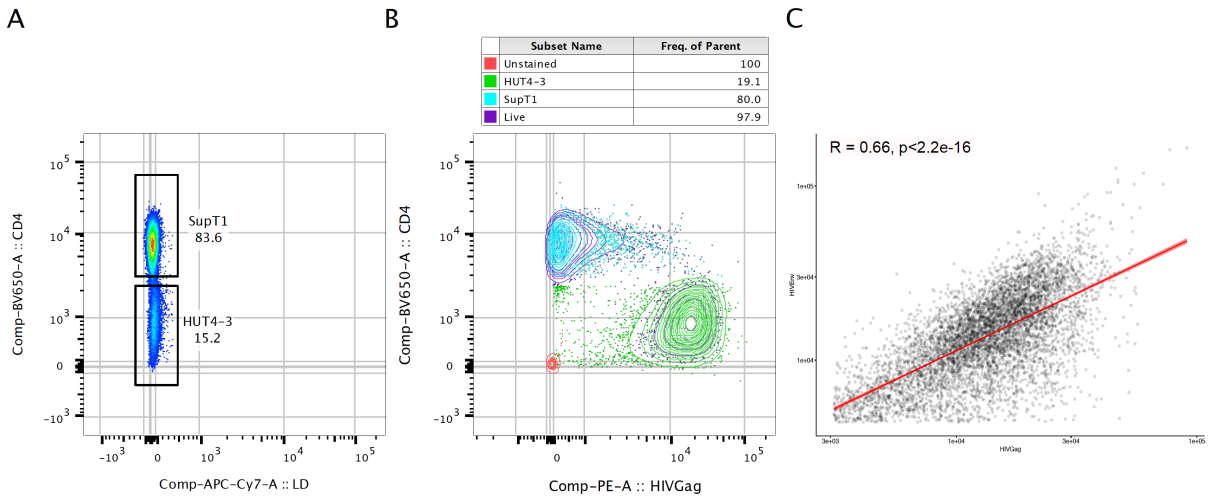

Supplemental Figure 3 related to Figure 7. GERDA staining establishment. A, B: FACS profiles of a mixed pool of infected (HUT4-3) and uninfected (SupT1) cells. SupT1 and HUT4-3 cells identified by CD4 vs Live/Dead (A) and CD4 vs HIV Gag (B). C: Gag (x-axis) vs Env (y-axis) correlation plot of Figure 7 Quadrant Q2

SUPPLEMENTAL FIGURE 4 Sensitivity of the GERDA system

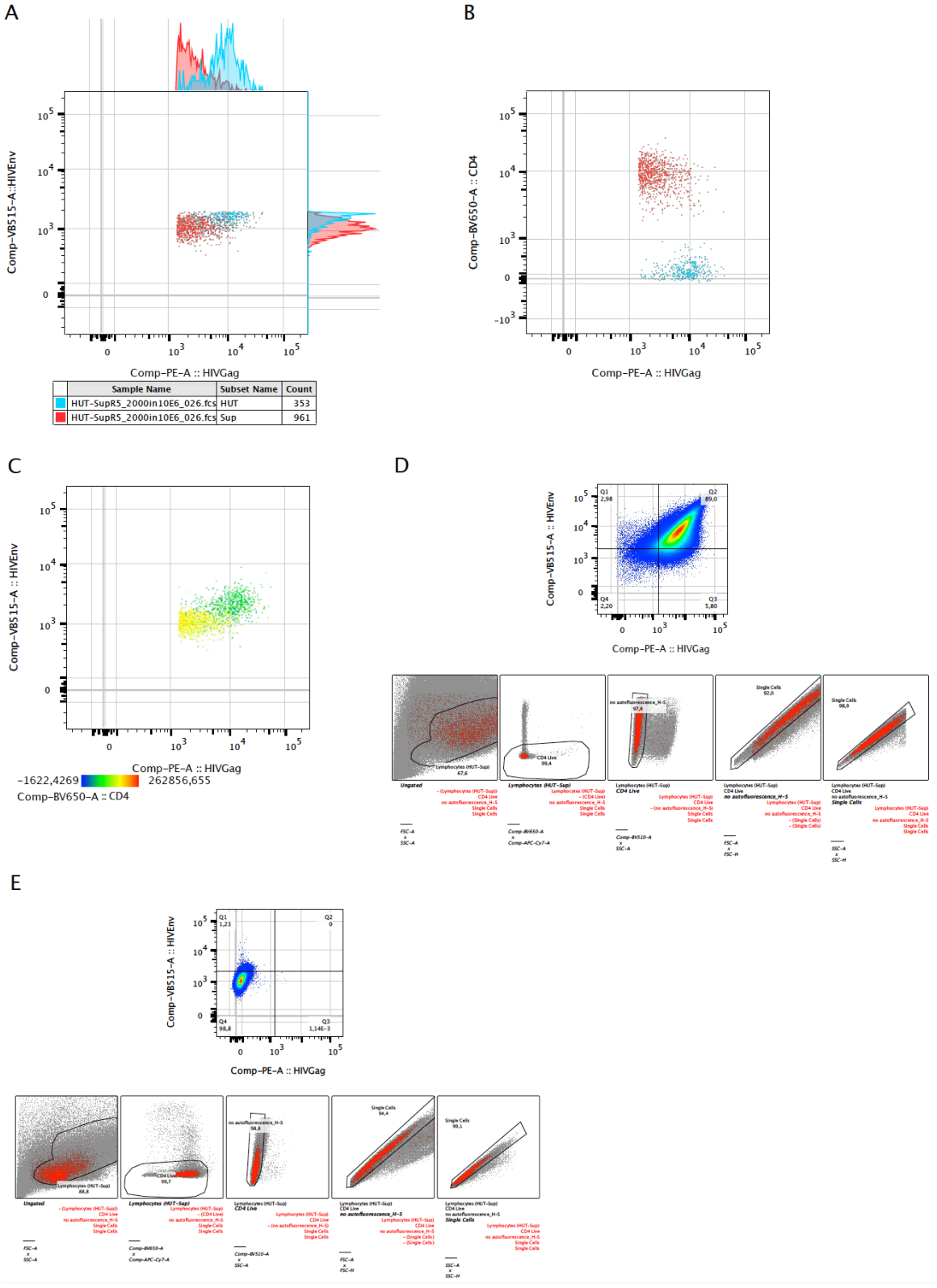

SUPPLEMENTAL FIGURE 4 Sensitivity of the GERDA system

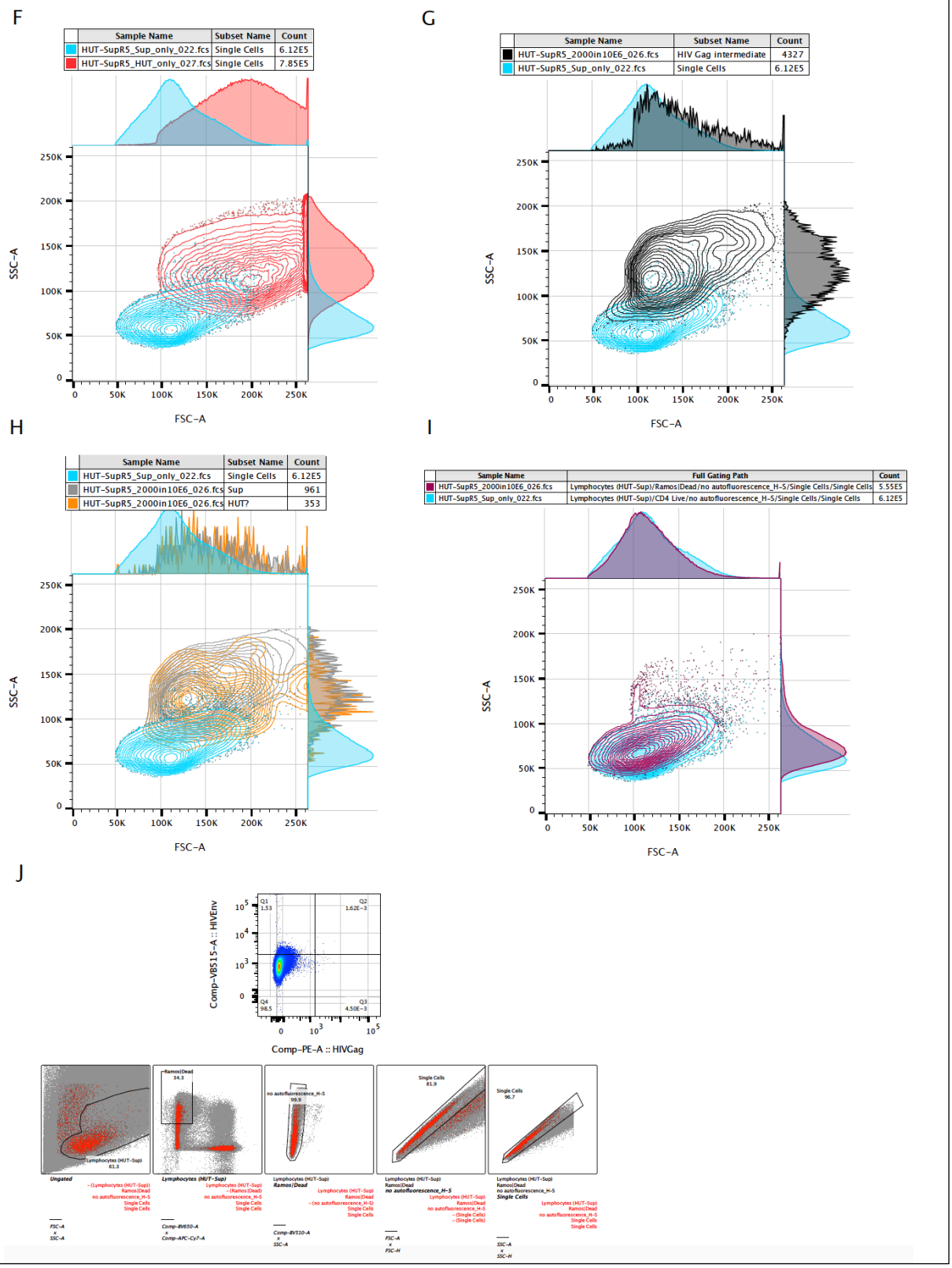

Supplemental Figure 4 related to Figure 8. GERDA sensitivity. 1600 input condition. A, B: Gag+Env+ (Q2) events pre-gated by CD4+ (SupT1, red) and CD4- (HUT4-3, blue) expressing cells looking at Gag vs Env expression (A) or CD4 vs Gag (B). C: HIV Gag vs HIV Env expression of Gag+ cells (Q2+Q3) with CD4 heatmap. D, E: Backgating (final gated population overlaid at each level in red) of HUT4-3 (D) or SupT1 cells (E). F-I: Scatter profile of individual cell lines: HUT4-3 (red) vs SupT1 (blue) (F), "HIV Gag intermediate gate"(black) vs SupT1 (blue) (G), Q3 CD4+ (SupT1, grey) gate vs Q3 CD4- (HUT4-3, orange) gate vs SupT1 (blue) (H) or Ramos cells (rose) vs SupT1 (blue) (I). J: Backgating (final gated population overlaid at each level in red) of Ramos/LD cells to HIV Gag/Env expression.

SUPPLEMENTAL FIGURE 5 GERDA establishment

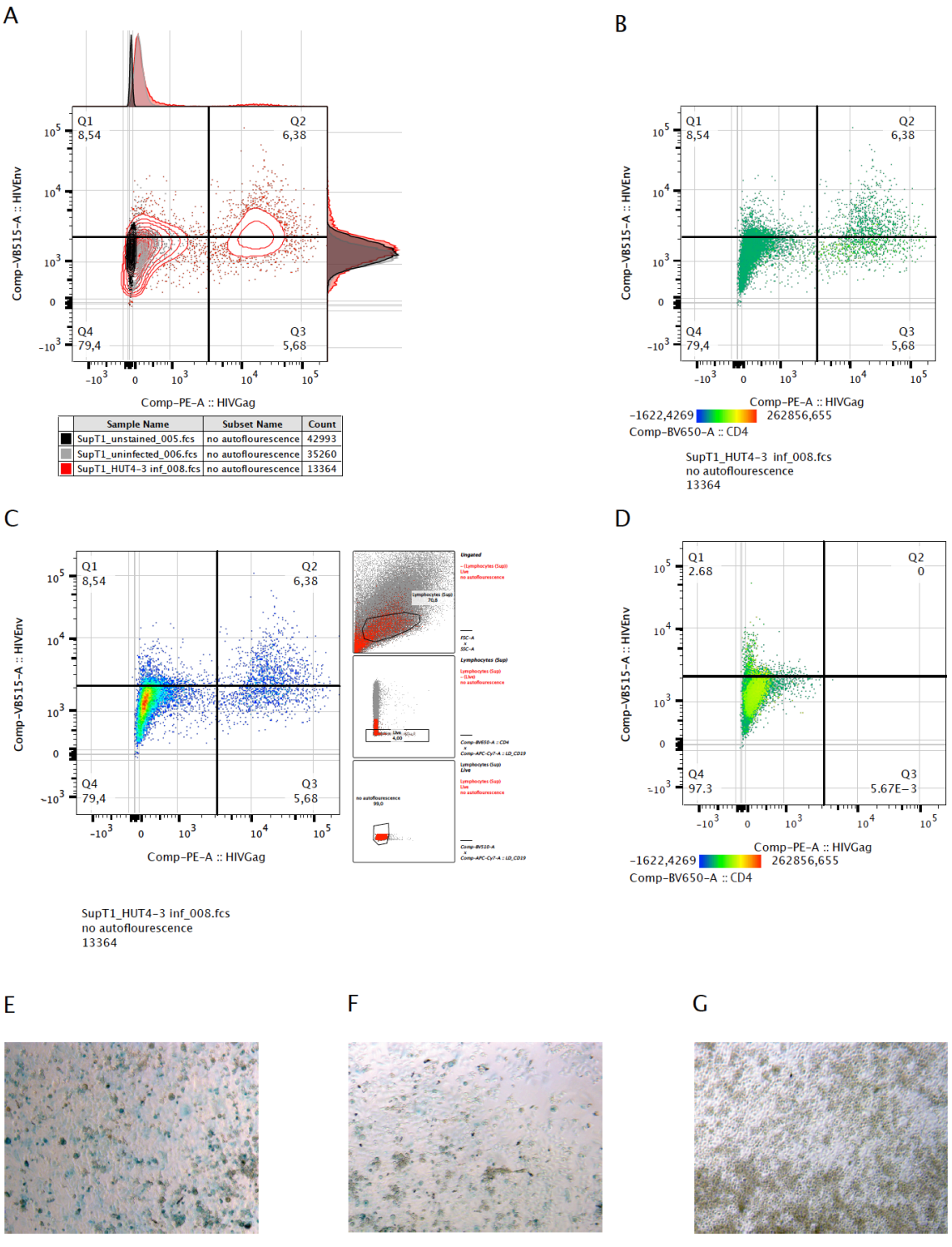

Supplemental Figure 5 related to Figure 7. GERDA staining establishment. A, B: HIV Gag/Env staining of HUT4-3 virus infected SupT1 cells. Infected cells (red) in comparison to unstained (black) and uninfected (grey) controls (A) or CD4 expression heatmap of infected SupT1 cells (B). C, H: Backgating (final gated population overlaid at each level in red) of SupT1 (C) or CD4+ T-cells (H). D, I: HIV neg controls of SupT1 (D) or CD4 (I) infections with CD4 heatmap. E-G, J-L: 6 days post infection X-Gal staining of SXR5 (E)/(J), TZM-bl (F)/(K) or uninfected control (G)/(L). Blue cells show individual infection events. M-O: Mal-2 infections of SupT1 cells looking at Gag vs Env (M), CD4 heatmap (N) or X-Gal staining (O). P-R: Ala-1/LAI infections of CD4+ PBMCs. Gag vs Env expression of LAI (orange,) or Ala-1 (blue) infection (P), X-Gal staining of Ala-1 (Q) or LAI infection (R). Blue cells show individual infection events.

SUPPLEMENTAL FIGURE 5 GERDA establishment

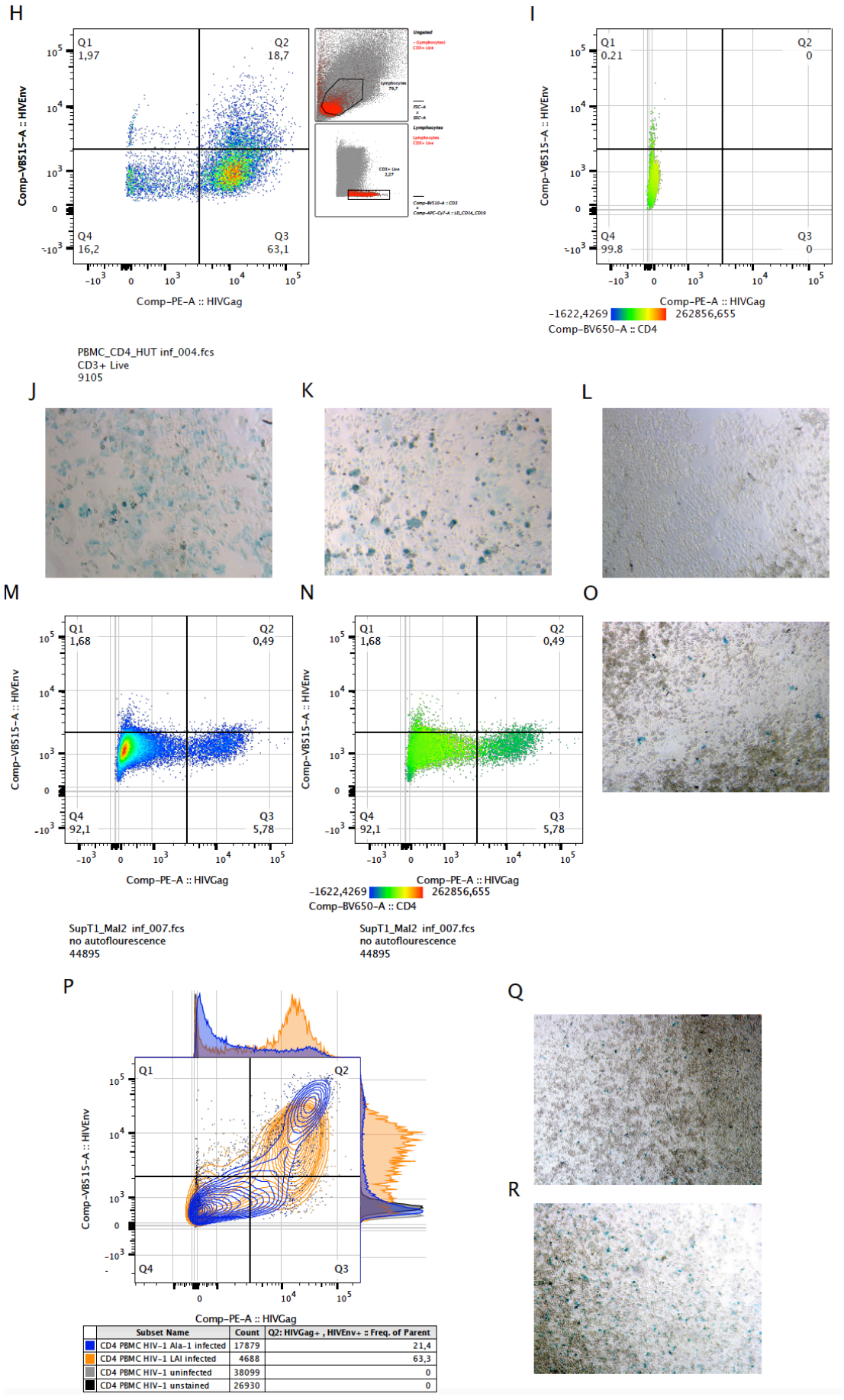

SUPPLEMENTAL FIGURE 6 GERDA applied on recent HIV-1 diagnosed individuals

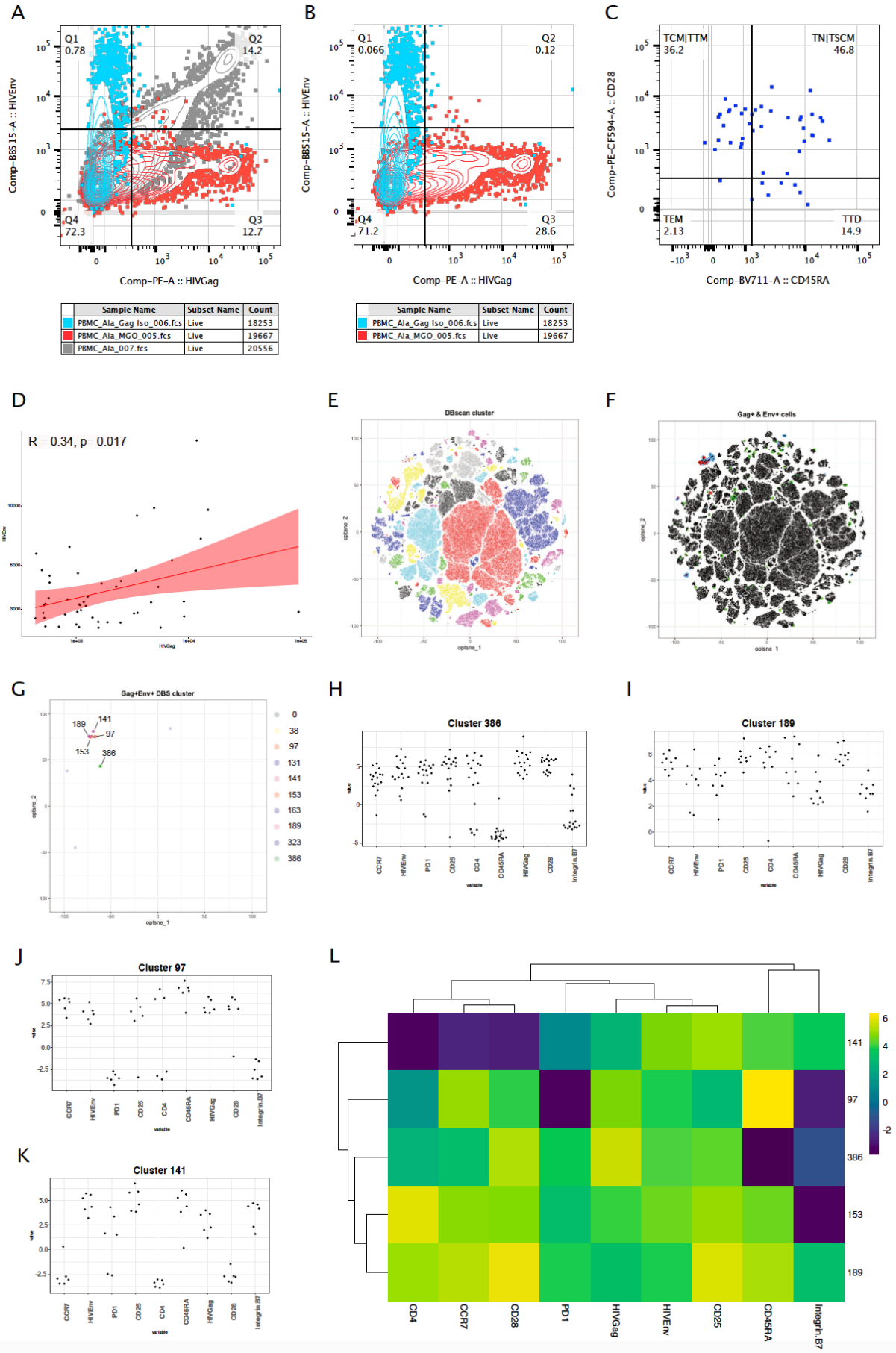

SUPPLEMENTAL FIGURE 6 GERDA applied on recent HIV-1 diagnosed individuals

M

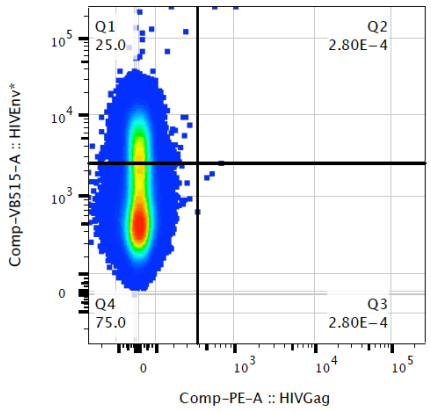

N

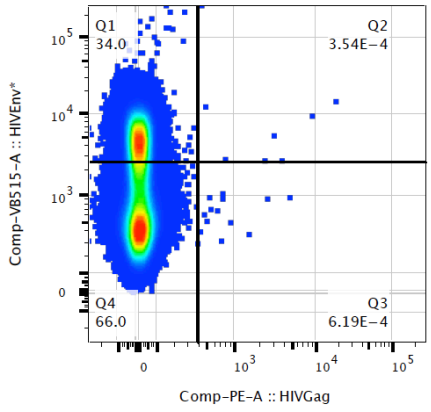

O

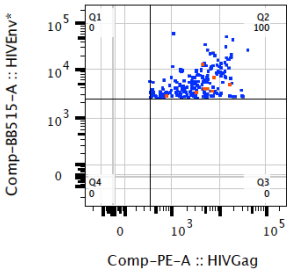

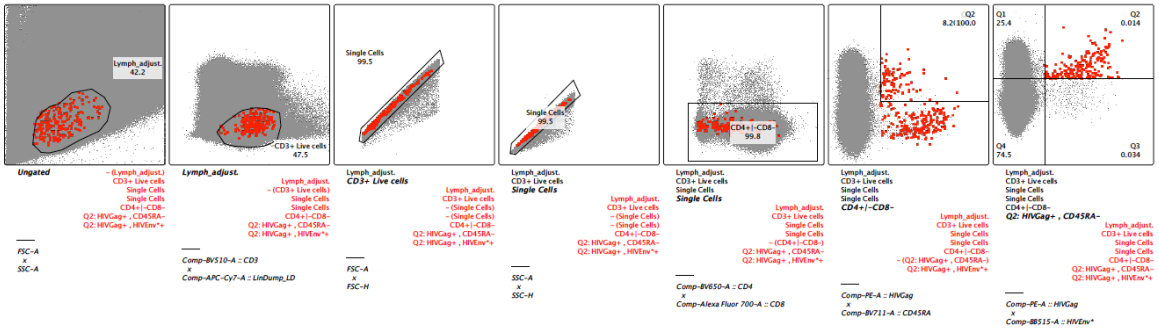

P

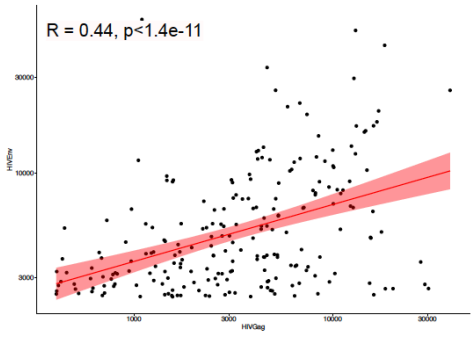

Q

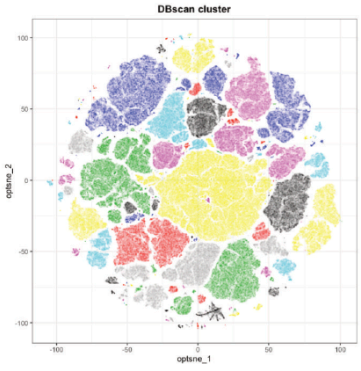

Supplemental Figure 6 related to Figure 9. GERDA staining on PBMCs of HIV-1 infected individuals. A, B: Isotype control stains of CD4+ PBMCs infected with Ala-1: MGO (red: bNAb Isotype, human IgG1), Gag Isotype control (blue) and usual Gag and bNAb stain (grey). Cryo-preserved pre-ART samples C-L. C: Gag+Env+ contribution of each memory compartment. D: Gag/Env correlation of Q2 Figure 9 A. E-G: t-SNE plots (each dot represents one cell as single data point, 6.85E105 cells in total) highlighting all identified DBSCAN clusters (Color palette does not allow to highlight each individual cluster in an individual color) (E), highlighting all Gag+ (blue) and Gag+Env+ (cyan) populations (F) or highlighting DBSCAN clusters of just Gag+Env+ cells (G). H-K: Marker expression of each individual cluster as indicated in Supp Figure 7 G. Related to recently diagnosed Patient P03 M-Q. M, N FACS control stains: uninfected (M), and same day stained individual P02 (N) for comparison to P03. O: Backgating (final gated population overlaid at each level in red) of DP events of patient P03. P: Gag/Env correlation of Q2 Figure 9 B. Q: t-SNE plot (each dot represents one cell as single data point, 1.41E106 cells in total) highlighting all clusters identified by DBSCAN (Color palette does not allow to highlight each individual cluster in an individual color)

SUPPLEMENTAL FIGURE 7 GERDA vs QVOA

A

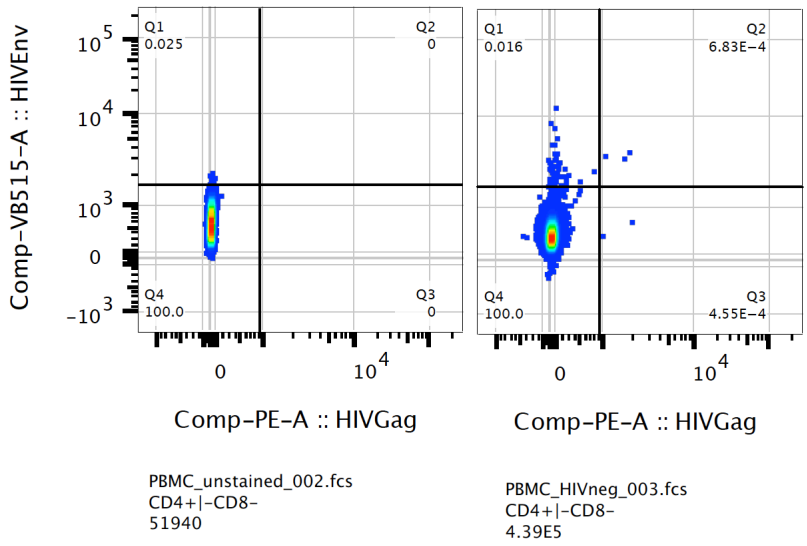

PBMC_unstained_002.fcs
CD4+|-CD8-
51940

PBMC_HIVneg_003.fcs
CD4+|-CD8-
4.39E5

B

Cell Fraction	Purity [%]
T_N	97.0 ± 2.9
T_{CM}	93.1 ± 0.14
T_{TM}	93.1 ± 0.42
T_{EM}	95.3 ± 2.19

C

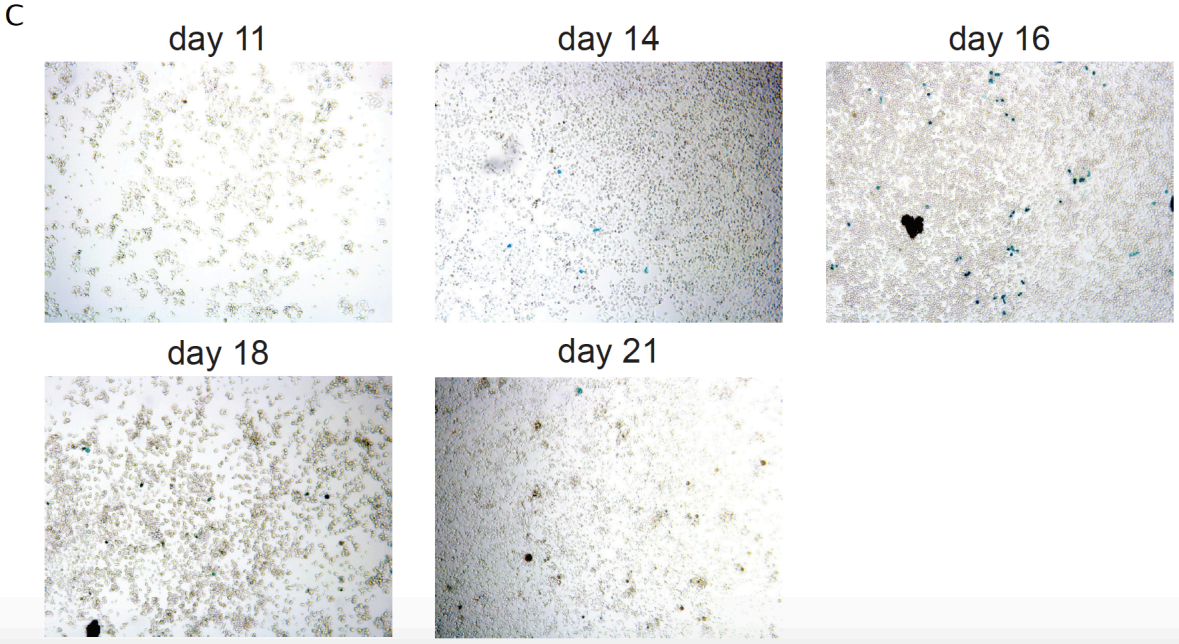

Supplemental Figure 7 related to Figure 11. GERDA performance during viral outgrowth. A, B: Control stains of day 14 post stimulation: unstained (left) and uninfected CD4+ T-cells (right). B: Purity of sorted fractions. Purities are given as % ± SD. C: Progression of viral reactivation visible as blue cells from same well over time by X-Gal staining. Blue cells show individual infection events. SD: standard deviation

SUPPLEMENTAL FIGURE 8 A PR-RT relatedness of P05 and P07

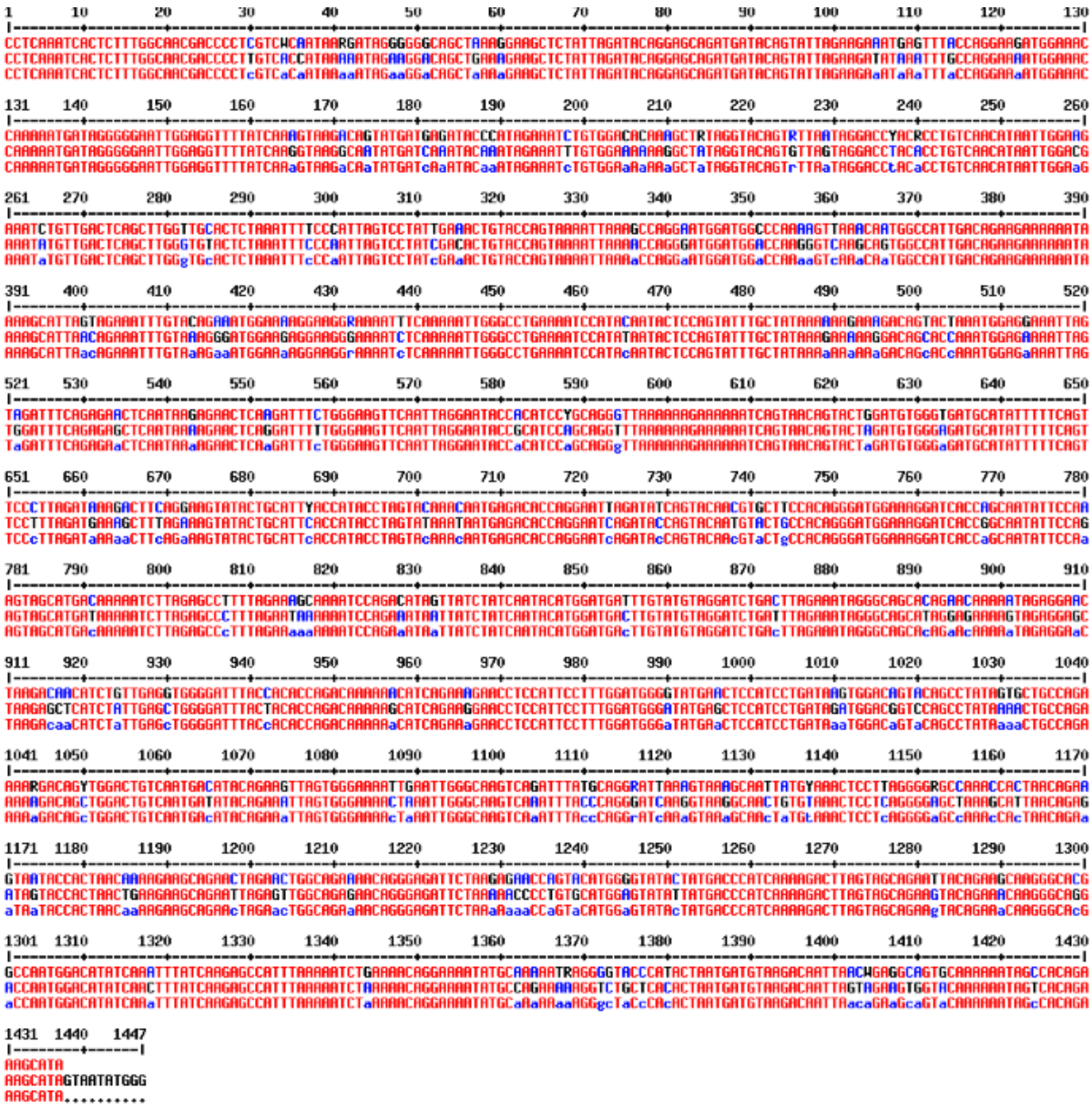

Supplemental Figure 8A. Relatedness of individual P05 and P07. Alignment of PR-RT sequence of P05 (top) and P07 (middle). Consensus sequence is shown on the bottom. Matches are colored in red, while mismatches are colored in Blue/black. Data was kindly supplied by MD Diagnostic University Hospital Basel/ Prof. Hans H Hirsch.

SUPPLEMENTAL FIGURE 8 B INT relatedness of P05 and P07

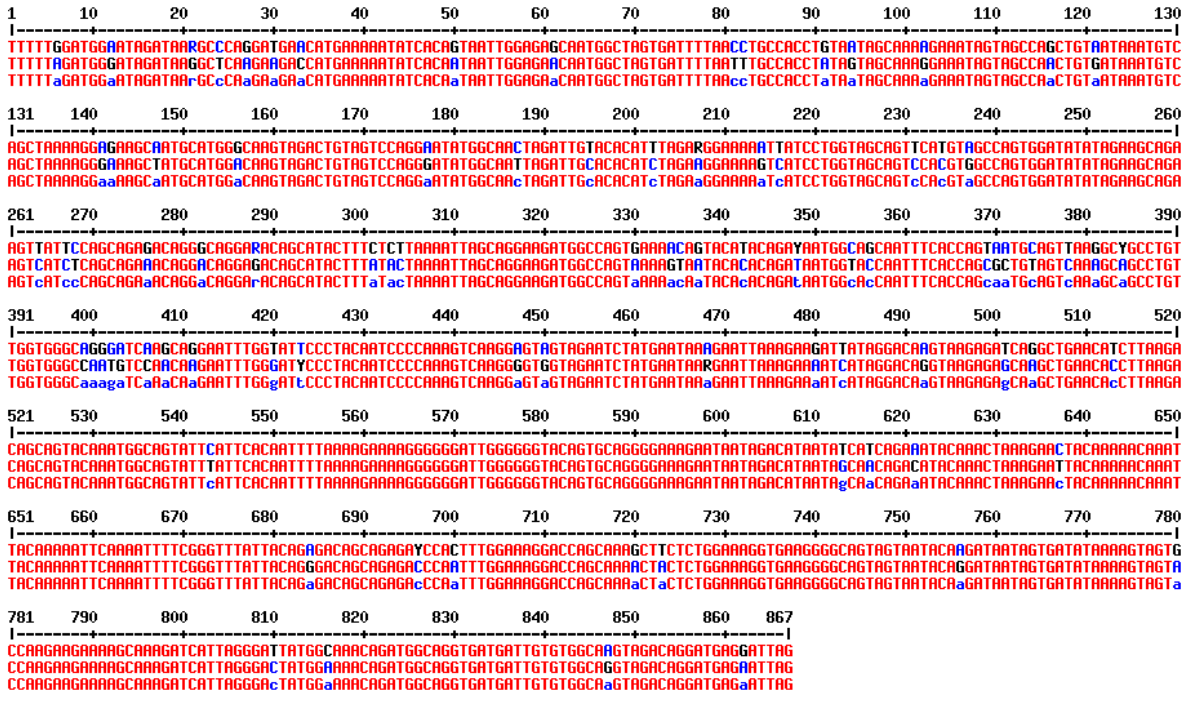

Supplemental Figure 8B. Relatedness of individual P05 and P07. Alignment of INT sequence of P05 (top) and P07 (middle). Consensus sequence is shown on the bottom. Matches are colored in red, while mismatches are colored in Blue/black. Data was kindly supplied by MD Diagnostic University Hospital Basel/ Prof. Hans H Hirsch.

SUPPLEMENTAL FIGURE 9 Patient visit schedule

Supplemental Figure 9 Patient schedule for recently HIV diagnosed individuals. Patient are indicated over time. First reactive antibody test must be confirmed by PCR and Western blot at a second visit shortly after first visit. ART is initiated generally 2 weeks after validation of HIV diagnosis. If the patient is doing fine after on month the visits are scheduled every 3 months. X marks the earliest sample used for analysis. The red asterisk marks the desired first timepoint for reservoir evaluation.

SUPPLEMENTAL FIGURE 10 GERDA profile of recent HIV-1 diagnosed individuals

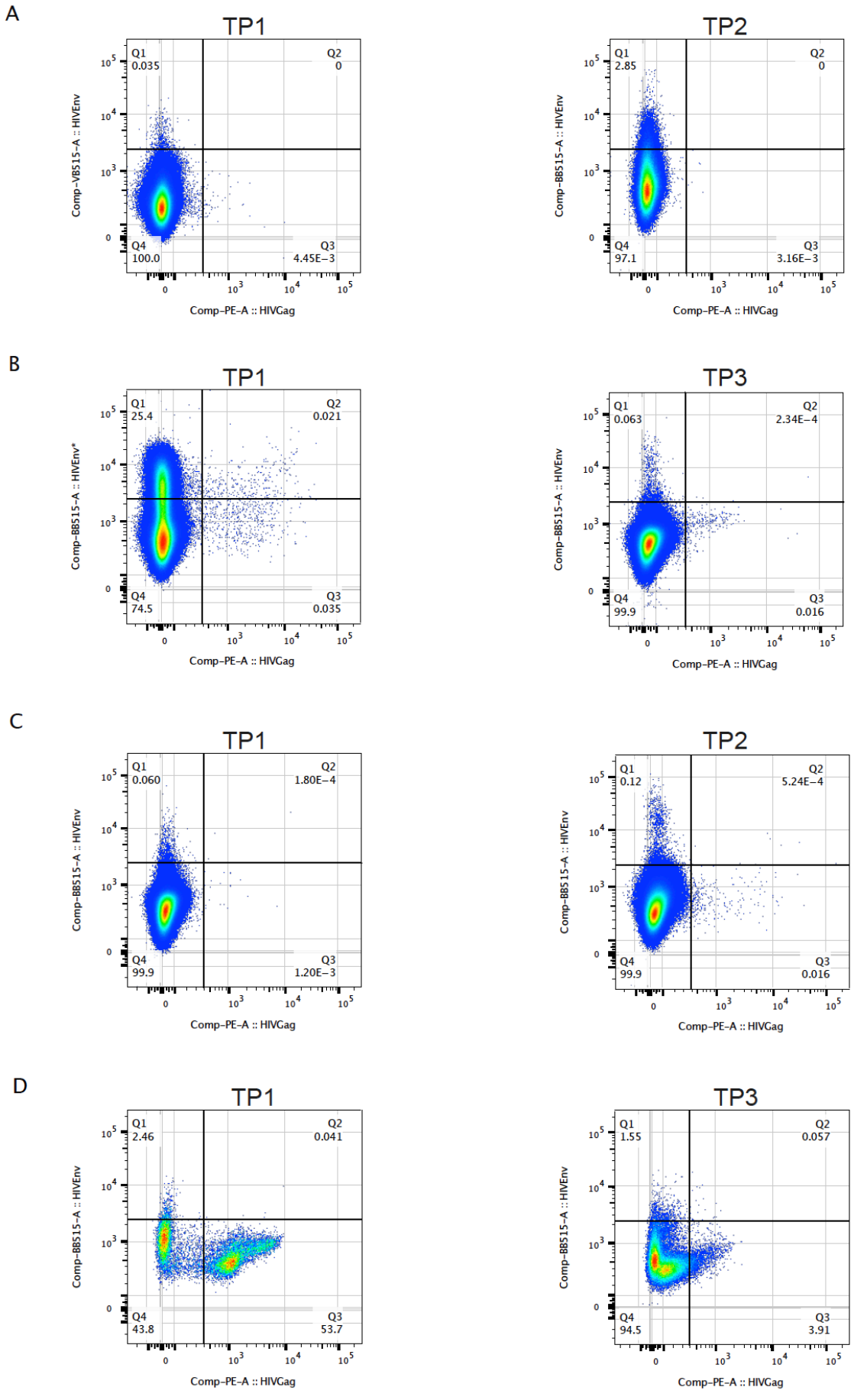

SUPPLEMENTAL FIGURE 10 GERDA profile of recent HIV-1 diagnosed individuals

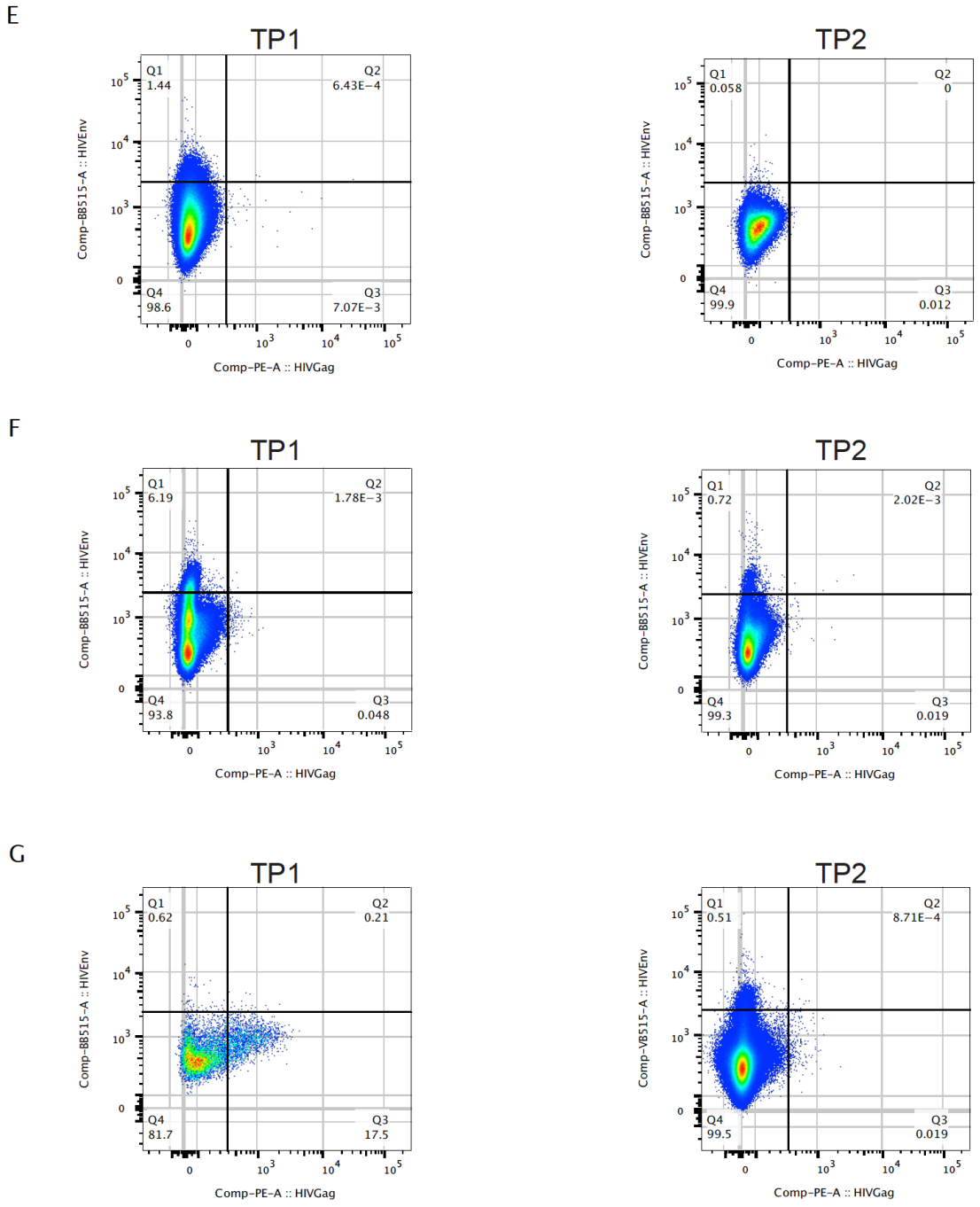

Supplemental Figure 10 related to Figure 9. GERDA staining on PBMCs of HIV-1 infected individuals: Gag vs Env expression of two consecutive timepoints for each examined individual. A: P01, B: P03, C: P04, D: P05, E: P06, F: P07, G: P08

SUPPLEMENTAL FIGURE 11 pMVQA plasmid map

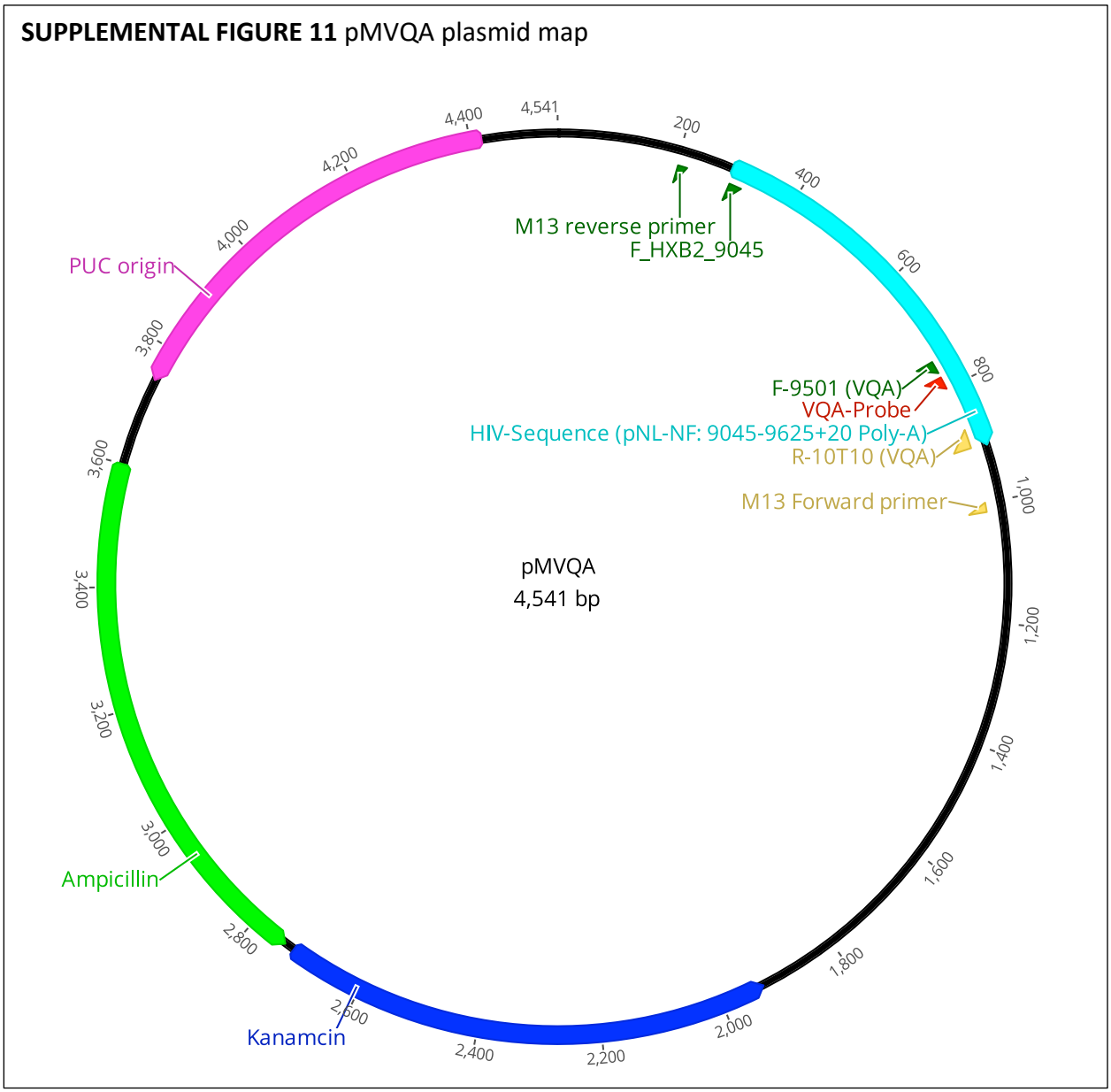

Supplemental Figure 11. Plasmid map of pMVQA. HIV sequence of reference plasmid pNL-NF was cloned from position 9045-9625 (cyan bar) with addition of a poly-A tail and cloned into TOPA-TA vector. Forward Primer (green), reverse primer (yellow) and Probe (red) binding sites are indicated by colored triangles. Origin of replication (magenta), Ampicillin (green) and Kanamycin (Blue) resistance cassettes are shown as respective colored bars.

XIV. Acknowledgement

I would like to thank all the people, friends and colleagues involved in the process and completion of my thesis.

First of all, I would like to thank my mentor and leading champion Prof. Thomas Klimkait placing his trust in me and giving me the opportunity to develop and "flourish" within my PhD project. Frankly speaking, at the beginning of my project you and I were quite naïve immunologists. But being naïve should never be confused with having no clue, or just to say it in an immunological term: it is just like naïve T-cells… you have the ability to develop in all kind of fates. Considering that I spent 1/6 of my life in your lab we have gone through many good times. It is basically your credit that I am now graduating as a PhD student. 9 years back in time I started in your lab as a "very naïve T-cell"/intern, still don't knowing where to go. Got to know the "big world" of small molecules, you really rouse my passion for life sciences. I really appreciate your eagerness as a tutor and teacher. You really deserve the title "Professor". I cannot remember having once a fight with you and am really thankful for all your support and the precious advices you gave as a lab veteran ☺. I always loved to listen to your old lab stories, always beginning with "back in times, when I was young…". Beside the glorious science side, I really can say that you truthfully have your heart at its right place! Thomas, I wish you all the best for your future as successful PI, husband, father and last but not least as a great * pause * grandfather! But it ain't over till the fat lady sings! Since fate has decided that you and I will continue our journey together, we will probably write a few more (successful) chapters with "Rocket science"… :-)

I would also like to thank Prof Christoph Dehio, my faculty representative, who always asked the right challenging and critical questions at all our progress reports. He always took his responsibilities seriously as a member of my thesis committee.

I am also very grateful to have had Prof. Angela Teresa Ciuffi as my external expert, who stepped in and immediately accepted my request to have her as my external Expert.

A very big "Thank you!" goes especially to Dr. Marcel Stöckle, who gave me access to the clinical samples and connected me to Kerstin Asal and Rebekka Plattner my holy study nurses. Kerstin always provided me with all patient related data and Rebekka always organized and scheduled all blood draws of my recruited patients. I was really grateful to have you as my contact person. Of course, all this would not have been possible without the help of all nurses who made all venipunctures. Same is true for "the Ladies" of MD diagnostics labs who supplied me with the first patient samples and had always a little bit of extra work, but still were willing

to help me out ☺. As last connecting piece I would also like to thank all the physicians that really did a marvelous job to win recently diagnosed patients for my project and in the end I am much obliged to those individuals who consent to donate blood for my project in times confronted with very aggravating circumstances.

Following to that, I would also like to thank Prof. Dr. Manuel Battegay, who accepted to have me in their weekly HIV reports, to discuss recent study cases and to introduce my project to all recruiting physicians at the University hospital Basel and who also hosted a really nice EACS conference 2019 in Basel.

I also like to thank Marek Basler for acting as a chairman at my defense. I guess he had to take the chair several times in a row for some Virologists at Petersplatz ☺

I was also very delighted to meet our German friends and colleagues from cologne Prof Florian Klein, who kindly supplied all bNAbs for my study and his great expertise for Virology and Immunology, and Prof Rolf Kaiser, who is possibly the best networking person in the world of Virology ;-) and also the organizer of world's best Virology conference Arevir! Along these lines I also want to thank Martin Däumer and Alexander Thielen from Kaiserslautern for helping us with all NGS data.

Faces have changed a lot in our lab in the last years. So I would like to thank:

- Jenny, who saved a lot of my abstracts from being rejected due to false wording :-P We really had a very nice time in the lab and also outside the lab. I will never forget the IAS conference in Mexico City and the dark streets we definitely should have never entered :-D. I really appreciated your perspicacious perception in scientific discussions but also your attitude in life. I was always astonished how many projects one person can deal with, but you are really a big champion ☺. If I would have to entrust my project in chaotic Africa to someone, I would definitely have my favorite one that I would choose for these challenges! I hope we will stay in touch beyond our PhDs ☺

- Lorena, who was the silent soldier in the background who managed all inquiries of the lab and always saved my ass to stand in for PBMC isolations of my patients whenever I was busy. I really like your style of working and learned a lot about working in an organized way! I was always amazed by all your trips and interesting stories you brought back from your adventurous vacations! I really enjoyed your company and hope for a further successful cooperation on our continuing way ☺

- Ulrike, who always pointed out what to change in my way to complicated presentations to make it understandable for the audience :-D. What I appreciated most is your time that you invest in the work for refugees and small kids as a volunteer, which is definitely not to be taken for granted!

- Nina, who was the poor PhD student that had to take over the integration site project that brought a lot of frustration with it. Nevertheless, you managed to get behind it and soon have very nice data! I will keep the Arevir meetings in Cologne especially for memories, where everyone was glad to end the 2 hour delayed workshops and have their Kölsch beers in the legendary "Bieresel" ☺

- Yuepeng, my little Padawan from China ☺ With small communication problems at the beginning we still managed to establish together the HIV poly-A quantification and to get really nice data out of "our" small patient cohort. I really enjoyed your company as co-worker and hope you could learn some aspects about the HIV reservoir and will pursue the project beyond my PhD and publish nice data out of it ☺

- Benni, Silvia and Rahel. You are basically the only ones that passed our lab and still are in my memories, especially Benni who was always good to have for an extensive talk and a little distraction from lab work. Same is true for Rahel, who "enlightened" me with her insights as a MD and all the funny stories she was sharing. Silvia it was also nice to have you as lab mate and you were definitely Bennis insurance for a well-organized lab book :-P

- Séverine, Vincent, Sarah and Joelle. Although most of you were mainly involved in my project as an intern I really appreciated my time back then with you. Severine and Vincent were always the ones that translated to me all of Thomas requests that had to be implemented. I really enjoyed my time with you guys at Inpheno next to Vesalgasse ☺. Sarah you were the first contact person (next to Christel, a wild person that I will definitely not forget :-D) and who provided me with all your deep knowledge about HIV. Joelle, a very interesting character and "the PhD" student when it comes to a brought record of very successful and numerous publications. We had a very nice time during my intern and also beyond, with nice memories at the autumn fair.

- Julian Spagnuolo, who kindly provided all his R codes for t-SNE and DBSCAN analysis, which made my life so much easier and smarter. I really appreciated your responsiveness and the term "that's an easy one…" :-P

- Julien Roux, who brought me into the bioinformatics network of the DBM. Although my conception of Bioinformatics is still rudimentary, I still benefited from your heatmap skills and you were definitely the fastest person when it came to responsiveness!!

- I also have to thank a lot of people that supported me with the introduction of FACS and MACS in our lab. Firstly, Carsten Wiethe from Biolegend who basically taught me all what I know about FACS via Facetime and telephone. I really appreciated your broad knowledge on all immunological aspects and your great responsiveness. Along those lines I also like to thank the guys from the Flowcytometry facilities in Basel and Zurich, with a special thanks to Telma Lopes and Mario Wickert. Timo Stahl, Andrin Wacker, Lisa Grupp and Alain Hirschy from Miltenyi who always advised my concerning all MACS issues.

-I would also like to thank the cleaning ladies, Juan, Ibrahim, Jean-Luc and Andy for keeping things running at Petersplatz! Especially Andy and Jean Luc, who were always very supportive, despite my exotic and numerous requests. I remember the “past 5 pm” times in the facility office listening to Nina Haagen and the old glorious success stories of Andy’s sidecar bike races.

A big thanks also to my PhD fellows of the DBM PhD club and especially the fellows of the Immuno PhD club: Mirela, Martin, Marianne, Jordan and Philippe to name only a few.

Bring up the big confetti guns for my Bachelor Kings and Queen graduates from 2015: Marina, Enja, Vinzenz, Aurel, Eron, Benni and David (the critical proofreader)… endless Uno fights and CRISPR Cas9 **chdüsch**… Enough said!

My deepest gratitude goes to my family. Mom and dad, who gave me so much love (sometimes even too much :-P) and overwhelming support during my whole life. I cannot spell out how inconceivable proud and lucky I am to have you as my parents and grandparents of my two little sunshines Mats and Leno. If I will succeed to be only half as capable as you as parents with my responsibility as a father for Mats and Leno I will have done the best job! Although we have currently a tough time and some more hurdles to come, I just want to let you know: Mama un Baba, ich lieb euch vo ganzem Herze!

To my brother Daniel aka Dänerle aka motivation coach aka idol aka best brother in the world! You are definitely someone I look up to. Always following your footsteps, if skateboarding, first cigarettes or fashion sins, there truly was no path I would not have followed you! I am proud to be the uncle of your two sweet boys Levin and Yonah and also grateful that you married the women of your life (finally after almost 10 years!!). You definitely made the right

choice! Although I am pretty much convinced that I am definitely stronger than you, I still have to admit: you are truly my hero! I love you! Brotherlove!

The last lines are dedicated to my two little sweet, adorable, handsome, smart, charming, extraordinary cute, sometimes mad, always on their toes, never exchangeable, inexpressible best gifts life has given to me, Mats and Leno. I am truly proud to be your father and hope that I can pass on some of my values and "lessons learned" about life! Whenever I got home after a horrible day (the notorious "today was a bad day for science"-Day) it was you that conjured a smile on my face and taught me that life is not just about success… it is about Love and Happiness! You are my "Odem", my motivation when I get up early from bed and the last thought I have before I fall asleep. I love you both from the bottom of my Heart! May the wind always be at your back and the sun upon your faces. And may the wings of destiny carry the both of you aloft to dance with the stars! Otter out …

XV. Poster

HIV-1 elimination from reservoirs - viral dynamics during suppressive ART

Otte, Fabian[1]; Metzner, Karin[2]; Klimkait, Thomas[1]
[1]Molecular Virology, University Basel, Department of Biomedicine Basel Switzerland
[2]University Hospital Zurich, Institute of Medical Virology Zurich Switzerland

Abstract message

- In pre-therapy situations CXCR4-tropic HIV-1 variants increase over time and with stage of disease, whereas under therapy CXR4-tropic variants become markedly reduced or vanish*
- The study aim was to identify, which lymphoid compartment(s) are responsible for the observed selective elimination of the CXCR4 infected cells looking at the homing potential of cells from the blood periphery
- Preliminary data from cell sortings reveal that Lymph node homing as well as gut homing properties of cells coincide with higher proviral loads
- Of note: most gut homing memory T-cells possess also lymph node homing properties
- tSNE visualization is a suitable tool for identifying essential marker co-expression on infected cells

Background

In the absence of any therapy X4 (CXCR4)-tropic HIV-1 is found to increase over time of infection, associated with an accelerated disease progression. More recent analyses during ART show that in most successfully treated patients the opposite is true: X4 viruses are diminished while R5 (CCR5) viruses are stable*. Antiretroviral therapy itself and the recovering immune system seem to readily detect and clear cells infected with X4 viruses . Our intention is to look at long lived memroy T-cell compartments in the periphery of patients during untreated and treated time points to determine which cells are involved in the viral dynamics and which lymphoid tissue is responsible fo reservoir formation, stability and viral clearance with special focus on X4- and R5- tropic virus compartmentalization.

Material & Methods

Our pilot study used MACS technology for the analysis of peripheral blood of arbitrarily chosen HIV-positive patient samples from the Swiss HIV cohort study. Non-relevant CD8+ (CTLs) and CD19+ (B-cells) were depleted and CD8-CD19- cells were selected for CD4 and Integrin B7 (gut homing) or CCR7 (lymph node homing). Proviral loads (pVLs) were determined by validated qPCR. For multi-dimensional data visualization the tSNE plugin of FlowJo was used.

Results

MACS preliminary results:
In order to evaluate which lymphoid homing marker might be of highest relevance, proviral loads of MACS sorted fractions revealed that CD4+CCR7+/-CD8-CD19- and CD4+B7+CD8-CD19- cells were clearly enriched for proviral DNA copies.

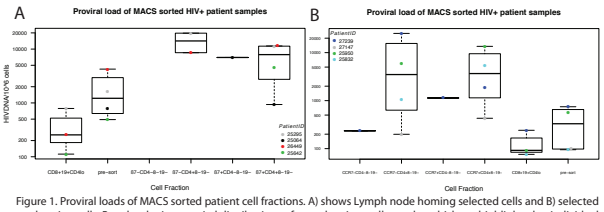

Figure 1. Proviral loads of MACS sorted patient cell fractions. A) shows Lymph node homing selected cells and B) selected gut homing cells: Boxplot depicts proviral distributions of sorted patient cell samples which are highlighted as individual data points in each graph. Median is indicated by black line inside each boxplot.

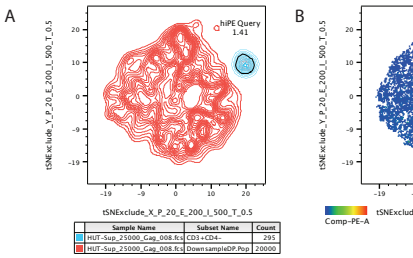

Figure 2. tSNE multi-parameter visualization for HIV-1 patient simulation. A) Depicts the clustered cell mixutre of 1% Gag expressing cells (HUT4-3: CD3+CD4-) titrated into uninfected Lymphocyte cell line (SupT1: CD3-CD4+) . Overlay shows CD3+CD4- highlighted in blue which is only expressed by infectious cells. The Heatmap of section B) shows PE-expression levels (HIV-1 Gag) in the clusterd cells. All PE high cells are clustered as a distinct, isolated population.

For the better interpretation of the complex multi-parameter data the tSNE algorithm was tested on patient simulated condition (1% HIV-1 infected cells) using HIV Gag::PE intracellular staining. As seen in Figure 2B all high PE expressing cells cluster in one population. Further analysis showed that those cells are indeed the infected cells. Further simulation of lower dilutions remain to be tested.

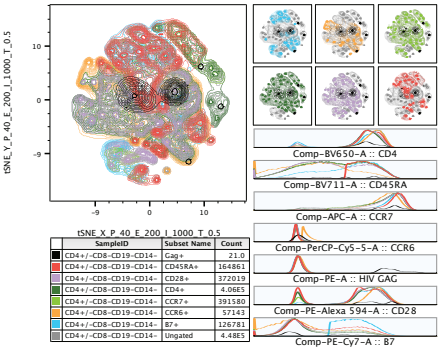

Figure 3. tSNE multi-parameter visualization of patient sample. Left graph shows contour plot of clustered cells (~500'000 cells). Cells were pre-gated on CD3+CD4+/-CD8-CD19-CD14- events. Each colour shown in table underneath shows respective positive fraction of each differentiation maker. Right top: tSNE overlays of each single marker superimposed on HIV-1 Gag and all other clustered events. Histoplot show marker expression of each gated poplation. Black events illustrate intracellular HIV-1 Gag expression as a proxy for infected cells that have late gene translation as well as viral budding from cell surfaces.

Patient condition (~200 HIV DNA copies/10^6 cells) multi-parameter stain on ~500'000 cells of interest (CD3+CD4+/-CD8-CD19-). HIV Gag+ cells are highlighted in plot as black. Data implies for this condition that HIV Gag+ cells co-express CD4, CCR7, CD28 and some Integrin B7.

Outlook

- *HIV Envelope broadly neutralizing antibodies will be used for tSNE analysis to identify potential intact proviruses of patients under suppressive cART and high proviral loads with much higher precision*
- *tSNE results will then highlight reservoir markers of interest for subsequent live cell sorts and the selective reactivation of latent proviruses*
- *scRNA sequencing of sorted cell fractions will give further insights into the role of immuno-modulating transcription profiles in HIV infected cells*
- *Finally, integrating all data from these cells, circulating in the periphery, will then be followed by a detailed analysis of the respective tissue(s) of interest (GALT/LN biopsies) using CyTOF imaging*

Contact: Fabian.Otte@unibas.ch

* Bader, J. et al. Therapeutic immune recovery prevents emergence of CXCR4-tropic HIV-1. Clin. Infect. Dis. ciw737 (2016).

Viral dynamics during suppressive ART - Towards HIV-1 elimination from reservoirs

Otte, Fabian [1]; Klimkait, Thomas [1] and the Swiss HIV Cohort Study

[1] Molecular Virology, University of Basel, Department of Biomedicine, Basel, Switzerland

Abstract message

- In pre-therapy situations CXCR4-tropic HIV-1 variants increase over time and with stage of disease, whereas under therapy CXR4-tropic variants become markedly reduced or vanish [1]
- The study aim was to identify, which lymphoid compartment(s) are responsible for the observed selective elimination of the CXCR4 infected cells looking at the homing potential of cells from the blood periphery
- Multi parametric FACS show active viral compartments beyond the periphery
- tSNE visualization is a suitable tool for identifying essential marker co-expression on infected cells

Background

In the absence of any therapy X4 (CXCR4)-tropic HIV-1 is found to increase over time of infection, associated with an accelerated disease progression. More recent analyses during ART show that in most successfully treated patients the opposite is true: X4 viruses are diminished while R5 (CCR5) viruses are stable [1]. Antiretroviral therapy itself and the recovering immune system seem to readily detect and clear cells infected with X4 viruses. Our intention is to look at long lived memory T-cell compartments in the periphery of patients during untreated and treated time points to determine which cells are involved in the viral dynamics and which lymphoid tissue is responsible for reservoir formation, stability and viral clearance with special focus on X4- and R5- tropic virus compartmentalization.

Materials & Methods

To study the properties of peripheral HIV-infected cells, we analyze T-cell memory, the lymphoid homing potential and HIV protein expression in stimulated patient cells by multi-parameter FACS, utilizing R based t-distributed stochastic neighborhood embedding (tsne) and DBScan [2] to identify specific target cell clusters.

Results

To evaluate our staining procedure we first tested if we can identify in a mixed pool of chronically infected (HUT4-3) and uninfected Lymphocytes (SupT1) HIV positive as well as HIV negative cell populations. As shown in Figure 1 viral active HUT4-3 cells localize as a clearly distinct double positive population in the second quadrant of the Contour plot whereas non-infected SupT1 cells are located in the double negative third quadrant.

Moving one step further to a more "patient-like" situation we used PBMCs infected with different HIV-1 strains (e.g. LAI and Ala-1, both Subtype B and X4-tropic). As illustrated in Figure 2 A and C both infections yield adequate levels of double positive cells. The Supernatants of each infection was further checked for the presence of functionally intact viruses (Fig. 2 B).

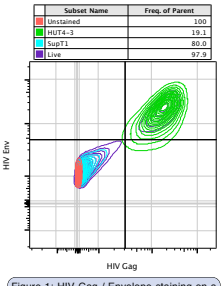

Figure 1: HIV Gag / Envelope staining on a mixed pool of infected (HUT4-3) and uninfected (SupT1) cells. Legend above highlights color coded ID of each population

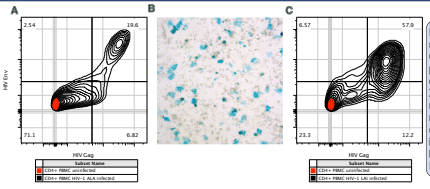

Figure 2: HIV Gag / Envelope staining of HIV-1 infected CD4+ T-cells. (A) Contour plot of Ala-1 infection condition. (B) Representative X-Gal stain of infected reporter cells. Each blue cell represents one infection event. (C) Contour plot of LAI infection condition. Legend below highlights color coded ID of each staining condition.

Finally primary material from pre cART timepoint of patients with high proviral loads was examined using T-cell memory, HIV protein and lymphoid homing markers. As seen in Fig. 3 A HIV Env^{hi} cells aggregate in the lower left part of the tsne map. If Gag signals, as seen in Fig 3 B, are considered as well, cell populations are identified that co-express Env and Gag.

Figure 3: tsne plots of patient derived data. (A) HIV Env heatmap highlighting HIV Env^{hi} cells as shown in scale next to pot. (B) tsne plot of Gag+ (blue), Env+ (in red) and Gag+Env+ (in black) cells.

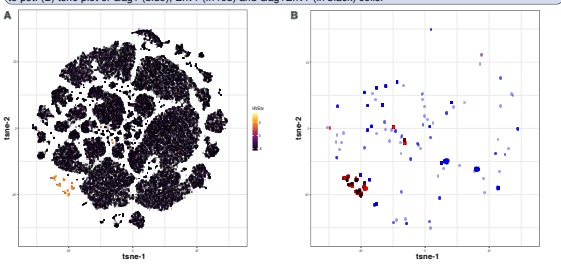

To have an unbiased view on the populations we clustered the data using DBScan. Each color in Fig 4 B represents one cell cluster identified by the algorithm. Fig. 4A next to the tsne cluster map depicts one selected cluster with Gag/Env double positive expression.

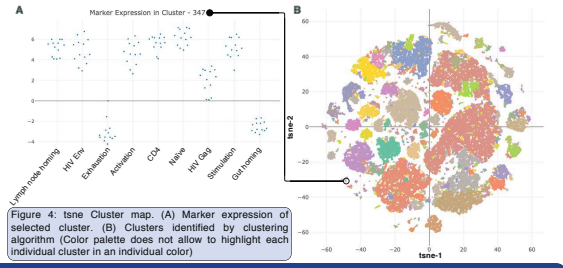

Figure 4: tsne Cluster map. (A) Marker expression of selected cluster. (B) Clusters identified by clustering algorithm (Color palette does not allow to highlight each individual cluster in an individual color)

Outlook

- tSNE results highlight reservoir markers of interest for subsequent live cell sorts and the selective reactivation of latent proviruses
- Matched integration site and proviral (MIP) sequencing of sorted cell fractions will give further insights in cellular compartmentalization and genomic landscapes of distinct viral species.
- Finally, integrating all data from these cells, circulating in the periphery, will then be followed by a detailed analysis of the respective tissue(s) of interest (GALT/LN biopsies) using CyTOF for deep immune profiling

Contact: Fabian.Otte@unibas.ch

[1] Bader, J. et al. Therapeutic immune recovery prevents emergence of CXCR4-tropic HIV-1. Clin. Infect. Dis. ciw737 (2016).
[2] FACkit (FACS Analysis Tool kit), version 0.1.0 developed by Julian Spagnuolo

XV.3. **23rd International AIDS Conference** *AIDS 2020 Virtual*, San Francisco & Oakland, USA (July 2020)

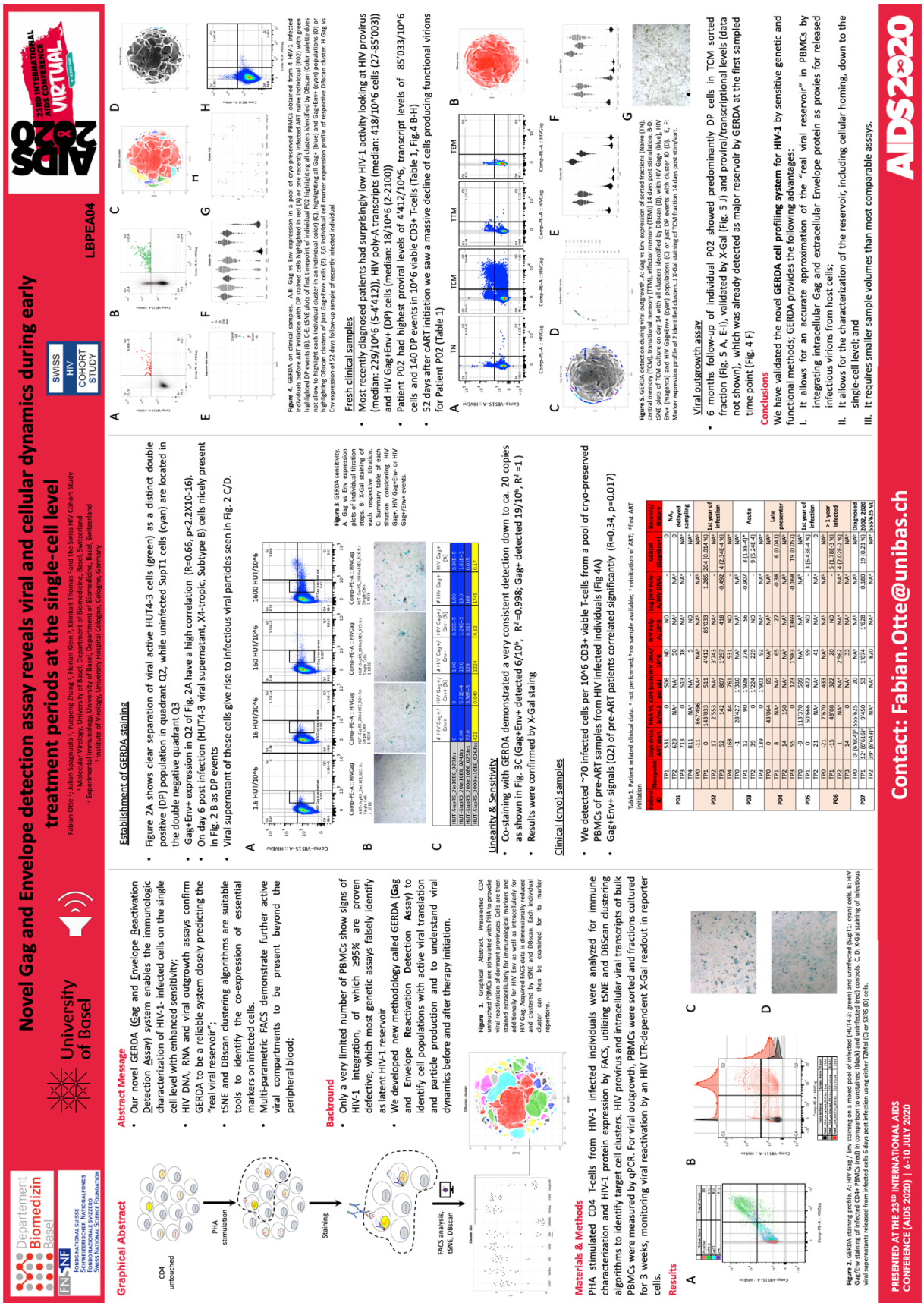

XVI. Curriculum Vitae

Personal Data

Name	Fabian Otte
Nationality	German
Date of birth	07th of February 1991
Email	Fabi.o@gmx.net
Phone	+49 176 382 353 76

Education Molecular Biology, Virology and Immunology

08/2016 – 10/2020 International PhD in Biomedicine, DBM, Basel
University of Basel (SUI), Department of Biomedicine, Prof. Dr. Thomas Klimkait

08/2015 – 07/2016 Master of Science Major in Molecular Biology (fast track),
University of Basel (SUI), Biocenter, Prof. Dr. Clemens Cabernard

09/2012 – 06/2015 Bachelor of Science Major in Molecular Biology
University of Basel (SUI), Biocenter

09/2001 – 06/2010 Academic High School
Kant Gymnasium, Weil am Rhein (GER)

Research Experience

08/2016 – 10/2020 **PhD in human biomedical Research**

Project scope: **Immunological** and **virological** characterization of the HIV-1 reservoir

- Developed novel highly sensitive **single-cell HIV detection assay**
- Successfully **liaised** state-of-the-art **technologies in Virology and Immunology**
- **Establishment of a sub cohort** of early HIV-1 diagnosed patients
- Analytical and reporting contribution for **two successful grant proposals** (SNF/Swiss HIV cohort Study: **50'000 CHF each**)

Publications

To be submitted soon: **Otte F**, Spagnuolo J, Wiethe C, Stoeckle M, Klein F, Klimkait T, and the Swiss HIV Cohort Study, *Preliminary working title*: Novel HIV-1 viral reservoir assay reveals viral and cellular dynamics at the single-cell level during early treatment periods

Tsankova A, Pham TT, Garcia DS, **Otte F**, Cabernard C, Cell cycle and polarity cues regulate baised Myosin activity and dynamics via *Drosophila* Rho Kinase/Drok and Protein Kinase N/Pkn during asymmetric cell division, Developmental Cell 2017

International Conferences

07/2020	**23rd International AIDS Conference** ***AIDS 2020 Virtual***, San Francisco & Oakland, USA **Late Breaker** Poster presentation "Novel Gag and Envelope detection assay reveals viral and cellular dynamics during early treatment periods at the single-cell level"
11/2019	**17TH European AIDS Conference**, Basel, CH **Scholarship** recipient and **oral** presentation "HIV-1 reservoir formation, stability and dynamics during cART"
07/2019	**10th IAS Conference on HIV science**, Mexico City, MX **Poster** presentation "HIV elimination from reservoirs – viral dynamics during suppressive ART"
05/2019	**17TH MEETING ON HIV & HEPATITIS, ROME, ITALY** **Oral** presentation of my data by supervisor "Viral dynamics during suppressive ART – Towards HIV elimination from reservoirs"
10/2018	**HIV DRUG THERAPY 2018, GLASGOW, UK** **Poster** presentation "HIV elimination from reservoirs – viral dynamics during suppressive ART"

Extracurricular scientific Skills

GCP + Swiss Supplement	TRREE (Training and Resources in Research Ethics Evaluation) certified (recognized by Swissethics)
HIV report USB	Scientific guest in HIV related clinical affairs at the University Hospital Basel
Immuno PhD club DBM	Immunology study club for scientific exchange of PhD projects and invited speakers

Biosafety	"Principals of Biosafety in Medical and Biological Research" Course UZH
Language	German (native) English (business fluent)
EDP	**R** for statistical computing, big data management and graphical excellence **FlowJo & Diva** Flow cytometry analysis **ImageJ/FIJI** and **Imaris** for scientific image analysis Adobe **Photoshop, Illustrator & Affinity Designer** **MS Office** Operating systems: **Windows & MacOS**

Interests

Family (2 kids), Freeletics, Cycling, Running, Snowboarding, Soccer

References

Prof. Dr. rer. nat. Thomas Klimkait (Supervisor PhD)
Head of Research Group Molecular Virology
Department of Biomedicine
University of Basel
Petersplatz 10 4051 Basel
T: +41 (0)61 267 32 72
thomas.klimkait@unibas.ch

Prof. Dr. Clemens Cabernard (Supervisor Master)
Assistant Professor
University of Washington
Department of Biology
24 Kincaid Hall
Seattle, WA 98195-1800
T: +1 206 616 7368
ccabern@uw.edu
www.cabernardlab.org